Model Predictive Control for Resilient Operation of Hybrid Microgrids

by

James Robert Nelson

A Dissertation Presented in Partial Fulfillment
of the Requirements for the Degree
Doctor of Philosophy

Approved October 2019 by the
Graduate Supervisory Committee:

Nathan Johnson, Chair
Michael Stadler
Wenlong Zhang

ARIZONA STATE UNIVERSITY

December 2019

ABSTRACT

This dissertation develops advanced controls for distributed energy systems and evaluates performance on technical and economic benefits. Microgrids and thermal systems are of primary focus with applications shown for residential, commercial, and military applications that have differing equipment, rate structures, and objectives. Controls development for residential energy heating and cooling systems implement adaptive precooling strategies and thermal energy storage, with comparisons made of each approach separately and then together with precooling and thermal energy storage. Case studies show on-peak demand and annual energy related expenses can be reduced by up to 75.6% and 23.5%, respectively, for a Building America B10 Benchmark home in Phoenix Arizona, Los Angeles California, and Kona Hawaii. Microgrids for commercial applications follow after with increased complexity. Three control methods are developed and compared including a baseline logic-based control, model predictive control, and model predictive control with ancillary service control algorithms. Case studies show that a microgrid consisting of 326 kW solar PV, 634 kW/ 634 kWh battery, and a 350 kW diesel generator can reduce on-peak demand and annual energy related expenses by 82.2% and 44.1%, respectively. Findings also show that employing a model predictive control algorithm with ancillary services can reduce operating expenses by 23.5% when compared to a logic-based algorithm. Microgrid evaluation continues with an investigation of off-grid operation and resilience for military applications. A statistical model is developed to evaluate the survivability (i.e. probability to meet critical load during an islanding event) to serve critical load out to 7 days of grid outage. Case studies compare the resilience of a generator-only microgrid consisting of 5,250 kW in generators and hybrid microgrid

consisting of 2,250 kW generators, 3,450 kW / 13,800 kWh storage, and 16,479 kW solar photovoltaics. Findings show that the hybrid microgrid improves survivability by 10.0% and decreases fuel consumption by 47.8% over a 168-hour islanding event when compared to a generator-only microgrid under nominal conditions. Findings in this dissertation can increase the adoption of reliable, low cost, and low carbon distributed energy systems by improving the operational capabilities and economic benefits to a variety of customers and utilities.

ACKNOWLEDGMENTS

I would like to express my deepest appreciation to Dr. Nathan Johnson. I am extremely grateful for his mentorship and limitless insights into all aspects of the energy industry and life. I would also like to thank the other two members of my committee, Dr. Michael Stadler and Dr. Wenlong Zhang, for providing guidance throughout my dissertation. I extend my sincere thanks to Samantha Janko, Shammya Saha, Nathan Webster, and the rest of the team at the Laboratory for Energy and Power Solutions (LEAPS). Without their endless motivation and assistance this dissertation would not have been possible. Lastly, I am extremely grateful for the support of my family and friends. I would not be the man I am today without their unwavering support.

TABLE OF CONTENTS

Page

LIST OF TABLES ix

LIST OF FIGURES xi

CHAPTER

INTRODUCTION 1

1.1. Motivation 1

1.2. Energy Industry Overview 2

1.2.1. Energy Markets 4

1.2.2. Reliability and Resilience 8

1.3. Distributed Energy Systems 10

1.3.1. DERs 10

1.3.2. Microgrids 12

1.3.3. Thermal Systems 14

1.4. Controls 16

1.4.1. Grid Controls 17

1.4.2. Microgrid Controls 18

1.5. Standards 21

1.6. Dissertation Organization 23

RESIDENTIAL COOLING USING SEPARATED AND COUPLED PRECOOLING AND THERMAL ENERGY STORAGE STRATEGIES 25

CHAPTER Page

2.1. Introduction 26

2.2. Location Data 30

2.3. Building Energy Model 34

2.4. Cooling Strategies 37

2.5. Optimal Precooling Set Points 40

2.6. Performance Comparison of Cooling Strategies 45

2.7. Conclusions 55

2.8. Acknowledgements 58

2.9. References 58

MODEL PREDICTIVE CONTROL OF MICROGRIDS FOR REAL-TIME ANCILLARY SERVICE MARKET PARTIPCATION 67

3.1. Introduction 68

3.2. Microgrid Control Algorithms 71

3.2.1. Logic-based Control 72

3.2.2. Model Predictive Control 74

3.2.2.1. Objective Function 74

3.2.2.2. Constraints 75

3.2.3. Model Predictive Control with Ancillary Services 79

3.2.3.1. Objective Function 79

CHAPTER Page

3.2.3.2. Constraints 80

3.3. Evaluation Metrics 83

3.4. Microgrid Portfolio 86

3.4.1. Microgrid Specification Data 86

3.4.2. Electric Rate Structure 88

3.4.3. Ancillary Service Market 89

3.5. Annual Performance Evaluation and Sensitivity Analysis 92

3.6. Intraday Dispatch 99

3.7. Conclusions 105

3.8. Acknowledgements 108

3.9. References 108

STATISTICAL DEVLOPMENT OF MICROGRID RESILIENCE DURING ISLANDING OPERATIONS 114

Abstract 114

4.1. Introduction 115

4.2. Statistical Development of Microgrid Survivability 119

4.3. Asset Dispatch During an Islanding Event 125

4.3.1. Objective Function 126

4.3.2. Constraints 127

CHAPTER Page

4.4. Microgrid Resilience Metrics 129

4.5. Microgrid Site Data 131

4.5.1. Installation Loads 131

4.5.2. Microgrid Assets 131

4.5.3. Microgrid Portfolios 133

4.6. Control Parameter Sensitivity Analysis 135

4.7. Performance Evaluations 139

4.7.1. On-site Fuel Reserves 139

4.7.2. Critical Load 140

4.7.3. Solar PV Generation 142

4.7.4. Battery Stack Starting State of Charge 143

4.8. Conclusions 145

4.9. Acknowledgements 148

4.10. References 148

DISSCUSION 156

5.1. Implications for Scientific and Electrical Power and Energy Communities 156

5.2. Future Work 162

5.3. Closing Remarks 164

REFERENCES 165

LIST OF TABLES

Table Page

2.1: Charges for the SRP Time-Of-Use Rate Structure (E-26) in Phoenix, Arizona..... 32

2.2: Charges for the LADWP Time-Of-Use Rate Structure (R-1B, Power Rate Ordinance No. 18413) in Los Angeles, California. 33

2.3: Charges for the HELCO Time-Of-Use Rate Structure (Revised Sheet No. 71) in Kona, Hawai'i..... 34

2.4: Building Characteristics and Parameter Values for the Building America B10 Benchmark Home (Wilson Et Al. 2014)..... 36

2.5: Major Characteristics of HVAC System for the Building America B10 Benchmark Home (Wilson Et Al. 2014). 36

2.6: Baseline Sizing Analysis of Heat Pump Cooling Capacity. 37

2.7: Optimal Precooling Parameter for Each Location for Strategies with and without a Set Back Temperature. 45

3.1: Annual Statistics of Electrical Load and Solar PV Generation for the ASU Fulton Center. 86

3.2: Charges for the APS E-32TOU M Rate Structure (Arizona Public Service 2017). .. 89

3.3: Total Number of Decision Variables Solved in Each Iteration of MPC Algorithms. 92

3.4: Statistics for Annual Simulation Using 24-Hour Prediction Time Horizon. 98

3.5: Statistics for Annual Simulation Using 48-Hour Prediction Time Horizon. 98

3.6: Statistics for Annual Simulation Using 168-Hour Prediction Time Horizon. 98

3.7: Statistics for Average Weekday in January for a 168-Hour Prediction Time Horizon. 102

Table Page

3.8: Statistics for Average Weekday in July for a 168-Hour Prediction Time Horizon. 105

4.1: Operational Characteristics of EOS Battery Storage Considered in the Hybrid Microgrid Portfolio (EOS, N.D.). 132

4.2: Generator, Solar PV, and Battery Economic Data Used to Calculate the Optimal Microgrid Portfolio. 133

4.3: Capacity of Energy Assets Included in Military Microgrid Portfolios. 135

4.4: Economics of Generator-Only and Hybrid Military Microgrid Portfolios. 135

LIST OF FIGURES

Figure Page

1.1: Historical, Current, and Forecasted Electricity Use in the U.S. (US Energy Information Administration 2017). 3

1.2: The Impact Of Disruptive Technology, Policy, and Market Forces That Create a "Vicious Cycle" in the Electric Power Industry (Ceres 2015). 4

1.3: Three Interconnection Areas and the Regional Transmission Organization/ Independent System Operator Market and Control Areas in the United States (United States Environmental Protection Agency 2017). 6

1.4: Generalized Timescale of the Grid Ancillary Services Needed to Maintain a Reliable Electric Grid (Hibbard Et Al. 2017). 8

1.5: Comparison of Grid Resilience and Reliability (Widergren Et Al. 2018)..... 10

1.6: The Volume Weighted Average Manufacturing Cost of Lithium-Ion Batteries from 2010 to 2017 (Chediak 2017). 12

1.7: Examples of a Civilian Microgrid (Left) and a Defense Microgrid (Right)..... 13

1.8: Prototype of a Residential TES, Heat Pump, and Cooling Coil Configuration..... 16

1.9: Hierarchical Control Structure of Electrical Power and Energy Systems (Meng Et Al. 2016). 17

1.10: Organizational Structures and Market Boundaries of Vertical Integrated and Horizontally Integrated Utilities (Pacific Northwest National Laboratory 2002). 18

1.11: Generalized Representation of a Model Predictive Controls Approach (ABB 2019). The Behavior of the System is Modeled over a Specified Prediction Horizon and Control Inputs Are Used to Achieve Desired Performance. 20

Figure Page

2.1: Average Annual Environmental Characteristics for Each Location. 31

2.2: Average Monthly Temperature and Relative Humidity for Each Location. 31

2.3: Building Envelope for the Building America B10 Benchmark Home. 35

2.4: Operating Mode Logic for Direct Expansion Cooling Coil and TES System. 40

2.5: Optimal Set Point Analysis Of Precooling Strategies for Phoenix. 42

2.6: Optimal Set Point Analysis Of Precooling Strategies for Los Angeles. 43

2.7: Optimal Set Point Analysis Of Precooling Strategies for Kona. 44

2.8: Outdoor Air Temperature and Intraday Electricity Use for the Average Day of July for Each Location. The Green Shaded Region Denotes the On-Peak Electric Rate Period. 47

2.9: Daily Electricity Use and Peak Demand for Off-Peak and On-Peak Times of Day in Each Location for the Average Day of July. 49

2.10: Monthly Electric Bill for Each Cooling Strategy in Each Location. 50

2.11: Change in Annual Electricity Charges, Annual Electricity Use, and Annual Peak Demand During the Off-Peak, On-Peak, and Total Billing Periods for Each Cooling Strategy with Changes Reported from the Baseline Simulation. 53

3.1: Control Process Flow for the Logic-Based Control Algorithm. 73

3.2: Average Annual Electrical Load and On-Site Solar PV Generation of the ASU Fulton Center. 87

3.3: Average Annual Required Capacity and Clearing Price for the Spinning and Non-Spinning Reserve Ancillary Service Markets in CAISO (California ISO, N.D.). 91

Figure Page

3.4: Annual Operating Expenses for Each of the Logic-Based, MPC Without Ancillary Services, and MPC With Ancillary Services Control Algorithms Using a 24-Hour, 48-Hour, and 168-Hour Prediction Time Horizon. 94

3.5: Annual Cumulative Distribution and Average Battery SOC for the Logic-Based, MPC Without Ancillary Services, and MPC With Ancillary Services Control Algorithms Using a 15 Min. Time Step and 168-Hour Prediction Time Horizon. 97

3.6: January Weekday Dispatch of Microgrid Using Logic-Based, MPC Without Ancillary Services, And MPC With Ancillary Services Control Algorithms. Green Shaded Region Indicates the On-Peak Time of the TOU Rate Structure. 101

3.7: July Weekday Dispatch of Microgrid Using Logic-Based, MPC Without Ancillary Services, and MPC With Ancillary Services Control Algorithms. Green Shaded Region Indicates the On-Peak Time of the TOU Rate Structure. 104

4.1: Survivability of a Generic Microgrid Containing Various Energy Assets. 121

4.2: Summary of On-Site Electrical Load. 131

4.3: Survivability of Microgrids with Various Values of the Resilience Weighting Factor Control Parameter. 137

4.4: Resilience Metrics of Control Parameters Sensitivity Analysis. 138

4.5: Sensitivity Analysis of On-Site Fuel Reserves on Performance Metrics for Generator-Only Microgrid (Top) And Hybrid Microgrid (Bottom). 140

4.6: Sensitivity Analysis of Critical Load Intensity on Performance Metrics for Generator-Only Microgrid (Top) and Hybrid Microgrid (Bottom). 142

Figure Page

4.7: Sensitivity Analysis of Solar PV Generation on Performance Metrics for Hybrid Microgrid. 143

4.8: Sensitivity Analysis of Battery Starting SOC on Performance Metrics for Hybrid Microgrid. 145

CHAPTER 1

INTRODUCTION

1.1. Motivation

Increasing demand for resilient and clean electric power is changing the way our societies produce, transmit, consume, and think about electricity. New technologies are supporting the paradigm shift of centralized generation to a more distributed approach, with expanding focus on distributed energy resources (DERs) such as solar photovoltaics (PV), energy storage, back-up conventional generation, and electric vehicles. Some approaches group energy assets into microgrids that consist of one or multiple DERs and loads that can be controlled as a single unit in parallel or islanded from the grid (ABB, n.d.). Microgrids are commonly deployed in applications that require more reliable electricity (e.g., hospitals, military bases, data centers, remote on-grid towns) or where it is too costly or infeasible to expand the main grid (e.g., cell towers, off-grid villages, mines, remote resorts) (Roberts, Chang, and Vox 2018). Ongoing research in microgrid controls is seeking ways to further increase reliability and resilience while also lowering the cost of operations.

Microgrid controller expenses currently account for a relatively low percentage of total microgrid costs, ranging from 2%-10% of the total project costs (Giraldez et al. 2018). However, controller expenses are expected to account for a larger portion of microgrid project costs as the expense for individual microgrid assets (e.g., solar PV, storage) continues to decrease (Load Management Leadership 2019). This suggests work is needed to decrease the cost of microgrid controllers to further improve project economics, and moreover, to increase the value of controls through reducing operating costs and enabling

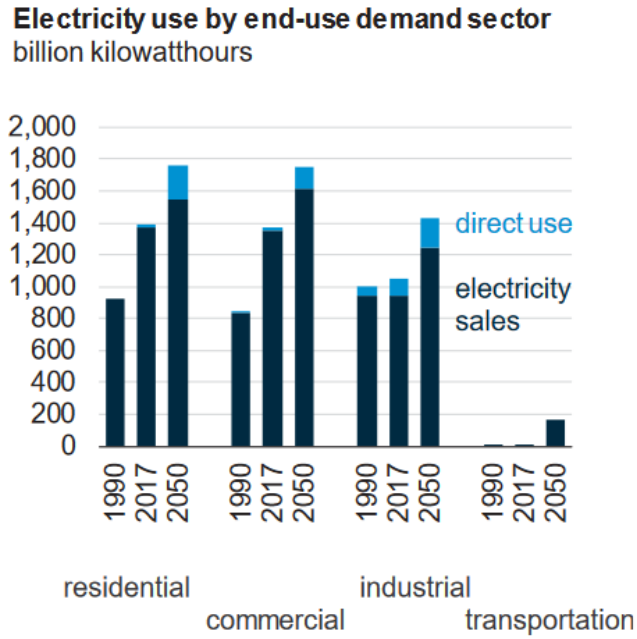
revenue generation. This additional financial value can be attained beyond the basic functionality to ensure stable operations in grid-connected and islanded mode (Zhou and Ho 2016)(Monesha, Kumar, and Rivera, n.d.). Microgrids and advanced controllers can also address technical challenges arising from high-penetration distributed generation that may otherwise lack integration and coordination with higher-level centralized generation and transmission scheduling (Hirsch, Parag, and Guerrero 2018), (Goyal and Ghosh 2016), (Raquel, n.d.).

1.2. Energy Industry Overview

The energy industry is undergoing unprecedented change. The percentage of the total electricity produced in the United States (U.S.) from solar and wind sources was 0% in 1980, 0.16% in 2000, and 7.62% in 2017 (Administration 2018). Over half of new generation sources in 2017 were renewable, with the majority coming from solar and wind (U.S. Energy Information Administration 2018b). Geothermal, hydro, and similar renewable generation sources are also growing in popularity but are expected to comprise a relatively small proportion of new generation capacity due to higher costs and restrictive project site requirements (Argonne et al. 2017). The increase in renewable generation is expected to continue with decreasing costs that rival natural gas (U.S. Energy Information Administration 2018a), economic incentives for renewables, growing societal concerns around climate change, and advances in storage technologies. Similar growth is occurring in energy storage. The University of Michigan estimates that the amount of U.S. energy storage projects increased by 174% from 2013 to 2018 (University of Michigan 2018). A major driver to this increase is rapidly falling costs of battery storage by 80% from 2010 to 2017 (Chediak 2017). The recent proliferation of renewable energy and energy storage

has provided energy producers and consumers with new options to source low-carbon power that is also reliable and low-cost.

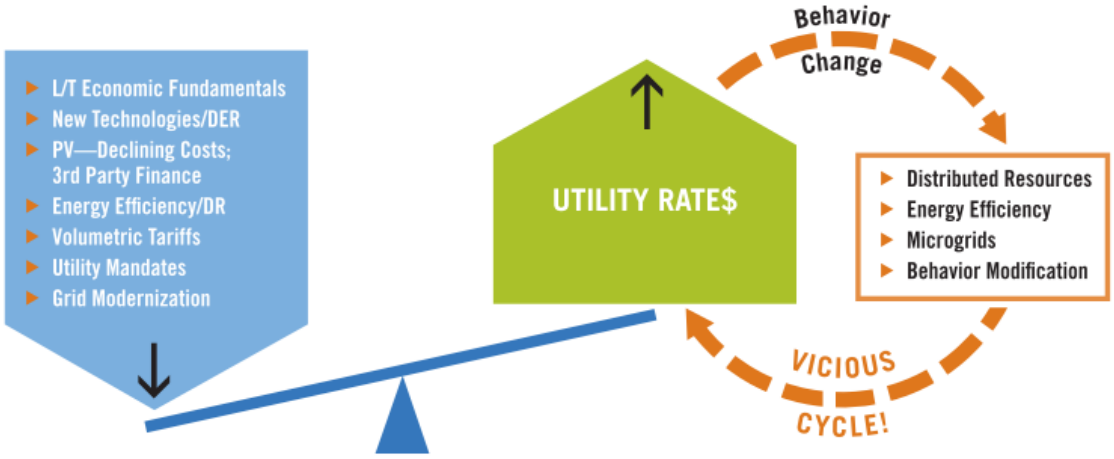
Changes are also occurring for energy consumers. In 2018, 38% of total energy consumption and 30% of the total electricity sales in the U.S. was from the residential and commercial sectors (U.S. Energy Information Administration, n.d.; EIA 2018). Fig. 1.1 shows how the overall electricity demand is projected to increase by 2050, and that residential and commercial sectors will still account for over half of nationwide demand. These sectors have potential to benefit from emerging technologies including DERs and microgrids. On-site DER and microgrid generation can supplement electricity purchases at either retail rates from utilities or wholesale rates if market access is allowed.



1.1: Historical, current, and forecasted electricity use in the U.S. (US Energy Information Administration 2017).

Electric utilities are increasingly seeing changes in the electric power industry and realizing that their business models will have to adapt. Fig. 1.2 shows how Peter Kind

describes these changes as a "Vicious Cycle" in which technology, policy, and market factors create a feedback loop that increases utility rates thereby causing disgruntled customers to look for other energy solutions (Ceres 2015). Recent publications have tried to envision how electric utilities will operate in the future to avoid such patterns, with some solutions posed such as revenue decoupling, equitable tariff design, localized energy management systems, and new market designs (Small and Frantzis 2010; Ceres 2015; PwC 2014).



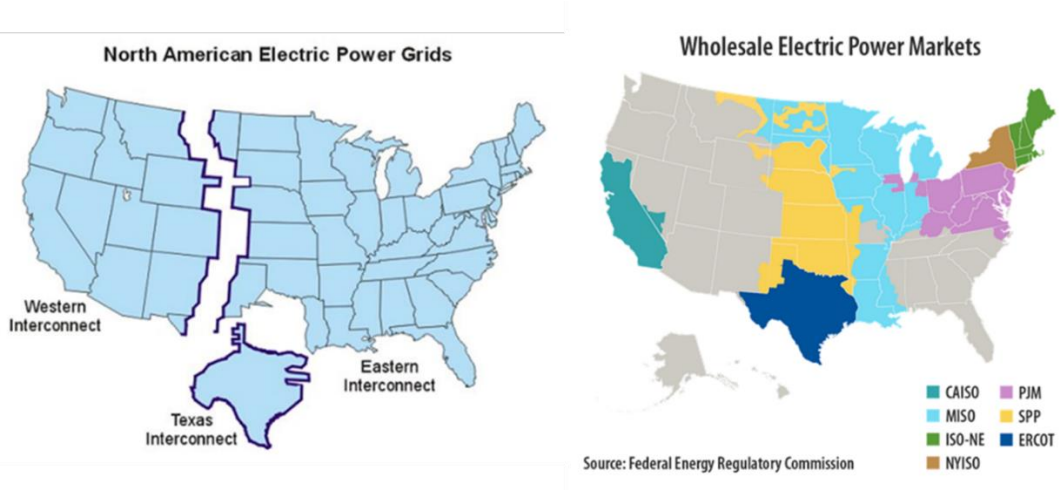
A confluence of factors are posing disruptive threats to the traditional utility business model.

1.2: The impact of disruptive technology, policy, and market forces that create a "Vicious Cycle" in the electric power industry (Ceres 2015).

1.2.1. Energy Markets

Energy markets are expected to change with the transforming energy industry. The Federal Energy Regulation Commission (FERC) is an independent agency within the U.S. Department of Energy that regulates interstate transmission of electricity and ensures consumers have access to reliable, efficient, and sustainable energy services at a reasonable cost (FERC, n.d.). To maintain independence as a congressional regulatory agency, no party within the U.S. government reviews decisions of FERC other than Federal courts

(Greenfield 2018). In 2005, FERC granted the North American Electric Reliability Corporation (NERC) the authority to regulate electrical markets according to specific reliability standards (U.S. Government Information 2005). NERC is a nonpartisan organization that has jurisdiction over the users, owners, and operators of the bulk power system and the responsibility to oversee and regulate electricity markets (NERC 2019a). Regional transmission organizations (RTOs) and independent system operators (ISOs) administer regional wholesale electricity markets and provide reliability planning for regions within the three interconnection areas of North America (Hoffman and Streit 2015). These markets were created to address the constant increase in electric prices and to encourage innovation through competition (PJM, n.d.). Fig. 1.3 shows the three interconnection areas and RTO/ISO regions within the continental United States. These markets coordinate both day-ahead and real-time purchases of electric energy, electric power capacity, and ancillary services. In general, the RTOs/ISOs take bids in ascending order and stop accepting bids when the needed power, capacity, or ancillary service is secured for a specified time interval (American Public Power Association 2018). All identified sellers within this time interval get compensated with the last bid price, also known as the clearing price. Recent studies have explored potential barriers to entry and system wide benefits of allowing distributed energy resources and microgrids to directly participate in these wholesale energy and ancillary service markets (Studies, Applications, and Benefits 2019), (Cochran et al. 2013).

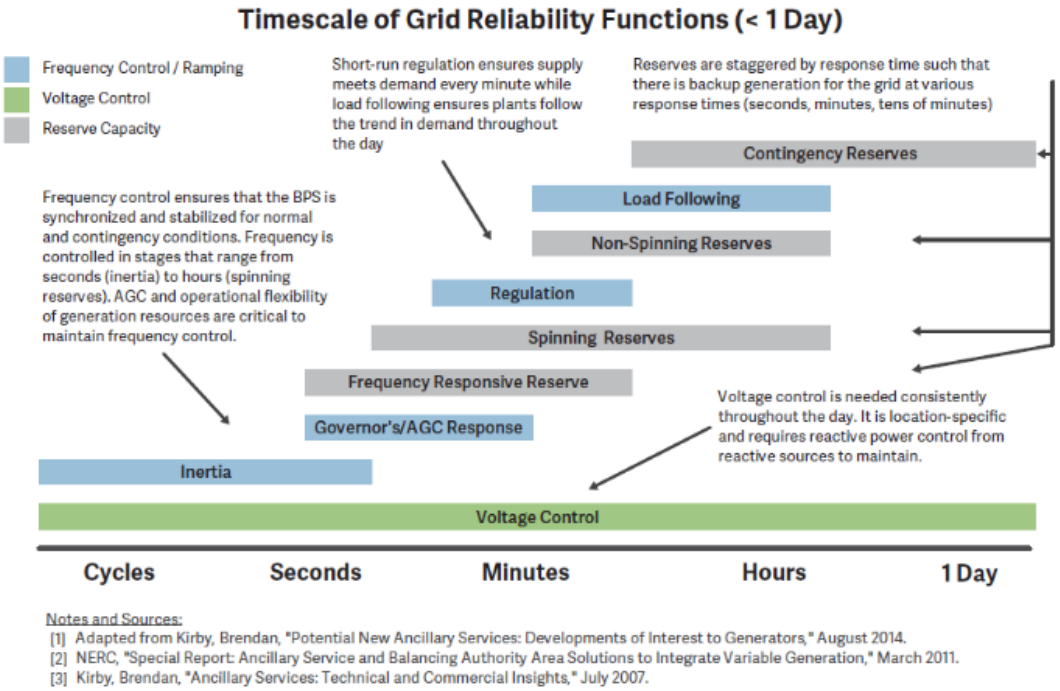


1.3: Three interconnection areas and the regional transmission organization/ independent system operator market and control areas in the United States (United States Environmental Protection Agency 2017).

Ancillary services describe asset-level capabilities that help ensure the reliability of the electrical grid (Reishus Consulting LLc 2017). These services ensure supply meets demand during normal operations to compensate for the uncertainty associated with imperfect load and renewable generation forecasts. Ancillary services also ensure enough generation capacity is reserved to replace a major failure within the network. These services can be automated or can be manually engaged by asset-level managers or electric grid operators. The nomenclature for each ancillary service varies between locations, balancing authority, and energy market, but in general there are four primary ancillary services arranged on a day-ahead, hour-ahead, or real-time basis (frequency regulation, spinning reserves, non-spinning reserves, and replacement reserves) and two secondary services that are arranged on a long-term basis (voltage support and black start) (CAISO, n.d.). Fig. 1.4 displays a generalized timescale of the different grid ancillary services that are needed to provide the flexibility to match variations in supply and demand, maintain frequency and voltage throughout the electrical grid, and can comprise as much as 25% of

the total bulk power costs (Hirst and Kirby 1996). Below are California Independent System Operator (CAISO) definitions of each of the ancillary services (CAISO, n.d.):

- **Frequency Regulation:** Generation that is on-line and synchronized with the grid frequency. Electricity generated can be increased or decreased instantaneously through automatic generation control (AGC). Regulation is used to maintain continuous balancing of resources and load within the ISO-controlled grid to maintain a stable grid frequency.
- **Spinning Reserves:** Generation that is on-line with capacity to ramp generation up or down within 10 minutes and remaining running for at least two hours.
- **Non-spinning Reserves:** Generation that is available but not on-line and is capable of being synchronized and ramped up within 10 minutes, and then capable of producing at that level of output for at least two hours.
- **Replacement Reserves:** Generation that is capable of starting if not already operating, synchronized with the ISO controlled grid, and ramped up within one hour and remain running for at least two hours.
- **Voltage Support:** Services provided by generating units or other equipment such as shunt capacitors, static var compensators, or synchronous condensers that are required to maintain grid voltage in a local area. This service is required for normal operation and system emergency conditions.
- **Black Start:** The procedure by which a generating unit starts without an external source of electricity. Typically occurs to restore power to the ISO Balancing Authority Area following system wide or local area blackouts.



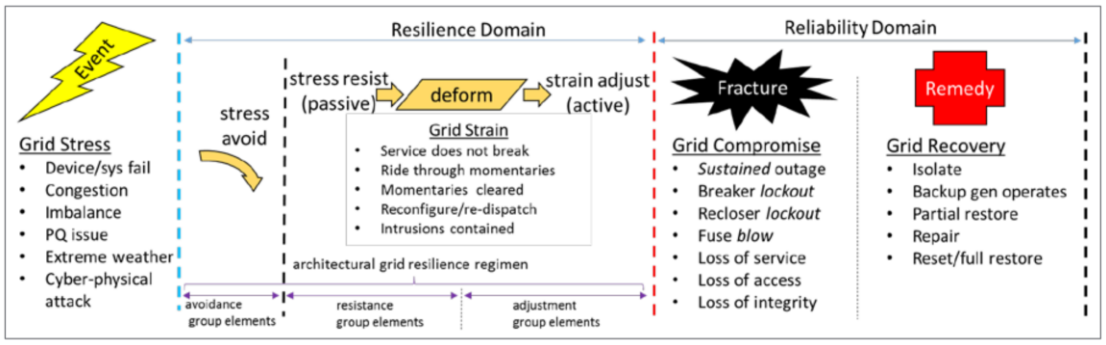
1.4: Generalized timescale of the grid ancillary services needed to maintain a reliable electric grid (Hibbard et al. 2017).

1.2.2. Reliability and Resilience

NERC defines grid reliability as "… the degree to which the performance of the elements of [the electrical] system results in power being delivered to consumers within accepted standards and in the amount desired." (Hirst and Kirby 2000). Historically, the reliability of electrical systems has been modeled and enhanced using contingency analyses (Müller et al. 2013), (Jamei et al., n.d.), (Miller 2008), (Momoh 2012). This type of analysis simulates failures to generation and transmission infrastructure to determine the impact on system capacity, stability, and the ability to meet load. The location and capacity of reserve generation is calculated to ensure balance of supply and demand, stabilize power, and eliminate possible congestion issues during these failures. Similar analyses have been conducted on microgrids and groups of microgrids to demonstrate their operation during islanding contingencies (Aghdam, Salehi, and Ghaemi 2018), (Goyal and Ghosh 2016),

(Mashayekh et al. 2017). Metrics for reliability are well-established and include the system average interruption duration index (SAIDI), system average interruption frequency index (SAIFI), and customer average interruption duration index (CAIDI) (Eto and Lacommare 2008). These metrics represent the duration and frequency of system interruptions and can indicate how reliable a system is (i.e. how often and how long do customers lose power) but do not directly indicate the resilience of a system. Reliability and resilience are separate concepts, and further, resilience does not have a standard definition, parameters, or metrics even though it has recently received significant attention (The Gridwise Alliance 2013), (Electric Power Research Institute 2016), (Ji et al. 2016), (Lammers 2017).

The definition of resilience used in this work is "… the ability to withstand grid stress events without suffering operational compromise or to adapt to the strain so as to minimize compromise via graceful degradation." (Taft 2017b). Grid stresses include, but are not limited to, congestion, imbalances, extreme weather, cyber-attacks, and device or system failure (Widergren et al. 2018). The result of these stresses can cause power quality issues, equipment failure, outages, and the loss of property, life, or finances. Fig. 1.5 compares consequences of grid stresses if the gird is reliable verses resilient. If a system is only reliable and a major stress occurs there is typically a high probability that the system will fracture or break causing a loss of service. However, if a system is resilient and the same stress occurs the system can adapt and still provide service without the need for external support.



1.5: Comparison of grid resilience and reliability (Widergren et al. 2018).

1.3. Distributed Energy Systems

The recent paradigm shift of implementing distributed generation instead of centralized generation within the energy industry has increased the prevalence of distributed energy solutions. The following subsections describe common distributed energy solutions.

1.3.1. DERs

Major advancements in power electronics and storage technologies have reduced the cost and improved the operational behavior of solar PV modules, inverters, generators, electric batteries, and controllable loads. The spot price for a solar PV module in the U.S. dropped by approximately 80% from 2010 (1.80 $/Watt) to 2017 (0.35 $/Watt) while the average module power and efficiency has steadily increased (Fu et al. 2017). The price of PV inverters and storage inverters are expected to have similar cost reductions in the upcoming years of 10%-12% per year and 12%-15% per year, respectively (Moskowitz 2017). Newer inverters are being manufactured with advanced functionality that includes active power control, active power ramping, reactive power control and compensation, soft start, and unintentional-islanding protection (National Renewable Energy Laboratory 2014). These advanced controls help smooth-out short-term variability in renewables, with

energy storage being added to smooth-out long-term variability. This allows operators to dispatch renewables similarly to traditional forms of generation by storing excess renewable generation and dispatching it when the renewable supply does not meet demand (Coppez, Chowdhury, and ... 2010). Fig. 1.6 shows how the price of lithium-ion batteries has decreased since 2010, giving more opportunities for storage to have an economic return on investment in energy applications such as microgrids (Chediak 2017). However, relying on battery storage and renewable energy to meet 80% of the U.S. energy demand would require a battery system that costs approximately $2.5 trillion (Temple 2018). Traditional forms of generation (e.g. fossil fuels generators) are needed to ensure reliability and reduce operating cost while phasing in renewables and storage. Microgrids can ease the transition to a low carbon electricity generation by using small thermal-based generators to supplement renewable generation and batteries. These distributed generations are becoming more fuel efficient and better at sharing load across multiple generation sources through variable speed drives and advanced control methods (Hadi, Hariyanto, and Choi 2016; Majumder et al. 2010).

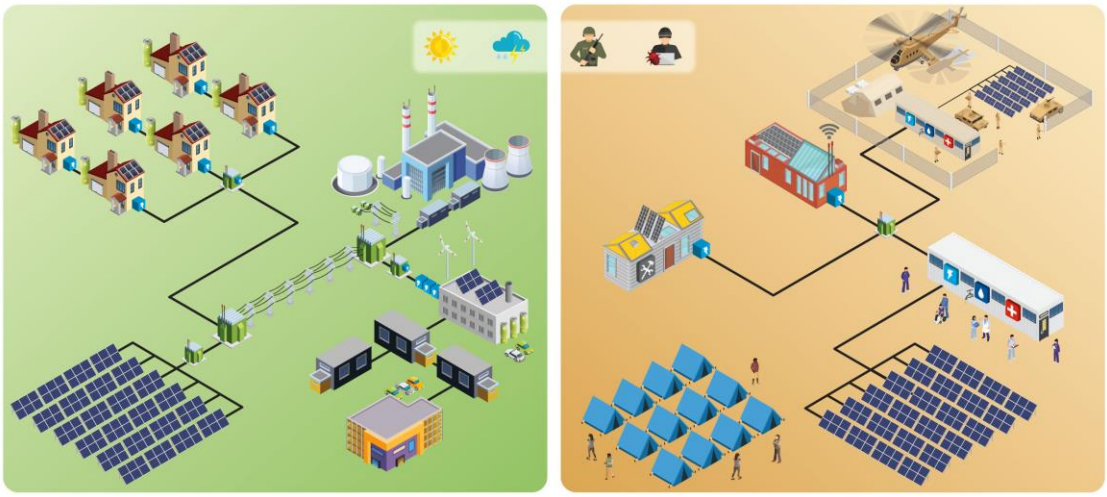


1.6: The volume weighted average manufacturing cost of Lithium-ion batteries from 2010 to 2017 (Chediak 2017).

1.3.2. Microgrids

The distributed nature of renewables and DERs has increased interest in microgrids and potential benefits that can be realized by controlling multiple DERs within a single controllable region. The Department of Energy (DOE) defines a microgrid as "a group of interconnected loads and distributed energy resources within clearly defined electrical boundaries that acts as a single controllable entity with respect to the grid. A microgrid can connect and disconnect from the grid to enable it to operate in both grid-connected or island-mode.'' (Ton and Smith 2012). It is important to note that this definition does not define a specific generation capacity. Stated differently, a microgrid can range from Watts to Megawatts as long as it has the operational capability to isolate and reconnect back to the grid with minimal to no loss load. Fig. 1.7 shows microgrid configurations for civilian and defense applications. Civilian applications typically consist of residential, commercial, and industrial loads paired with renewable generation and storage to reduce energy expenditures. Defense applications typically consist of commercial and industrial loads

paired with renewable generation, storage, and back-up generators to reduce cost and ensure a reliable energy supply in the event of a grid outage.



1.7: Examples of a civilian microgrid (left) and a defense microgrid (right).

The first microgrid was constructed in 1882 when the first centralized power plant, the Manhattan Pearl Street Station, was built to provide power to 80+ customers in 1882 (Applications et al. 2009). Economies of scale motivated the consolidation of microgrids into large electrical grids with multiple control regions and stakeholders during the 20th century. Recently, worldwide interest in microgrids has been growing due to the expanding demand for accessible, safe, reliable, affordable, and sustainable energy sources. Navigant Research projects that the worldwide microgrid market will become a $30.9 billion industry by 2027 with 4,475 new microgrid projects deployed in 2019 (Navigant Research 2018) (Navigant Research 2019). Successful microgrid projects involve a variety of stakeholders. These stakeholders include:

- **Client/Customer** – Owner of project. Can be one or multiple parties.
- **Electric utility** – Oversees the interconnection with electrical grid. Can also be the microgrid owner or co-owner.

- **Developer/Integrator** – Delivers engineering, construction, and procurement (EPC) services for designing, installing, and commissioning.
- **Technology vendor** – Supply subsystems and energy assets.
- **Financer** – Provides capital and contractual underwriting.
- **Regulator** – Provides policy incentives and regulatory requirements.
- **Operator** – Ensures safe and reliable operations after commissioning.
- **Technician** – Performs routine maintenance and repair of equipment.

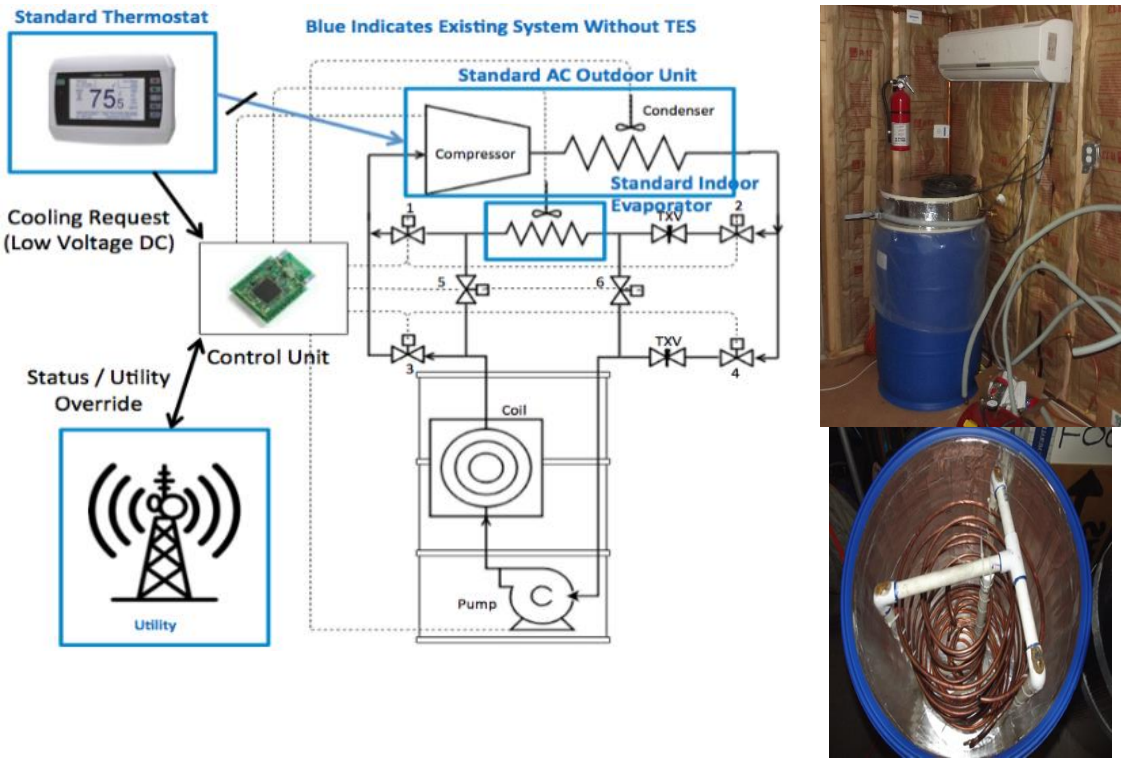
Collaboration between each stakeholder is necessary to ensure all parties requirements are met and that a microgrid project can be delivered on time and on budget. Project risk grows if any of these stakeholders are neglected during the lifetime of the project.

1.3.3. Thermal Systems

Over 40% of residential energy use and nearly 30% of commercial energy use in the U.S. is for heating ventilation and cooling (HVAC) (US Department of Energy 2008). In warmer climates, peak cooling times (i.e. afternoon) require more expensive electricity generation that often leads to higher utility tariffs. These market mechanisms economically incentivize building owners to reduce or shift their cooling loads. This can result in unideal temperature ranges that research has shown to negatively affect occupant comfort and performance (Brager 2013). This provides an opportunity for thermal solutions that can shift or reduce thermal loads while maintaining comfortable indoor air temperatures. Fig. 1.8 shows one such solution, a thermal energy storage (TES) system, that can store hot or cold thermal energy during times of low electricity rates and dispatch this energy during times of higher electricity rates to reduce peak demands. Precooling is another solution that

building managers and owners are using to reduce cooling costs. Precooling shifts a portion of electricity used for cooling during high electricity rate periods by cooling a space by passive (e.g. opening windows during the night) or active (e.g. operating the cooling system) means during times of low electricity rates.

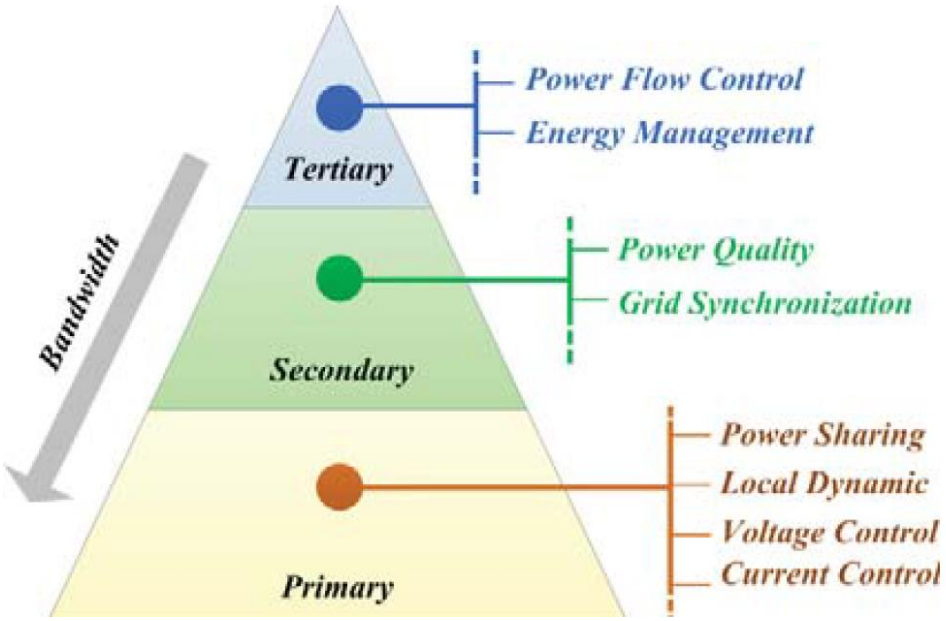
Research of precooling strategies for commercial and residential applications has shown wide applicability to multiple climatic zones (J. E. Braun and Lee 2006; K.-H. Lee and Braun 2008; K. Lee and Braun 2008b, 2008a; German et al. 2014; Arababadi and Parrish 2015; Herter and Okuneva 2014) with simulation results showing economic benefits (Keeney and Braun 1997; J. E. Braun and Lee 2006; K.-H. Lee and Braun 2008; K. Lee and Braun 2008b, 2008a; Springer and Group 2007; Turner, Walker, and Roux 2015) and peak load reduction (Keeney and Braun 1997; J. E. Braun and Lee 2006; K.-H. Lee and Braun 2008; K. Lee and Braun 2008b, 2008a; Springer and Group 2007; Turner, Walker, and Roux 2015). Research has also shown similar economic and operational benefits are possible using TES systems (Musgrove, Ehmke, and Stocks 1989; Arcuri, Spataru, and Barrett 2017; Bell 1998). Recent studies have shown that further economic and operational benefits can be achieved by combining precooling and TES systems for commercial applications (Kintner-Meyer and Emery 1995; Henze and Krarti 1999; Krarti, Henze, and Bell 1999; Hajiah and Krarti 2012a, 2012b). However, further research is needed to understand the effects of combined cooling strategies (precooling and TES) in the residential sector.



1.8: Prototype of a residential TES, heat pump, and cooling coil configuration.

1.4. Controls

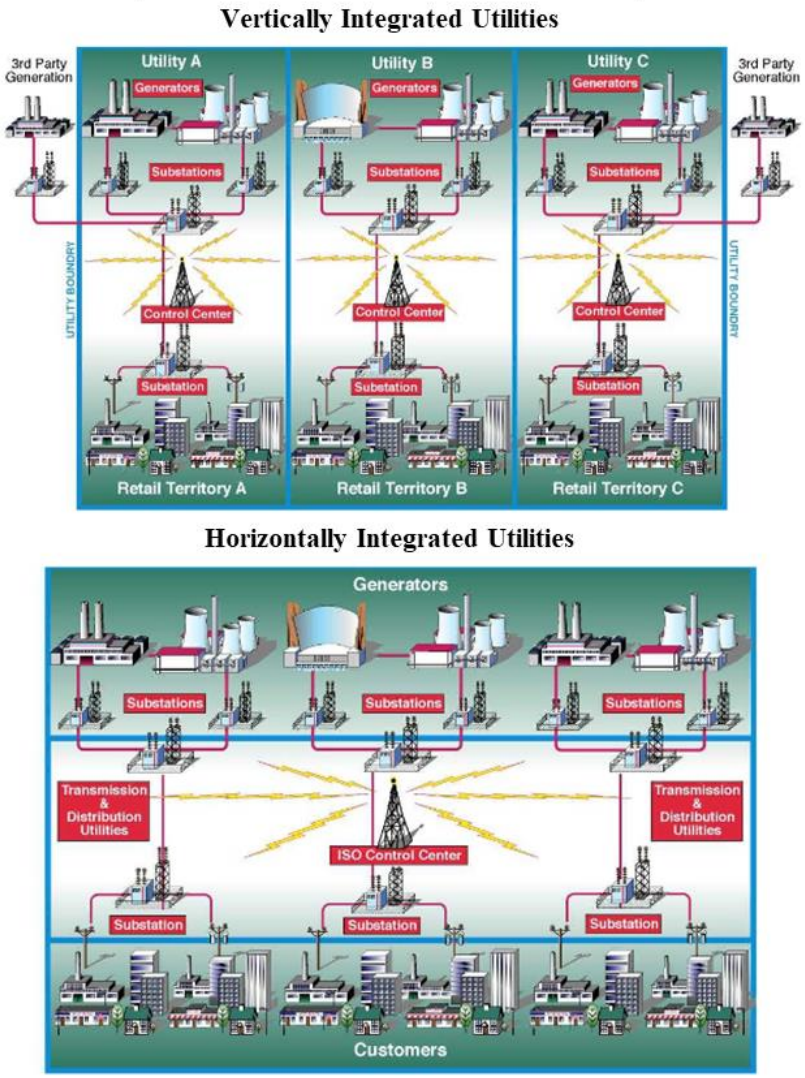
Electrical systems traditionally use hierarchical control architectures that consist of three levels of controls that operate at different time scales to ensure that supply meets demand and power quality standards are met. Fig. 1.9 depicts the primary, secondary, and tertiary levels of controls and the prominent control functions executed in each domain. Primary control is responsible for regulating grid frequency through immediate and autonomous generator control (Undrill 2018). Secondary control balances and initially dispatches reserves for disturbances using higher level generation controls and manual actions taken by dispatchers (NERC Resources Subcommittee 2011). Tertiary control is responsible for full deployment and restoration of reserves to handle current and future contingencies (NERC Resources Subcommittee 2011).



1.9: Hierarchical control structure of electrical power and energy systems (Meng et al. 2016).

1.4.1. Grid Controls

The electrical power and energy industry is comprised of vertically integrated utilities that own and control generation facilities, transmission networks, and local distribution networks (Taft 2017a), and horizontally organized utilities that participate in generation, transmission, and retail markets. Fig. 1.10 shows the different organizational structures and market boundaries that they typically participate in. Vertically integrated utilities typically use traditional controls (hierarchical) with less reliance on energy markets than horizontally organized utilities because vertically integrated utilities own generation (Taft 2017a).

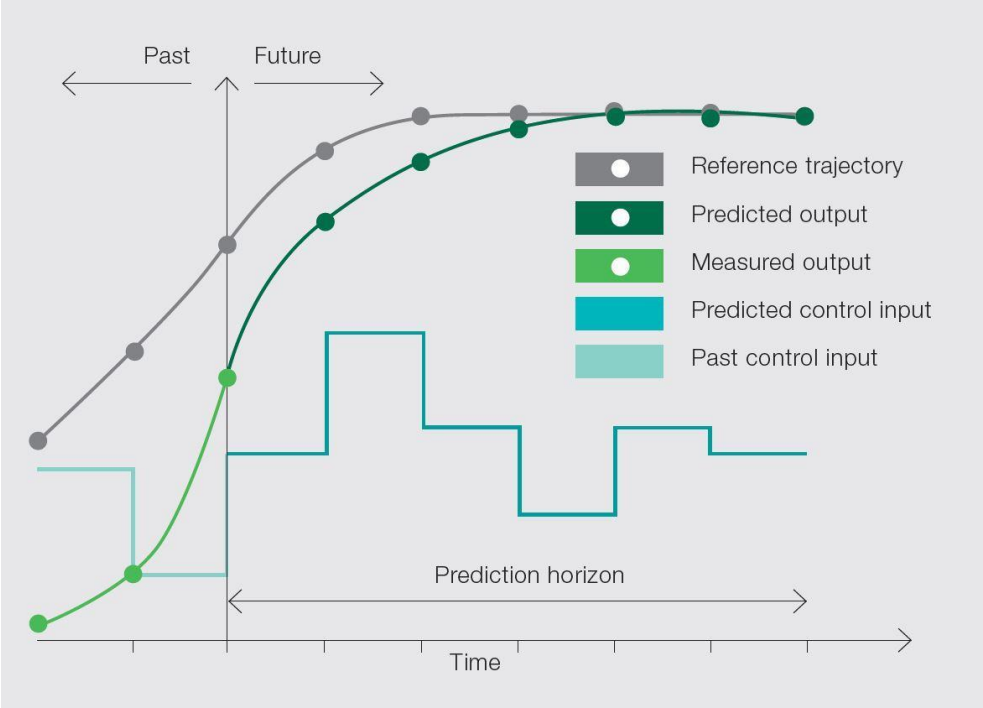


1.10: Organizational structures and market boundaries of vertical integrated and horizontally integrated utilities (Pacific Northwest National Laboratory 2002).

1.4.2. Microgrid Controls

Hierarchical control has been implemented in microgrids to coordinate and control assets internal to the microgrid and sometimes in conjunction with the connected utility or ISO (Khongkhachat and Khomfoi 2015). Common classifications of microgrid controls include centralized, decentralized, and distributed controls (Sen and Kumar 2018). Each classification can be used for a variety of control functions similar to those of the main grid

such as droop control, voltage and frequency control, active and reactive power sharing, energy management, and market participation (Sen and Kumar 2018). These control methodologies use closed loop controls, open loop controls, logic-based controls, optimization, or a combination of these methodologies to accomplish the control tasks. Optimization techniques can range from metaheuristic optimization methods to linear and non-linear programing algorithms (Fathima and Palanisamy 2015). Recent research in energy management and market participation has focused on employing model predictive control (MPC) or receding horizon optimization approaches to dispatch energy assets while considering the uncertainty of renewable generation and loads. Fig. 1.11 shows a representation of an MPC approach in which the system behavior is modeled over a specified prediction horizon and control inputs are used to achieve desired performance. For cost-optimal operations of microgrids, MPC algorithms typically use real-time information along with historical data to predict future environmental conditions, pricing signals, and energy asset status over a specified horizon. The algorithm uses this information as inputs for an optimization formulation that calculates the optimal dispatch of energy assets over the time horizon and executes dispatch choices in the first time step. With each time step, new forecasts are calculated and used to execute the optimal energy asset dispatch for the next time step.



1.11: Generalized representation of a model predictive controls approach (ABB 2019). The behavior of the system is modeled over a specified prediction horizon and control inputs are used to achieve desired performance.

Current research has shown that MPC techniques can enhance economic and technical metrics for electrical power and energy systems (Fathima and Palanisamy 2015; Gruber et al. 2015; Pereira, Munoz De La Pena, and Limon 2016; Parisio, Rikos, Glielmo, et al. 2014; J. Xu, Zou, and Niu 2014; X. Zhang et al. 2017; Prodan and Zio 2014; Ghanbarian et al. 2017) and for HVAC systems and building thermal comfort (Castilla et al. 2014; Acosta et al. 2016; Schirrer et al. 2016; Hazyuk, Ghiaus, and Penhouet 2012; Prívara et al. 2011; Afram and Janabi-Sharifi 2014; West, Ward, and Wall 2014; X. Chen, Wang, and Srebric 2015). MPC techniques in microgrids have also been developed to provide reactive power support services (Gandhi et al. 2018; Ratnam and Weller 2018). Others have investigated optimal bidding strategies and participation in ancillary service

marketplaces (Gomes and Saraiva 2010; Shi, Luo, and Tu 2014; Jianxiao Wang et al. 2017; Majzoobi and Khodaei 2017).

Multiple U.S. patents are related to controls for microgrids. A small sample of relevant patents include: Hybrid robust predictive optimization method of power system dispatch (Patent Number 7991512), Microgrid energy management system and method for controlling operation of a microgrid (Patent Number 9733623), and Energy management system in a power and distribution system (Patent Number 7085660). However, no current patents detail the control functionality needed for microgrids to participate in real-time energy markets or ensuring resilience for islanding events. A provisions patent has been filed based on the control algorithms discussed in Chapter 3 of this work (Serial Number 62/853,966) and an invention disclosure/ provision patent is currently being developed for the controls and modeling discussed in Chapter 4 of this work.

1.5. Standards

Multiple regulatory entities have introduced standards to guide the deployment and operation of DER and microgrid technologies in energy marketplaces. Examples include IEEE 1547, IEEE 2030, FERC order 841, and ANSI C84.1.

- **IEEE Standard for Interconnection and Interoperability of Distributed Energy Resources with Associated Electric Power Systems Interfaces (IEEE 1547):** Details the technical specifications and testing of interconnection and interoperability between the utility electric power system and DERs. This standard helps ensure safe and reliable operations of DERs and provides guidance on the advanced operational behavior that distributed generation assets can provide to the grid (e.g. voltage support).

- **IEEE Guide for Smart Grid Interoperability of Energy Technology and Information Technology Operation with the Electric Power System (EPS), End-Use Applications, and Loads (IEEE 2030):** Provides best practices for achieving smart grid interoperability. This standard details networking and communication needed for DERs to successfully integrate with the utilities and RTOs/ISOs.
- **IEEE Standard for the Specification of Microgrid Controllers (IEEE 2030.7) and IEEE Standard for the Testing of Microgrid Controllers (IEEE 2030.8):** Details the operational functions, testing procedures, and minimum requirements associated with the proper operation of microgrid controllers. These standards help guide the development and testing of microgrid controllers that can help improve the adoption of DERs and microgrids with the central grid.
- **FERC order 841 (Item no. E-1):** Allows for the participation of electric storage resources in the capacity, energy, and ancillary services markets operated by Regional Transmission Organizations and Independent System Operators. This order enables value stacking of batteries to provide benefits to both customers/owners and utilities/regulatory organizations.
- **American National Standard for Electric Power Systems and Equipment – Voltage Ratings (60 Hertz) (ANSI C84.1):** Establishes nominal voltage ratings and operating tolerances for 60 hertz electric power systems above 100 volts. This standard and similar standards ensure that newly integrated DERs and microgrids can maintain a reliable grid.

These standards and orders have potential to improve the economics of DERs and microgrids by enabling the advanced operation and control of DERs and microgrids to participate in energy marketplaces and coordinate with the larger electric power system.

1.6. Dissertation Organization

The dissertation is organized into five chapters:

- **Chapter 1: Introduction –** Provides an introduction to the energy industry, distributed energy resources, microgrids, grid controls, wholesale markets, ancillary services, and microgrid controls. A brief description of the work completed in Chapters 2 through 4 are also presented.
- **Chapter 2: Residential Cooling Using Separated and Coupled Precooling and Thermal Energy Storage Strategies** – This journal article evaluates economic and operational benefits of several air-cooling strategies for residential applications. Precooling and thermal energy storage cooling strategies are simulated separately and in combination for a typical single-family home in Phoenix, AZ, Los Angeles, CA, and Kona, HI. Analyses examine optimal precooling parameters, intraday operations, and annual performance to compare cooling strategies with respect to environmental conditions, utility rate structures, and payback periods. This article was published in *Applied Energy* in October 2019.
- **Chapter 3: Model Predictive Control of Microgrids for Real-time Ancillary Service Market Participation** – This journal article develops advanced microgrid control algorithms with results demonstrated for retail and wholesale markets. Economic and operational benefits are shown for a case study involving a commercial-scale microgrid. Logic-based, model predictive control, and model

predictive control with ancillary services algorithms are used to dispatch assets within a hybrid microgrid to achieve least cost operation. Annual performance and intraday operational details are examined to understand the value of advanced controllers and how they adjust dispatch to participate in real-time energy markets. This article will be submitted in November 2019.

- **Chapter 4: Statistical Modeling of Microgrid Resiliency During Islanding Operations** – This journal article develops and examines a resilience modeling framework with control algorithms for operating a microgrid during an islanding event. A Markov chain model expresses the survivability of the microgrid over a 168-hour islanding event and an optimal control algorithm is developed to simulate microgrid dispatch during islanding operations. Sensitivity analyses and performance evaluations compare the resilience of a generator-only microgrid and a hybrid microgrid with diesel generators, energy storage, and solar photovoltaics (PV). This article will be submitted in November 2019.
- **Chapter 5: Discussion** – Results from Chapters 2 through 4 are comprehensively discussed. Benefits of advanced control algorithms for hybrid microgrids with various operational goals are described and future research opportunities are defined.

CHAPTER 2

RESIDENTIAL COOLING USING SEPARATED AND COUPLED PRECOOLING AND THERMAL ENERGY STORAGE STRATEGIES

Authored by James R. Nelson, Nathan G. Johnson, Prudhvi Tej Chinimilli, & Wenlong Zhang

Published in *Applied Energy* Vol. 252 October 2019

https://doi.org/10.1016/j.apenergy.2019.113414

Abstract

Increased residential cooling loads often correlate with peak electricity demand in warm and temperate climates. Solutions such as precooling and thermal energy storage (TES) being separately shown to shift energy use to off-peak times and reduce electricity expenses for commercial and residential applications. This study advances prior research to jointly implement and optimize precooling and TES strategies, and further develops a precooling strategy that dynamically adjusts precooling set points with respect to outdoor temperatures. Six strategies for residential cooling are evaluated and compared on metrics including system sizing, intraday dispatch, electricity use, energy expenditures, and investment rate of return. Case study data include a simulated one-year period for the cities of Phoenix, Los Angeles, and Kona in the United States. After accounting for capital cost, operating cost savings, and discount factors, a smart thermostat with the proposed dynamic precooling technique is found to have the best return on investment with payback rates between 0.2-6.2 years across all locations and rate structures. However, if technology costs lower or electricity rates change, it could be beneficial to use a combined approach with TES and precooling that gives the greatest reduction in daily on-peak demand and energy

use at 75.6% and 78.5%, respectively. These individual and combined strategies provide value to ratepayers and electric utilities by reducing energy expenditures and shifting cooling loads to reduce system-wide peak demand.

2.1. Introduction

Residential buildings account for 21.4% of total annual energy use in the United States (EIA 2016) with space heating and space cooling comprising 41% of that (Berardi 2015). In areas with a warmer climate, intraday electricity peaks for building cooling normally coincide with peak electricity system demand (Energy Information Administration 2017). Utilities have sought to reduce system peak by installing advanced metering infrastructure (AMI) in over 43% of homes in the United States (Cappers et al. 2016) and implementing time-of-use (TOU) rate structures to incentivize customers to shift loads to other parts of the day (Zhao, Yang, and Lee 2017). Further reductions in peak load can be obtained using automated demand response technologies that turn off certain loads during periods of the day with higher electricity prices (McKane 2010). Solar photovoltaics (PV) paired with battery storage have also been used to reduce system peak demand (i.e., peak shave) (Janko, Arnold, and Johnson 2016), (Luerssen et al. 2019). A similar option is charging a thermal energy storage (TES) system during off-peak periods and discharging the TES during on-peak periods (Musgrove, Ehmke, and Stocks 1989). Another thermal-based load shifting method includes precooling a building before the onset of on-peak TOU rates to reduce the use of chillers during on-peak times (Caves and Christensen 1980). Either cooling strategy can benefit the customer and electric utility by reducing on-peak energy demand and hence energy expenditures, yet minimal analytical inquiry has been

completed for combinations of both precooling and TES for shifting residential cooling loads.

Studies of precooling strategies for peak load reduction have primarily focused on commercial buildings (Rismanchi et al. 2012), (Xue and Shengwei 2012), (P. Xu 2006), (Y. Xu et al. 2013) using simulations to demonstrate economic benefits (Yau and Rismanchi 2012), (Keeney and Braun 1997), (J. E. Braun and Lee 2006), (K.-H. Lee and Braun 2008), (K. Lee and Braun 2008b), (K. Lee and Braun 2008a). Keeney and Braun demonstrated cost savings averaging 10% per month for the peak cooling season (Keeney and Braun 1997), while work by Xu et al. demonstrated reductions in cooling energy use by 25-50% during peak hours (P. Xu 2006). Braun and Lee expanded on these works using a case study involving a small commercial building that showed additional cost savings could be achieved using multiple zone temperatures optimized for different intraday needs (J. E. Braun and Lee 2006), (K.-H. Lee and Braun 2008), (K. Lee and Braun 2008b), (K. Lee and Braun 2008a).

Research of precooling strategies for residential buildings has become more common given increases in AMI, TOU rate structures, and smart thermostats. Results show wide applicability to multiple climatic zones (German et al. 2014), (Arababadi and Parrish 2015), (Herter and Okuneva 2014) with demonstrated reductions in energy cost (Springer and Group 2007; Turner, Walker, and Roux 2015) by dynamically updating thermostat set points based on user occupancy and comfort preferences. Booten and Tabares-Velasco validated a residential EnergyPlus building model that uses precooling strategies by comparing energy usage to empirical data collected from an actual home in Sacramento, California (Booten and Tabares-Velasco 2012). Braun and Chaturvedi developed inverse

models from EnergyPlus results to predict cooling load demand and test advanced precooling controls through simulations (J. E. Braun and Chaturvedi 2002). Fu Xiao and Wang showed a 26% reduction power of demand for a residence in Hong Kong using optimization algorithms with a combination of temperature set-point resets and precooling strategies (Hu, Xiao, and Wang 2019). These studies can be expanded to increase economic benefit by dynamically updating thermostat set points with respect to outdoor air temperature to precool more, or less, based on expected cooling demand.

Similar reductions in electricity expenditures can be achieved using TES systems (Musgrove, Ehmke, and Stocks 1989), (Arcuri, Spataru, and Barrett 2017), (Bell 1998), (Kintner-Meyer and Emery 1995), (Farah, Liu, and Saman 2019), (Luo et al. 2017), (Ruan et al. 2016), (Tang and Wang 2019). TES systems can be passive or active. Passive TES systems typically rely on the building's thermal mass or utilize phase change materials to regulate indoor air temperature (Johra and Heiselberg 2017), (Wijesuriya, Brandt, and Tabares-Velasco 2018) and active TES systems are coupled to an air conditioner or chiller for charging and later discharging to cool a building (Navarro et al. 2016). Passive and active TES systems use storage media with energy stored in sensible heat, latent heat, or a combination of the two (Lizana et al. 2017). Storage medias may include solid materials (e.g., rock, concrete), water or organic material (e.g., paraffin), and inorganic materials (e.g., salts) (Hasnain S.M. 1998). Of these, ice and chilled water are common for active systems because they are inexpensive, have high specific heats and latent heats that are preferable for energy storage, and have long term stability across many cycles (Arcuri, Spataru, and Barrett 2017), (Oró et al. 2012).

Recent studies have suggested that additional economic benefits can be obtained by co-optimizing air conditioning controls with active TES systems (Henze and Krarti 1999; Krarti, Henze, and Bell 1999; Bell 1998) or passive TES systems (J. E. Braun, Montgomery, and Chaturvedi 2001), (T. Y. Chen 2001), (Klaassen, House, and Center 2002). Kintner-Meyer and Emery demonstrated the value of combining cold storage and building thermal mass to achieve up to a 35% reduction in energy use during peak periods while reducing daily energy expenditures by 6-18% for a benchmark 33,600 m^2 office building simulated for locations including the island of Hawai'i, Phoenix, San Diego, and Seattle (Kintner-Meyer and Emery 1995). Work by Hajiah and Krarti used building thermal capacitance and ice storage to reduce on-peak cooling loads with simulated results validated in an HVAC laboratory (Hajiah and Krarti 2012a). An additional study by the same authors identified further economic benefits by optimizing system sizing through parametric analysis of the chiller and ice storage tank capacity (Hajiah and Krarti 2012b). These research methods for commercial-scale buildings have not been completed for residential buildings with different building designs and specifications, occupancy patterns, load profiles, and cooling technologies. Further, differences in building envelopes, rate structures, and technology cost-performance curves indicate that findings from prior industrial and commercial applications may not perfectly map to residential applications and used to infer findings for that unexplored space in the literature.

This study develops six cooling strategies and completes a side-by-side techno-economic comparison of electricity use and costs for a benchmark residential building simulated with Building America B10 Benchmark specifications. HVAC components are sized and controlled to reduce energy costs for different environmental conditions and

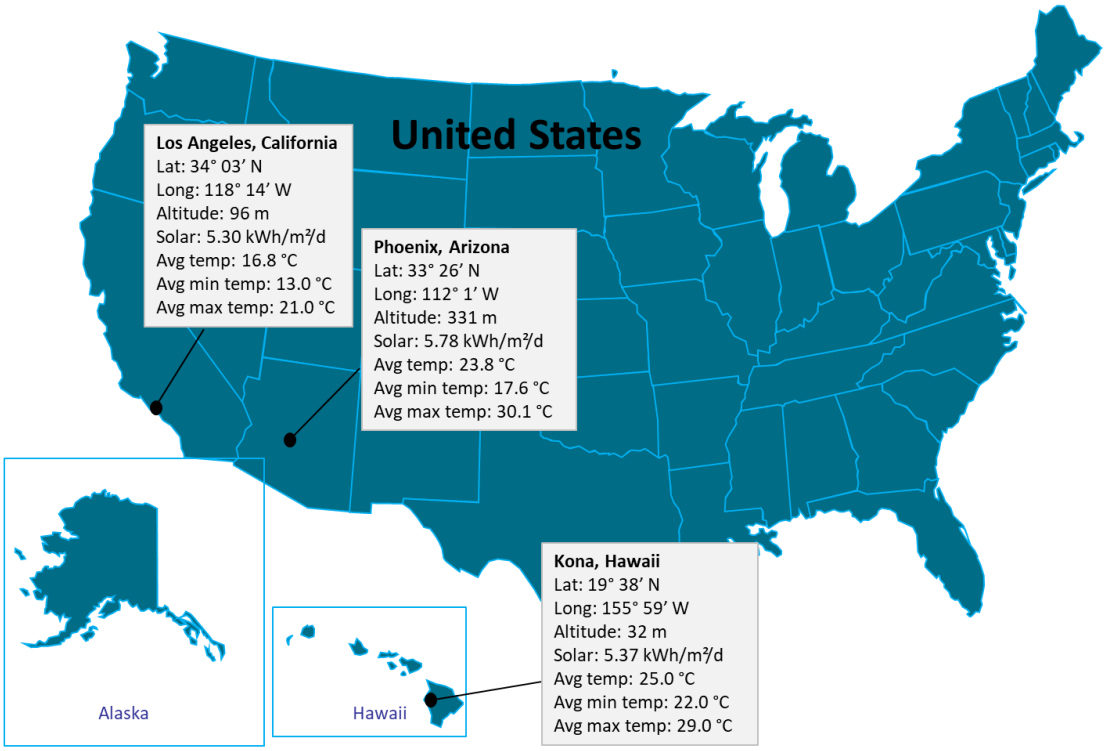
TOU rate structures in three cities in the United States. Performance evaluation and sensitivity analyses provide the following contributions to literature:

- Development of two optimized residential precooling strategies that dynamically update set points based on outdoor air temperature.
- Technical development and optimal sizing of a coupled precooling and TES system for a benchmark residential home.
- Energetic and financial comparison of six cooling strategies including precooling, TES, and combined techniques across three locations with different environmental conditions and TOU electric rate structures.
- A comparison of findings between residential and commercial applications indicate the relative performance of precooling, TES, and combined techniques does not hold between use cases with different building envelopes, rate structures, and technology cost-performance curves.

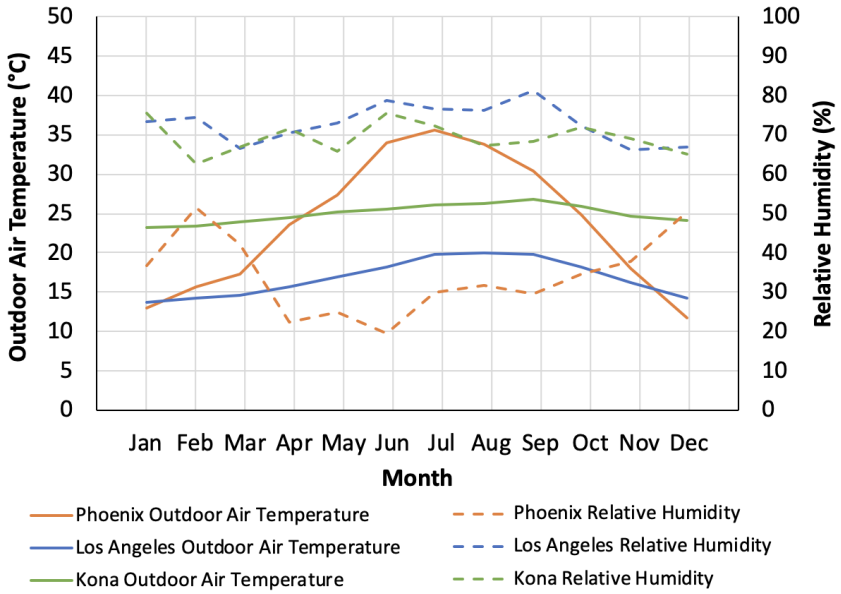
2.2. Location Data

2.2.1. Environmental Data

Three case study locations were selected in the United States including Phoenix and Los Angeles as Hot-Dry climates, and Kona as a Hot-Humid climate (Pacific Northwest National Laboratory 2010). Local hourly environmental conditions were taken from the nearest international airport with typical meteorological year (TMY3) weather data (Wilcox and Marion 2008). Fig. 2.1 shows the location of each city with average annual environmental statistics and Fig. 2.2 displays the average monthly outdoor air temperature and relative humidity in each city.



2.1: Average annual environmental characteristics for each location.



2.2: Average monthly temperature and relative humidity for each location.

2.2.2. Electric Rate Structures

Tables 2.1-2.3 summarize the electric rate structures for each location with prices that vary by season and time of day. The Hawai'i Electric Light (HELCO) rate structure for Kona maintains the same on-peak hours and price for every day of the year. For Phoenix, the Salt River Project (SRP) rate structure has three seasonal rates including winter, summer, and summer peak with different on-peak and off-peak TOU periods for winter and summer months. The Los Angeles Department of Water and Power (LADWP) rate structure includes four seasons and off-peak, low-peak, and high-peak TOU periods. For the LADWP rate structure, the high-peak rate is considered on-peak for June to September, while from October to May both the low-peak rate and high-peak rates are considered on-peak given they are equivalent. Each utility includes additional taxes and fees, as shown in Tables 1-3, with SRP and LADWP including fees in the base energy charge and HELCO itemizing fees.

Table 2.1: Charges for the SRP Time-of-Use Rate Structure (E-26) in Phoenix, Arizona.

Charge Description	TOU Period	Value
Energy Price Off-Peak (Nov-Apr) (Project 2015)	Weekdays: 9pm-5am, 9am-5pm; Weekends: All day	7.11 Cents/kWh
Energy Price On-Peak (Nov-Apr) (Project 2015)	Weekdays: 5am-9am, 5pm-9pm	10.20 Cents/kWh
Energy Price Off-Peak (May-June, Sept-Oct) (Project 2015)	Weekdays: 8pm-1pm; Weekends: All day	7.38 Cents/kWh
Energy Price On-Peak (May-June, Sept-Oct) (Project 2015)	Weekdays: 1pm-8pm	19.57 Cents/kWh
Energy Price Off-Peak (July-Aug) (Project 2015)	Weekdays: 8pm-1pm; Weekends: All day	7.41 Cents/kWh
Energy Price On-Peak (July-Aug) (Project 2015)	Weekdays: 1pm-8pm	22.26 Cents/kWh
Service Charge (Project 2015)	-	20 $/month
City Tax (Phoenix) (Salt River Project n.d.)	-	2.9%
County and State Tax (Salt River Project n.d.)	-	6.3%

Table 2.2: Charges for the LADWP Time-of-Use Rate Structure (R-1B, Power Rate Ordinance No. 18413) in Los Angeles, California.

Utility Charge Description	TOU Period	Value
Energy Price Off-Peak (Jan-Mar) (Los Angeles Department of Water and Power 2016)	Weekdays: 8pm-10am; Weekends: All day	14.872 Cents/kWh
Energy Price Low-Peak (Jan-Mar) (Los Angeles Department of Water and Power 2016)	Weekdays: 10am-1pm, 5pm-8pm	18.401 Cents/kWh
Energy Price High-Peak (Jan-Mar) (Los Angeles Department of Water and Power 2016)	Weekdays: 1pm-5pm	18.401 Cents/kWh
Energy Price Off-Peak (Apr-May) (Los Angeles Department of Water and Power 2016)	Weekdays: 8pm-10am; Weekends: All day	15.092 Cents/kWh
Energy Price Low-Peak (Apr-May) (Los Angeles Department of Water and Power 2016)	Weekdays: 10am-1pm, 5pm-8pm	18.621 Cents/kWh
Energy Price High-Peak (Apr-May) (Los Angeles Department of Water and Power 2016)	Weekdays: 1pm-5pm	18.621 Cents/kWh
Energy Price Off-Peak (June) (Los Angeles Department of Water and Power 2016)	Weekdays: 8pm-10am; Weekends: All day	15.092 Cents/kWh
Energy Price Low-Peak (June) (Los Angeles Department of Water and Power 2016)	Weekdays: 10am-1pm, 5pm-8pm	18.621 Cents/kWh
Energy Price High-Peak (June) (Los Angeles Department of Water and Power 2016)	Weekdays: 1pm-5pm	24.198 Cents/kWh
Energy Price Off-Peak (July-Sept) (Los Angeles Department of Water and Power 2016)	Weekdays: 8pm-10am; Weekends: All day	14.788 Cents/kWh
Energy Price Low-Peak (July-Sept) (Los Angeles Department of Water and Power 2016)	Weekdays: 10am-1pm, 5pm-8pm	18.816 Cents/kWh
Energy Price High-Peak (July-Sept) (Los Angeles Department of Water and Power 2016)	Weekdays: 1pm-5pm	25.601 Cents/kWh
Energy Price Off-Peak (Oct-Dec) (Los Angeles Department of Water and Power 2016)	Weekdays: 8pm-10am; Weekends: All day	15.278 Cents/kWh
Energy Price Low-Peak (Oct-Dec) (Los Angeles Department of Water and Power 2016)	Weekdays: 10am-1pm, 5pm-8pm	19.306 Cents/kWh
Energy Price High-Peak (Oct-Dec) (Los Angeles Department of Water and Power 2016)	Weekdays: 1pm-5pm	19.306 Cents/kWh
Service Charge (Jan-June) (Los Angeles Department of Water and Power 2016)	-	12.85 $/month
Service Charge (July-Dec) (Los Angeles Department of Water and Power 2016)	-	21.20 $/month
City Tax (R. Lee n.d.)	-	10%

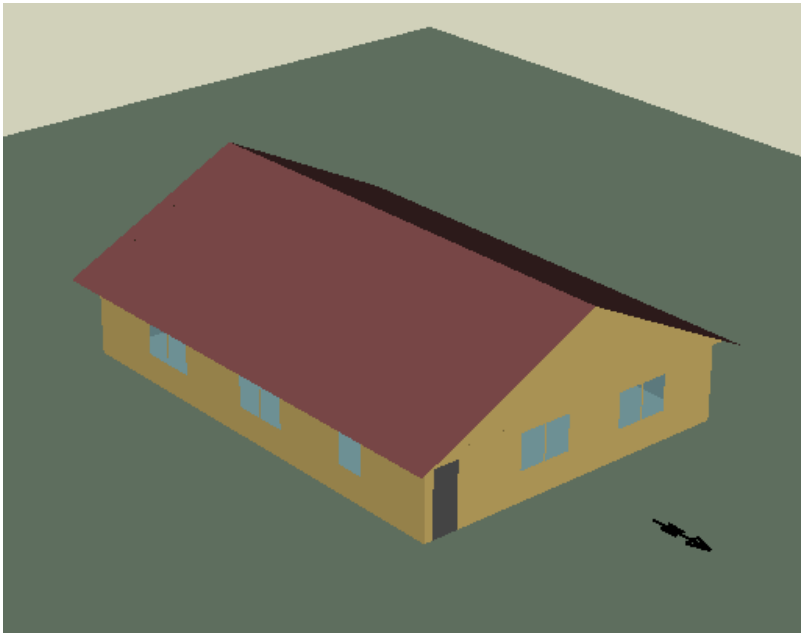
Table 2.3: Charges for the HELCO Time-Of-Use Rate Structure (Revised Sheet No. 71) in Kona, Hawai'i.

Charge Description	TOU Period	Value
Energy Price Off-Peak (Hawaii Electric Light 2016)	Daily: 8pm-3pm	23.4506 Cents/kWh
Energy Price On-Peak (Hawaii Electric Light 2016)	Daily: 3pm-8pm	44.4506 Cents/kWh
Usage Charge (under 300 kWh) (Hawaii Electric Light 2016)	-	0 Cents/kWh
Usage Charge (300-1000 kWh) (Hawaii Electric Light 2016)	-	3.3518 Cents/kWh
Usage Charge (over 1000 kWh) (Hawaii Electric Light 2016)	-	4.4510 Cents/kWh
Public Benefits Fund Surcharge (Hawaii Electric Light 2017a)	-	4.2440 Cents/kWh
Purchase Power Adjustment Clause (Hawaii Electric Light 2017c)	-	2.2291 Cents/kWh
Revenue Balancing Account Provision (Hawaii Electric Light 2017d)	-	0 Cents/kWh
Service Charge (Hawaii Electric Light 2016)	-	11.50 $/month
Green Infrastructure Fee (Hawaii Electric Light 2017b)	-	1.34 $/month
Tax	-	0%

2.3. Building Energy Model

EnergyPlus (U.S. Department of Energy 2017) was used to model a benchmark single-family home and simulate hourly energy use according to local environmental forcings in each city. EnergyPlus is the Department of Energy's (DOE's) open-source whole-building energy modeling engine that has been extensively tested and validated in (Berkeley, Renewable, and Ridge, n.d.), (Henninger and Witte, n.d.), (Henninger et al. 2003), (Witte, Henninger, and Crawley 2004), (Henninger and Witte, n.d.), (Im 2016). Home specifications were taken from the Building America B10 Benchmark specifications, which are consistent with the 2009 International Energy Conservation Code and commonly used as a baseline to track progress toward multiyear energy savings goals (Wilson et al. 2014). The building envelope was constructed in BEopt with advanced simulation parameters completed in EnergyPlus (National Renewable Energy Laboratory 2016). Median home sizes for Phoenix and Los Angles were identified to be 200.4 m^2 (2157 ft^2) and 167.2 m^2 (1800 ft^2), respectively (Muresan 2016), while the median home size for the

Island of Hawai'i was found to be 128.3 m^2 (1381 ft^2) (Ohama 2017). The average of these sizes yielded a home of 165.3 m^2 (1780 ft^2) that was adjusted to 167.2 m^2 (1800 ft^2) to maintain a rectangular shape with dimensions 11 m by 15.2 m (36 ft by 50 ft). Fig. 2.3 visualizes the building envelope for the single-story home comprised of three bedrooms and two bathrooms. This building was used in each city to permit direct comparison. A separate carport or unattached garage was not modeled. Table 2.4 details major building characteristics and associated parameter values. Lighting loads, appliance and plug loads, and people density were taken to be 1571.46 kWh/yr, 8998.17 kWh/yr, and 63.3 m^2/person, respectively, per the Building America B10 Benchmark specifications for a three bedroom dwelling with 167.2 m^2 footprint (Wilson et al. 2014).



2.3: Building envelope for the Building America B10 Benchmark home.

Table 2.4: Building characteristics and parameter values for the Building America B10 Benchmark home (Wilson et al. 2014).

Building Characteristic	Parameter Values
Walls	R-13 fiberglass batt, 2×4, 40.6 cm o.c.
Attic	Ceiling #-30 cellulose, GR-1, Vented
Roof	Asphalt shingles, Medium
Windows	0.15 WWR, Low-E, Double, Non-metal, Air, L-Gain
Floor	Uninsulated slab-on-grade
Infiltration	7 ACH50
Thermal Mass	80% carpet, 1.27 cm drywall all walls and ceilings
Wall Height	2.4 m

2.3.1. HVAC System Sizing

Table 2.5 summarizes major characteristics of the HVAC system using the Building America B10 Benchmark specifications (Wilson et al. 2014). The standard gas furnace and air conditioning combination was replaced with a heat pump given the latter are more common in the selected climates with limited to no heating needs (Energy 2017), (U.S. Department of Energy, n.d.).

Table 2.5: Major characteristics of HVAC system for the Building America B10 Benchmark home (Wilson et al. 2014).

Component	Description
Supply Fan	On/off control, Blow through placement, Maximum flow rate – 635 m^3/min
Ductwork	R-8, Leakage – 15%
Heating Coil	Single speed direct expansion capacity – 15.7 kW
Supplemental Heating Coil	Electric coil capacity – 5.3 kW
Cooling Coil	Single speed direct expansion capacity – location dependent, Nominal sensible heat ratio – 0.72, Nominal coefficient of performance – 4.07

A sizing study identified the minimum heat pump size needed to provide cooling in each location without any unmet cooling in the simulated year. Table 2.6 shows results with minimum sizes of 10.55 kW (3 tons) for Phoenix, 3.52 kW (1 ton) for Los Angeles, and 5.28 kW (1.5 tons) for Kona. In Los Angeles and Kona, cooling electricity use decreased with increasing heat pump capacity because the unit could operate for a shorter

duration of the year while still meeting the required cooling requirements. Conversely in Phoenix, annual electricity use increased from the 0.5 ton unit to the 1.0 ton unit because the smaller unit operated frequently at maximum load and was unable to meet cooling requirements that could be served by a larger unit. Units above 1.0 ton permitted faster cooling and a reduction in operating hours that reduced total annual electricity use in Phoenix.

Table 2.6: Baseline sizing analysis of heat pump cooling capacity.

Cooling Capacity (kW/ton)	Annual Electricity Use (MWh/yr)			Annual Electric Bill ($/yr)			Annual Cooling Hours Not Met (hrs/yr)		
	PHX	LA	KONA	PHX	LA	KONA	PHX	LA	KONA
1.76/0.5	14.67	7.89	18.77	1745.37	1555.81	7221.78	4771.67	41.83	6673.00
3.52/1.0	15.32	7.30	16.29	1842.86	1442.87	6457.38	3419.83	0	20.50
5.28/1.5	15.11	7.24	14.34	1867.95	1431.26	5671.87	1436.00	0	0
7.03/2.0	14.38	7.18	13.70	1836.37	1421.17	5417.83	256.83	0	0
8.79/2.5	13.75	7.12	13.40	1777.86	1409.76	5314.17	0.17	0	0
10.55/3.0	13.29	7.08	13.11	1715.97	1401.00	5218.69	0	0	0
12.31/3.5	12.96	7.05	12.79	1671.38	1395.14	5112.55	0	0	0
14.07/4.0	12.73	7.01	12.46	1643.76	1388.97	4996.92	0	0	0

Note: PHX, LA, and KONA are abbreviations for Phoenix, Los Angeles, and Kona, respectively.

2.4. Cooling Strategies

Six cooling strategies were developed and simulated with resulting intraday dispatch behaviors and annual performance compared.

2.4.1. Baseline Cooling Strategy

The baseline cooling strategy uses a constant thermostat set point of 24.4 °C according to the Building America B10 Benchmark specifications (Wilson et al. 2014).

Cooling load increases as outdoor air temperature rises to maintain a maximum interior temperature of 24.4 °C.

2.4.2. Precooling Strategies

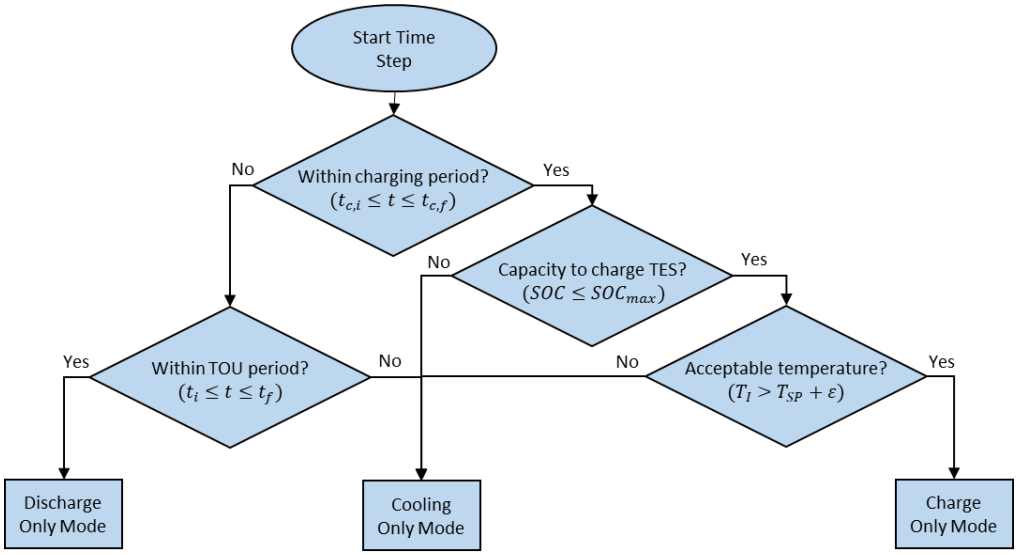
The precooling strategy adjusts the precooling thermostat set point, T_{SP}, using an adjustable scaling parameter, δ, multiplied by the difference between the outdoor air temperature, T_O, and the baseline temperature, T_B. Precooling occurs if the outdoor air temperature is hotter than the baseline temperature. A set back variable, σ, was used to evaluate the effect of increasing the on-peak thermostat set point to further reduce energy use during that period of day. Eq. 1 shows precooling strategy control logic where t is the current time, $t_{p,i}$ is the start time of the precooling period, and t_i and t_f are the starting and ending times of on-peak TOU electricity pricing, respectively. Two precooling strategies were formulated: one without set back (denoted as Precooling No Set Back), and one with set back (denoted as Precooling Set Back). Sensitivities are performed with respect to the precooling duration, scaling parameter, and location to identify optimal set points.

$$T_{SP} = \begin{cases} T_B & t < t_{p,i} \\ T_B - \delta(T_O - T_B) & t_{p,i} \le t < t_i \text{ and } T_O \ge T_B \\ T_B & t_{p,i} \le t < t_i \text{ and } T_O < T_B \\ T_B + \sigma & t_i \le t < t_f \\ T_B & t \ge t_f \end{cases} \quad \text{(Eq. 1)}$$

2.4.3. TES Strategy

A single-speed direct expansion cooling coil was paired with a TES system in EnergyPlus called *Coil:Cooling:DX:SingleSpeed:ThermalStorage*. The TES was right-sized to meet 100% of energy requirements if the heat pump was operated at full capacity for all on-peak hours to yield sizes of 73.85 kWh for Phoenix, 14.08 kWh for Los Angeles,

and 26.40 kWh for Kona. Specifications were taken for the Lennox KCA060S4 cooling coil with performance data related to operational characteristics (e.g., cooling capacity, energy input ratio, and part load fraction) and indoor and outdoor conditions (e.g., evaporator entering wet-bulb temperature, dry-bulb temperature for the condenser, evaporator air flow rate, and part load ratio of the cooling capacity of the evaporator) (Units 2017). Similar small-scale TES systems have been marketed for residential and small commercial applications, such as Ice Bear technology at 28-140 kWh capacity (Ice Energy 2018a), (Ice Energy 2018b). Manufacturer data and relationships in EnergyPlus were used to generate the sensible heat ratio, charging curve, and discharging curve for the different sized cooling units in each city. Charging and discharging performance of the TES unit was assumed independent of state of charge (SOC) between 5% and 95% to match findings of high performance TES systems described in (Mammoli and Robinson 2018). Fig. 2.4 shows a flow chart of the control strategy for cooling, charging, and discharging modes where $t_{c,i}$ is the start of the charging time, $t_{c,f}$ is the end of the charging time, SOC is the state of charge of the TES, SOC_{max} is the maximum state of charge of the TES, ε is the allowable range that the indoor air temperature can increase while in charging mode, and T_I is the measured indoor air temperature at time t. This control logic adequately charged the TES while maintaining the indoor air temperature within the specified range of the ANSI/ASHRAR Standard 55-2013 by allowing an increase up to 2 °C above the baseline set point (ANSI/ASHRAE 2013). The ability of the heat pump to simultaneously cool and charge the TES was not evaluated due to insufficient data from the manufacturer.



2.4: Operating mode logic for direct expansion cooling coil and TES system.

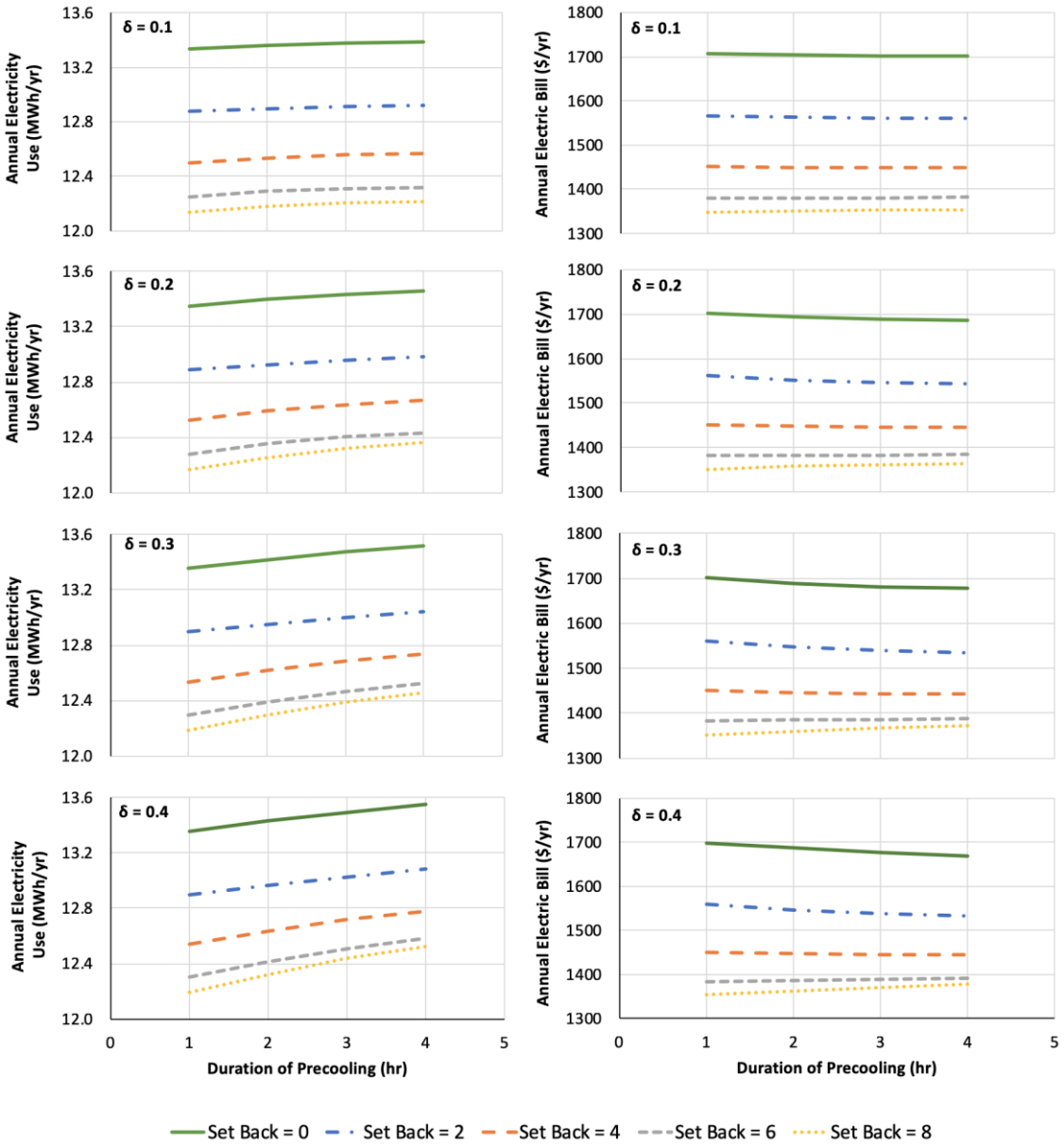
2.4.4. Combined Strategies

Two strategies were evaluated that combined both precooling and TES. One combined strategy employed the optimal precooling set back temperature (denoted as Combined Set Back), whereas the second combined strategy did not use a set back temperature (denoted as Combined No Set Back). The duration and time of day for charging the TES was kept similar between the TES-only strategy and both combined strategies to enable direct comparison. TES charging began at midnight and ended four hours before the on-peak hours to ensure the TES did not attempt to charge while the building was being precooled.

2.5. Optimal Precooling Set Points

Optimal precooling strategies were identified by evaluating the effect of the scaling parameter, precooling duration, and set back value on the annual electricity use and annual electricity bill. Results in Fig. 2.5 for Phoenix show a positive relationship between precooling duration and annual electricity use, and a negative correlation with annual

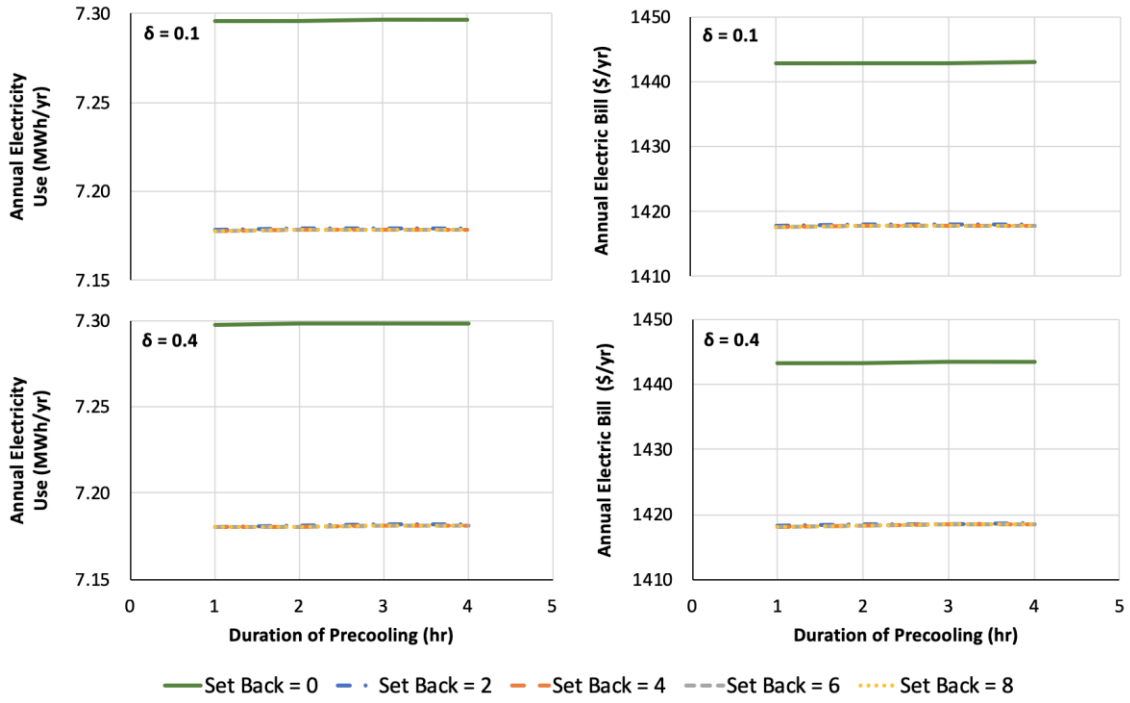
electricity expenditures that indicates financial savings with longer precooling durations. This trend holds for all four values of the scaling parameter and all set back temperatures up to 6 °C, at which point annual electricity costs level off or increase for higher set back temperatures and trend upwards for higher values of the scaling parameter. This occurs because the indoor air temperature does not always drift up to the specified set back temperature during on-peak hours. Therefore, as precooling duration increases, annual electricity use and expenditures increase because cooling is applied unnecessarily and creates a larger temperature difference between indoor and outdoor temperature that increases energetic losses through the building envelope.



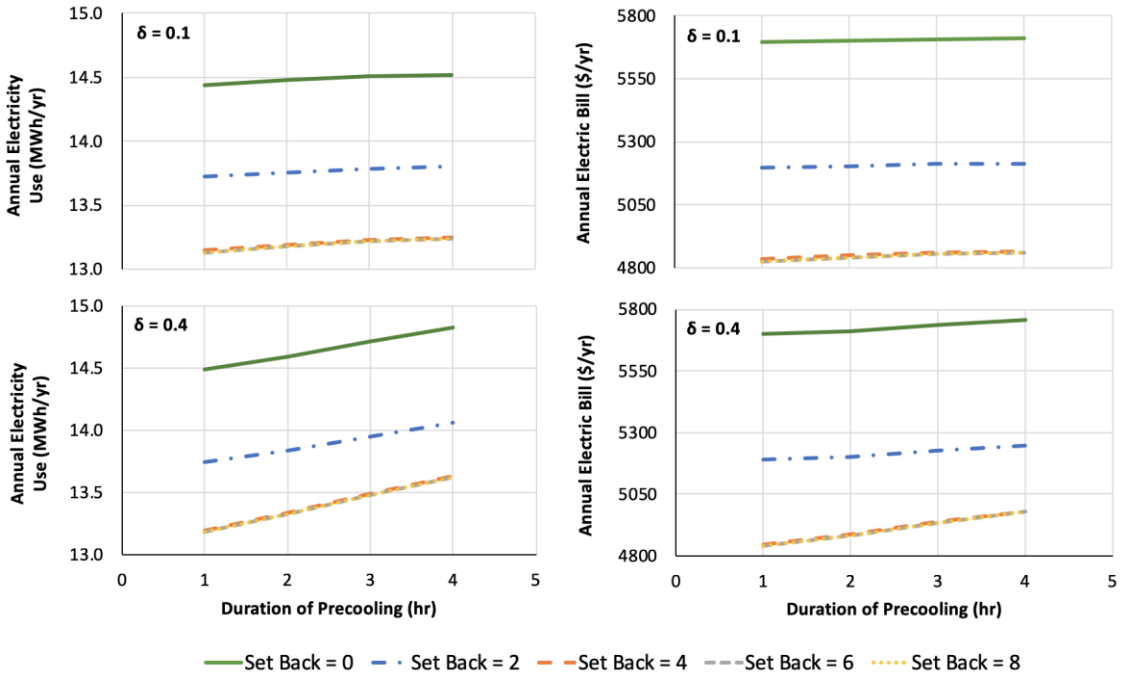
2.5: Optimal set point analysis of precooling strategies for Phoenix.

Similar graphical summaries are provided in Figs. 2.6 and 2.7 for Los Angeles and Kona, respectively. Trends are shown only for scaling parameter values of 0.1 and 0.4 because the same relationships exist for all scaling parameters with slight increases observed in electricity use and expenses as the scaling parameter and precooling duration increases. This is a result of the heat pump operating at a higher capacity to meet the lower

thermostat set point during the precooling duration over the course of the year. Increasing the set back temperature beyond 2 °C for Los Angeles and 4 °C for Kona had a negligible effect on annual electricity use and expenditures due to the indoor temperature rarely drifting up to the set back thermostat temperature during the on-peak time of day.



2.6: Optimal set point analysis of precooling strategies for Los Angeles.



2.7: Optimal set point analysis of precooling strategies for Kona.

Table 2.7 summarizes optimal precooling parameters and the resulting energetic and financial details for comparison. For Phoenix, the optimal precooling duration and scaling parameter is one hour and 0.1 when using a set back temperature, and four hours and 0.4 when a constant indoor temperature is maintained during on-peak times. This results in energetic and financial savings of 21.4% and 8.7% when employing a set back and a 2.7% decrease and 2.0% increase when maintaining a constant thermostat temperature during on-peak times, respectively. If just examining the hotter summer months, findings show that longer precooling durations and more significant dynamic precooling set points (larger scaling parameter) are more economical when no set back is employed but can result in increases in annual electricity use. Results for Los Angeles show minimal energetic and financial savings due to the outdoor air temperature remaining close to the thermostat temperature for the duration of on-peak periods. Findings for Kona indicate 8.4% and 14.9% energetic and financial savings, respectively, for a precooling

strategy with the maximum set back value. This is in contrast to a precooling strategy without set back that uses 0.7% more electricity and results in a 0.4% increase in annual electricity expenditures over the baseline strategy. Results from Figs. 2.5-2.7 and Table 2.7 indicate a precooling strategy with set back can provide energetic and economic benefits for all three climates whereas a precooling strategy with no set back provides economic benefit for hotter climates like Phoenix.

Table 2.7: Optimal precooling parameter for each location for strategies with and without a set back temperature.

Precooling Parameter	Baseline			Precooling Set Back			Precooling No Set Back		
	PHX	LA	KONA	PHX	LA	KONA	PHX	LA	KONA
Duration (hr)	0	0	0	1	1	1	4	1	1
Scaling (-)	0	0	0	0.1	0.1	0.1	0.4	0.1	0.1
Set back Temperature (°C)	0	0	0	8	6	8	0	0	0
Annual Electricity Use (MWh/yr) and (Change (%))	13.29 (-)	7.30 (-)	14.34 (-)	12.13 (-8.7)	7.18 (-1.6)	13.13 (-8.4)	13.55 (+2.0)	7.30 (0.0)	14.44 (+0.7)
Annual Electric Bill ($/yr) and (Change (%))	1715.97 (-)	1442.87 (-)	5671.87 (-)	1348.67 (-21.4)	1417.78 (-1.7)	4824.21 (-14.9)	1670.01 (-2.7)	1442.84 (0.0)	5695.37 (+0.4)

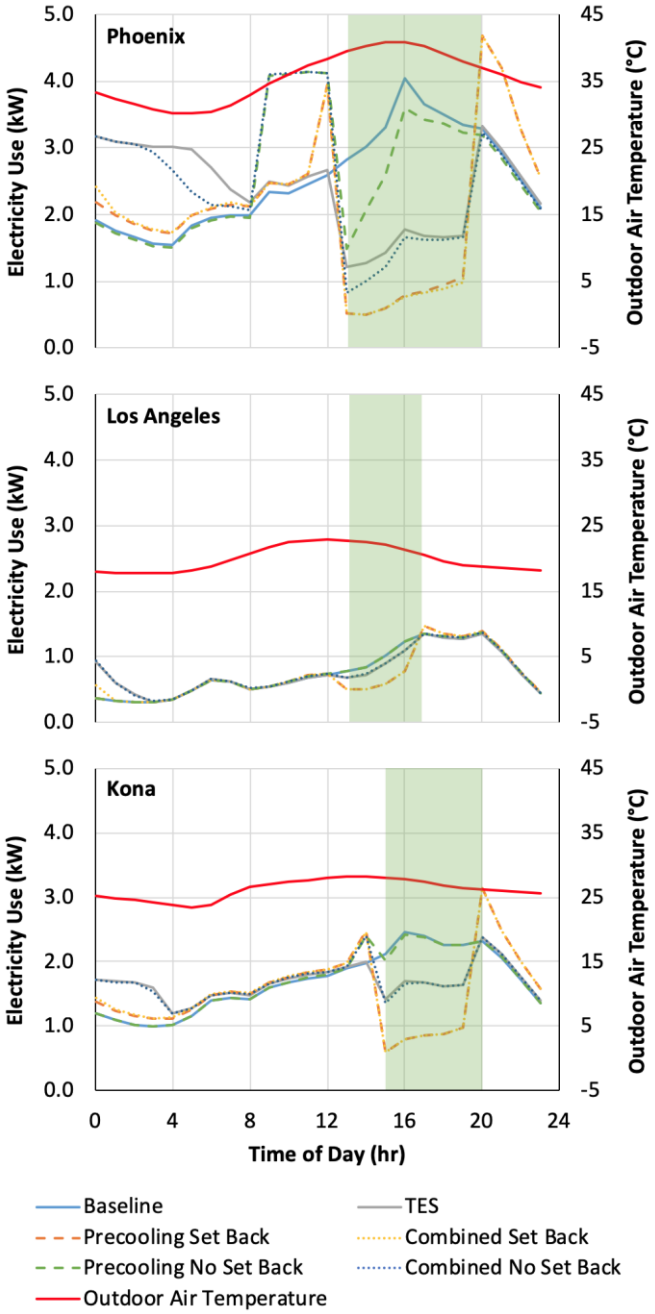
Note: PHX, LA, and KONA are abbreviations for Phoenix, Los Angeles, and Kona, respectively.

2.6. Performance Comparison of Cooling Strategies

Performance comparisons were completed for six cooling strategies including the baseline strategy, two dynamic precooling strategies, the TES system, and two combined strategies. Simulations used hourly data from each location with results provided for (a) intraday operational behavior for an average day in the summer, (b) electrical expenditures for each month of the year to assess financial benefits with respect to changes in environmental conditions and rate structures that change during the year, and (c) performance characteristics and financial benefits for the entire year.

2.6.1. Intraday Operational Behavior

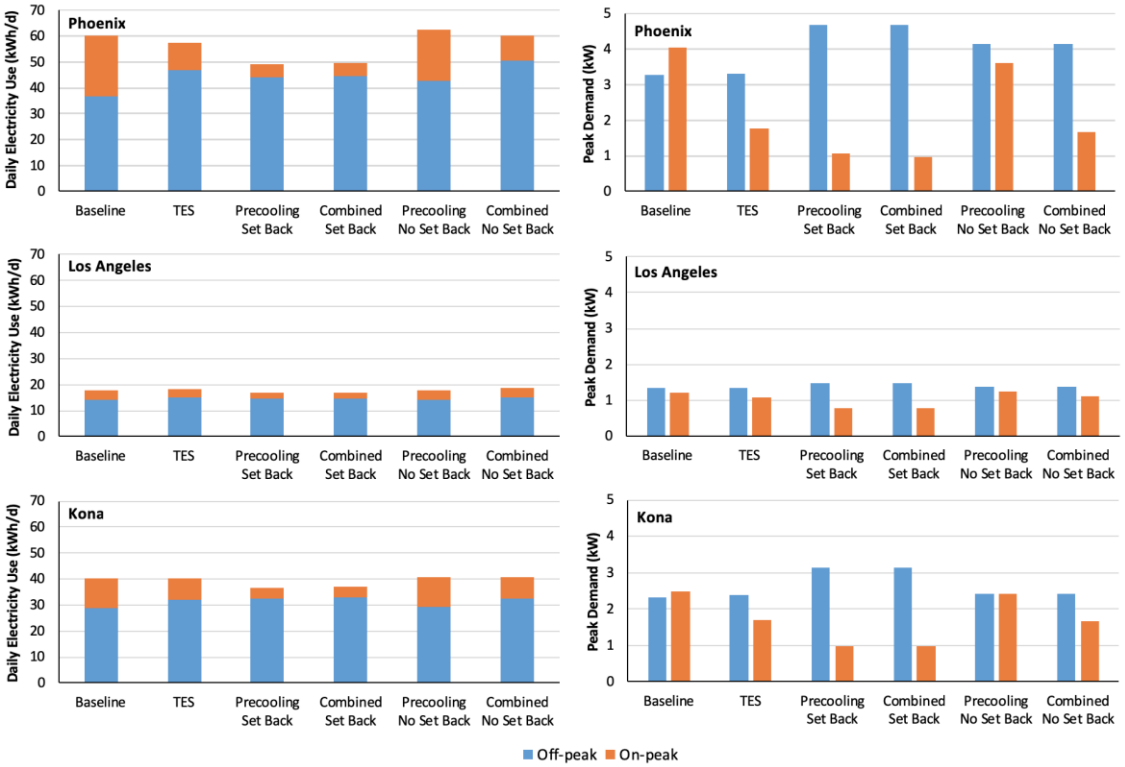
Intraday results in Fig. 2.8 show peak shaving and load shifting capabilities for each cooling strategy and each location. On-peak electricity rates are shaded in green and the average hourly outdoor air temperature is plotted for context. The hourly temperature and energy use represent the “average day” in July by averaging data across all days in the month with highest TOU rates and temperatures; weekends were omitted in Phoenix and Los Angeles because they lacked peak TOU pricing. Fig. 2.8 shows that for Phoenix and Kona, the combined set back and precooling set back strategies resulted in a large ramp of electricity consumption when the peak pricing period ends, a result of the HVAC system operating at its maximum cooling capacity to bring the indoor temperature back to the baseline set point. The other three cooling strategies mirror the baseline electricity consumption profile for the evening hours past peak pricing period.



2.8: Outdoor air temperature and intraday electricity use for the average day of July for each location. The green shaded region denotes the on-peak electric rate period.

Fig. 2.9 provides a quantitative summary of load shifting and peak shaving during on-peak times. The five cooling strategies changed on-peak electricity use between +1.1% and -78.5% and reduced on-peak demand by +0.7% and -75.6%. In Phoenix, four strategies

including precooling set back, combined set back, TES, and combined no set back reduced electricity consumption, with the precooling set back strategy resulting in the greatest reduction of 18.4%. The combined set back, TES, and combined no set back strategies reduced daily electricity consumption by 18.1%, 4.8%, and 0.1%, respectively, while the precooling no set back strategy increased daily electricity consumption by 3.6%. Results for Los Angeles show minimum benefit in load shifting due to the short on-peak period and average outdoor air temperature being close to the 24.4 °C baseline thermostat set point during on-peak times. Although the economic advantage of the investigated cooling strategies is minimal for Los Angeles under the current rate structure, the load shifting and peak shaving capabilities indicated in Fig. 2.9 can benefit the utility by reducing peak load by up to 37.9% during on-peak hours. Results for Kona show a 30.0% to 64.4% reduction in on-peak electricity use for all cooling strategies, except the precooling no set back strategy which caused minimal reduction to the indoor temperature during precooling, resulting in the HVAC system operating similar to the baseline strategy during on-peak times. The TES and combined no set back strategies avoid the late afternoon ramps produced by the other cooling strategies by shifting a portion of the electricity use to the morning hours when the TES is being charged. However, the combined no set back strategy results in a larger off-peak demand due to precooling while the TES charging maintains a similar off-peak demand as the baseline strategy because the TES is charged during low demand times (i.e., early morning hours).

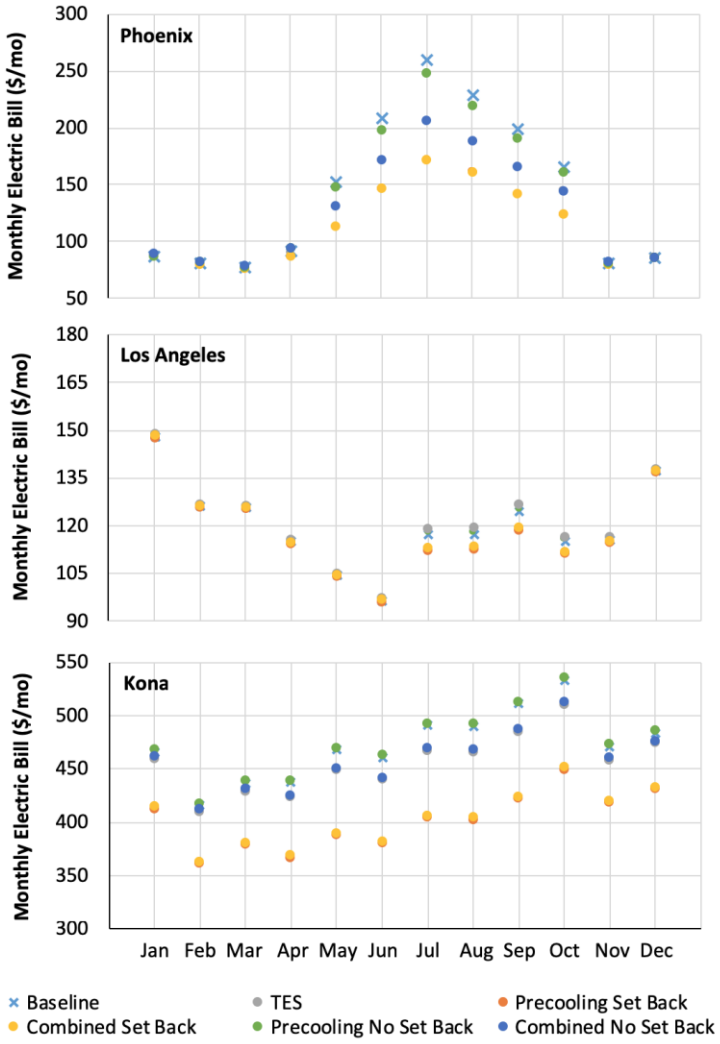


2.9: Daily electricity use and peak demand for off-peak and on-peak times of day in each location for the average day of July.

2.6.2. Monthly Simulations

Fig. 2.10 shows monthly electricity expenditures for each location and cooling strategy. Results for Phoenix show that any cooling strategy offers reduced expenses relative to the baseline case for months May to October. Lowest monthly expenses are achieved using the precooling set back strategy for ten months of the year and the combined set back strategy for the remaining months of July and August. These data allow HVAC designers and homeowners to adjust cooling strategies during the year to maximize savings. For example, in Phoenix, the combined set back strategy is best suited for July through August and the precooling set back strategy is best suited for the months of September through June. Results for Los Angeles show that both strategies with a set back

provide a modest reduction in expenditures for months July to September. For Kona, every cooling strategy, except for the precooling no set back strategy, provides a reduction in monthly electricity expenditures relative to the baseline case. For both Los Angeles and Kona, the precooling set back strategy provides the lowest electric bills for all twelve months of the year and doesn't require changes in the cooling strategy beyond the use of a dynamic precooling set point that updates automatically.



2.10: Monthly electric bill for each cooling strategy in each location.

2.6.3. Annual Performance Evaluation

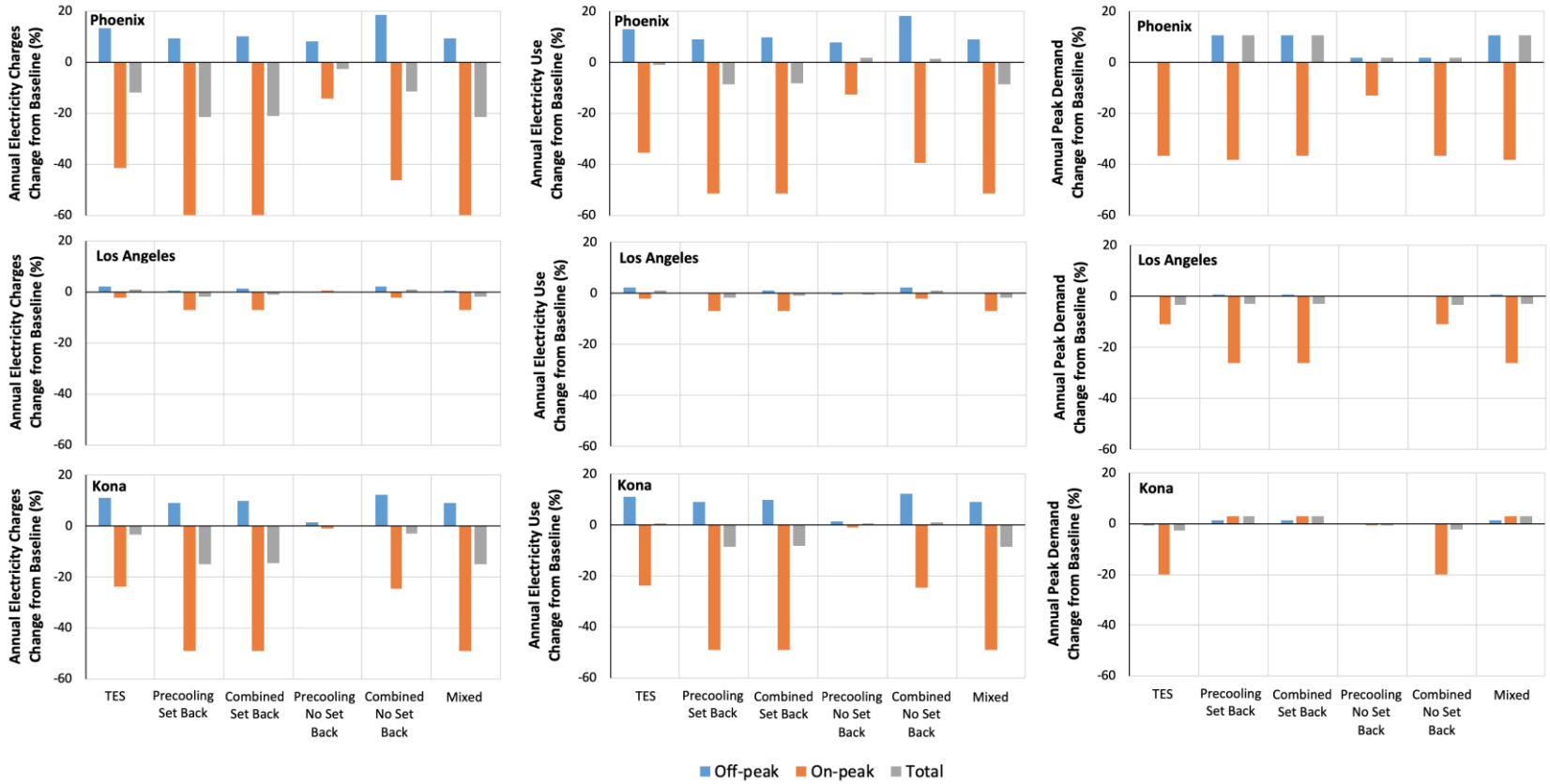
Annual simulations of the proposed cooling strategies were completed to explore the relative differences in performance and economics over a full year. Fig. 2.11 shows results with the percentage change from baseline for the annual electricity charges, annual electricity use, and annual peak demand for the off-peak, on-peak, and total billing periods for each location. Off-peak and on-peak electricity charges are associated with the TOU energy charges of each rate structure while the total electricity charges include fees and taxes.

The precooling set back strategy provided the greatest savings in total annual electricity charges for Phoenix, Los Angeles, and Kona with reductions of 23.5%, 1.7%, and 14.9%, respectively. The combined set back strategy provided similar economic and operational benefits in all locations, indicating that any strategy employing a set back temperature reduced cooling load during on-peak times and hence electricity expenditures. Precooling set back and combined set back strategies also reduced annual electricity use in all three locations by minimizing heat pump operation during the hottest parts of the day when the heat pump operates at a lower efficiency. The precooling no set back and TES strategies shifted energy use to reduce on-peak loads but had only a modest effect on annual electricity use for Phoenix and Kona. None of the proposed cooling strategies significantly affected total annual electricity use or total annual peak demand for Los Angeles, and further, only the two strategies using a set back provided financial savings relative to the baseline case.

Each of the cooling strategies increased total annual peak demand for Phoenix with the strategies employing a set back causing the greatest increase of 10.9% in off-peak

periods due to the heat pump operating at a high capacity after the on-peak time period to bring the indoor temperature back to the baseline value. However, each of the cooling strategies in Phoenix reduced on-peak demand by 12.8% to 38.3%. In Kona, cooling strategies with a set back also increased annual peak demand by up to 3.2%, however, strategies without a set back temperature lowered annual peak demand because the heat pump was not operated near full capacity following the on-peak period. In Los Angeles, total annual peak demand and on-peak demand decreased for every strategy, except for precooling with no set back because the afternoon peak was not affected. Total annual peak demand increased for Phoenix and Kona and decreased for Los Angeles, however, there was no effect on electricity charges because residential rate structures did not include demand charges.

Optimal cooling strategies for each month were selected from Section 6.2 and combined to create a "mixed" strategy, as shown in Fig. 2.11, to obtain greater financial savings by selecting the least cost strategy from each month. Los Angeles and Kona had the simplest mixed strategy because the precooling set back strategy was the least cost option in all months. In Los Angeles, this occurred because raising the thermostat set point during on-peak times decreased the total heat pump operating hours over a year and increased the average annual heat pump efficiency. Whereas in Kona, locational differences including the single non-seasonal rate structure and minimal changes in intraday air temperatures over the year favored precooling with set back. Phoenix used a combination of the precooling set back strategy (September to June) and combined set back strategy (July to August) to maximize the amount of energy shifted to off-peak times during the hottest months of the year.



2.11: Change in annual electricity charges, annual electricity use, and annual peak demand during the off-peak, on-peak, and total billing periods for each cooling strategy with changes reported from the baseline simulation.

The ten-year rate of return and payback period for each cooling strategy was calculated for each location. Capital costs given in Table 2.8 include the TES system for each location calculated using methodology available in (Sanaye and Hekmatian 2016), (Sanaye and Shirazi 2013), (Venkata Rao 2018), (Navidbakhsh, Shirazi, and Sanaye 2013) and the average capital cost of market-ready smart thermostats from (Delaney 2018). The average inflation rate of 2.18% from 2000-2018 (COINNEWS MEDIA GROUP LLC, n.d.) was used as the discount rate and applied to annualized savings calculations to yield the rate of return given in Table 2.9. The TES and combined no set back strategies result in a negative rate of return for all locations, indicating that operational savings do not make up for the capital cost of a TES system. Precooling provides a consistent positive rate of return for each location, and the greatest rate of return, due to the low capital cost of the smart thermostats and monthly monetary savings that were as good or greater than savings with TES alternatives. Investment in a smart thermostat with the proposed dynamic precooling strategy provides a payback period of 0.4, 6.2, and 0.2 for Phoenix, Los Angeles, and Kona, respectively.

Table 2.8: Capital cost of thermal energy storage and smart thermostat for each location.

	Phoenix TES	Los Angeles TES	Kona TES	All Locations Smart Thermostat
Cost ($)	6212.70	3285.64	4151.96	150.45

Table 2.9: Ten-year rate of return of each cooling strategy and technology for each location.

Cooling Strategy	Rate of Return (%)		
	Phoenix	Los Angeles	Kona
TES	-70.20	-103.28	-57.85
Precooling	2119.81	51.63	5022.90
Combined	-48.14	-95.40	74.63
Precooling No Set Back	177.76	-99.82	-242.02
Combined No Set Back	-71.55	-103.17	-64.88
Mixed	-47.47	-93.36	79.14

2.7. Conclusions

This study performed techno-economic evaluations of six cooling strategies for a B10 Building America Benchmark residential building in the cities of Phoenix, Los Angeles, and Kona of the United States. Time-of-use rate structures were applied from each local utility to assess the viability of implementing precooling strategies and ice thermal energy storage (TES) systems that were optimized separately and together in a combined strategy (precooling and TES). Results were evaluated and compared on system sizing, intraday dispatch, electricity use, and electricity cost across daily, monthly, and annual simulations. Significant findings include:

- An optimal heat pump and TES system was sized for each location based on local environmental conditions and utility rate structures to yield a heat pump and TES capacity of 10.55 kW (3 tons) and 73.85 kWh for Phoenix, 3.52 kW (1 ton) and 14.08 kWh for Los Angeles, and 5.28 kW (1.5 tons) and 26.40 kWh for Kona, respectively.
- When looking at the hottest days of the year using an average simulated day in July, the combined (precooling and TES) strategy with set back temperature provided the greatest reductions in on-peak demand and on-peak energy use, with results showing reductions of 75.6% and 78.5% for Phoenix, 36.9% and 37.9% for Los Angeles, and 60.7% and 64.4% for Kona, respectively.
- The TES system alone was able to maintain a consistent indoor air temperature while reducing daily on-peak demand and on-peak electricity consumption between 11.1%-55.8% and 11.5%-54.6% when compared to the baseline cooling strategy across all three locations, respectively.

- When examining performance over the entire year, the precooling set back strategy provided the greatest reductions in annual on-peak demand and annual on-peak energy use with results showing reductions of 38.3% and 51.5% for Phoenix, and 26.2% and 7.0% for Los Angeles, respectively. In Kona, the TES strategy provided the greatest reduction in annual on-peak demand of 20.0%, whereas the precooling set back strategy provided the greatest reduction in annual on-peak energy use of 49.0%.
- The precooling strategy with no set back provided a 4.8% reduction in annual electricity charges for hotter climates, such as Phoenix, with minimal economic benefit realized for the more temperate climates of Los Angeles and Kona.
- Analyses completed for precooling strategies with set back showed that dynamically updating precooling set points provided further cost savings using a simple automated routine that adjusted set points as a function of outdoor air temperature and daily weather patterns. This strategy resulted in an annual economic savings of 23.5%, 1.7%, and 14.9% for Phoenix, Los Angeles, and Kona, respectively. However, the total annual peak demand increased by 10.9% and 23.9%, for Phoenix and Kona, respectively.
- Precooling set back and combined set back strategies used the heat pump at nearly an equivalent load factor over the year, in contrast to the baseline model, by shifting heat pump use from on-peak to off-peak times and thereby decreasing total annual electricity charges by 1.2% to 23.5% and operating the heat pump at a higher efficiency to reduce total annual electricity use by 1.1% to 8.7% across all three locations.

- The combined set back strategy was generally not used but provided a close economic savings to that of precooling set back for both Phoenix and Kona. The combined set back strategy was used in the mixed strategy for Phoenix in periods of the year with the highest on-peak electricity rates and hotter temperatures.
- A full financial assessment was completed to identify the ten-year rate of return and payback period. Findings showed that TES and combined no set back strategies result in a negative rate of return for all locations, indicating that operational savings do not make up for the capital cost of a TES system over a ten-year period. The precooling strategy provides a consistent positive rate of return for each location, and the greatest rate of return, due to the low capital cost of the smart thermostats and monthly monetary savings that were as good or greater than savings with TES alternatives. Investment in a smart thermostat with the proposed dynamic precooling technique provides a payback period of 0.4, 6.2, and 0.2 for Phoenix, Los Angeles, and Kona, respectively.

Generalized findings indicate that precooling strategies were effective at reducing residential electricity expenditures for all locations, with TES systems demonstrating some but lesser benefit in locations such as Phoenix with high cooling requirements that may warrant the financial investment of a TES system. The relative cost savings of these strategies increased with rate structures having longer on-peak periods and greater differences between on-peak and off-peak rates that promoted load shifting. Results show that precooling strategies increased total annual peak demand for Phoenix and Kona. This did not affect energy expenditures because residential rate structures did not include demand charges, which is in contrast to cooling studies for commercial and industrial

buildings that often include demand charges and hence utilize different cooling technologies and controls strategies to reduce overall energy expenditures. For example, a study performed by Kintner-Meyer and Emery implemented precooling and TES to achieve a 21% reduction in peak power demand, 41% reduction in on-peak energy use, and 6% reduction in daily operating costs for a benchmark 33,600 m^2 office building simulated in Phoenix (Kintner-Meyer and Emery 1995). Findings from this study using precooling and TES for the benchmark 167.2 m^2 residential home in Phoenix demonstrated a 16.0% increase in peak power demand, 78.5% reduction in on-peak energy use, and 44.7% reduction in daily operating costs. These two studies demonstrate that quantitative findings, and more importantly the ranked order of cooling alternatives, can be different based on the building envelope, rate structure, and economies of scale for the selected technologies.

Not all of the evaluated cooling strategies provided a reduction in annual electricity use or electric bill. However, these strategies can still provide value to electric utilities by shifting cooling loads to reduce system-wide peak demand and shifting energy use to off-peak times. Such savings for the utility could be passed onto the consumer through rate adjustments. Further work could explore rate structures with demand charges to compensate customers for peak load reduction. Extending this study with empirical testing including user comfort is another area for investigation.

2.8. Acknowledgements

This study was funded in part by Salt River Project.

2.9. References

ANSI/ASHRAE. 2013. “Thermal Environmental Conditions for Human Occupancy.”

Arababadi, Reza, and Kristen Parrish. 2015. “Developing and Modeling Potential Precooling Strategies for Residential Buildings in the Phoenix Climate.” *ASHRAE*

Transactions, 1–7.

Arcuri, Bruno, Catalina Spataru, and Mark Barrett. 2017. "Evaluation of Ice Thermal Energy Storage (ITES) for Commercial Buildings in Cities in Brazil." *Sustainable Cities and Society* 29: 178–92. https://doi.org/10.1016/j.scs.2016.12.011.

Bell, Dagfinn. 1998. "Evaluation of Optimal Control for Ice-Based Thermal Energy Storage Systems." University of Colorado.

Berardi, Umberto. 2015. "Building Energy Consumption in US, EU, and BRIC Countries." *Procedia Engineering* 118: 128–36. https://doi.org/10.1016/j.proeng.2015.08.411.

Berkeley, Lawrence, National Renewable, and Oak Ridge. n.d. "Validation and Uncertainty Characterization for Energy Simulation."

Booten, Chuck, and Paulo Cesar Tabares-Velasco. 2012. "Using EnergyPlus to Simulate the Dynamic Response of a Residential Building to Advanced Cooling Strategies." In *2nd International Conference on Building Energy and Environment, Boulder, Colorado*.

Braun, James E., and Nitin Chaturvedi. 2002. "An Inverse Gray-Box Model for Transient Building Load Prediction." *HVAC&R Research* 8 (1): 73–99.

Braun, James E., and Kyoung-Ho Lee. 2006. "An Experimental Evaluation of Demand Limiting Using Building Thermal Mass in a Small Commercial Building." *ASHRAE Transactions* 112 (1).

Braun, James E., Kent W. Montgomery, and Nitin Chaturvedi. 2001. "Evaluating the Performance of Building Thermal Mass Control Strategies." *HVAC&R Research*, 403–28. https://doi.org/10.1080/10789669.2001.10391283.

Cappers, Peter, C Anna Spurlock, Patrick Baylis, Meredith Fowlie, and Catherine Wolfram. 2016. "Time-of-Use as a Default Rate for Residential Customers: Issues and Insights." *Lawrence Berkeley National Laboratory*, no. June: 1–53.

Caves, Douglas W., and Laurits R. Christensen. 1980. "Econometric Analysis of Residential Time-of-Use Electricity Pricing Experiments." *Journal of Econometrics* 14 (3): 287–306. https://doi.org/10.1016/0304-4076(80)90029-9.

Chen, T. Y. 2001. "Real-Time Predictive Supervisory Operation of Building Thermal Systems with Thermal Mass." *Energy and Buildings* 33 (2): 141–50.

COINNEWS MEDIA GROUP LLC. n.d. "Current US Inflation Rates: 2009-2019." US INFLATION CALCULATOR.

https://www.usinflationcalculator.com/inflation/current-inflation-rates/.

Delaney, John R. 2018. “The Best Smart Thermostats for 2019.” PCmag. 2018. https://www.pcmag.com/article/356755/the-best-smart-thermostats.

EIA. 2016. “Annual Energy Outlook 2016.” *U.S. Energy Information Administration*, ES-5. https://doi.org/EIA-0383(2016).

Energy Information Administration. 2017. “2016 EIA Form 861:Electric Power Sales, Revenue, and Energy Efficiency.” https://eia.gov/electricity/data/eia861.

Energy, U.S. Department of. 2017. “Heat Pump Systems.” 2017. https://energy.gov/energysaver/heat-pump-systems.

Farah, Sleiman, Ming Liu, and Wasim Saman. 2019. “Numerical Investigation of Phase Change Material Thermal Storage for Space Cooling.” *Applied Energy* 239 (January): 526–35. https://doi.org/10.1016/j.apenergy.2019.01.197.

German, Alea, Marc Hoeschele, David Springer, and Davis Energy Group. 2014. “Maximising the Benefits of Residential Pre-Cooling.” *ACEEE Summer Study on Energy Efficiency in Buildings*, 71–83.

Hajiah, Ali, and Moncef Krarti. 2012a. “Optimal Control of Building Storage Systems Using Both Ice Storage and Thermal Mass - Part I: Simulation Environment.” *Energy Conversion and Management* 64: 499–508. https://doi.org/10.1016/j.enconman.2012.02.016.

———. 2012b. “Optimal Controls of Building Storage Systems Using Both Ice Storage and Thermal Mass - Part II: Parametric Analysis.” *Energy Conversion and Management* 64: 509–15. https://doi.org/10.1016/j.enconman.2012.02.020.

Hasnain S.M. 1998. “Review on Sustainable Thermal Energy Storage Technologies, Part I: Heat Storage Materials and Techniques.” *Energy Conversion and Management* 39 (11): 1127–38. https://doi.org/10.1016/S0196-8904(98)00025-9.

Hawaii Electric Light. 2016. “REVISED SHEET NO. 71, Effective September 21, 2016.” 2016. https://www.hawaiianelectric.com/Documents/my_account/rates/hawaii_electric_light_rates/helco_rates_sch_tou_r.pdf.

———. 2017a. “REVISED SHEET NO. 50.4 , Effective July 1, 2017.” 2017. https://www.hawaiianelectric.com/Documents/my_account/rates/hawaii_electric_light_rates/helco_rates_pbf_current.pdf.

———. 2017b. “REVISED SHEET NO. 53, Effective January 1, 2018 to June 30,

2018.” 2017. https://www.hawaiianelectric.com/Documents/my_account/rates/hawaii_electric_light_rates/helco_rates_gi_fee_surcharge.pdf.

———. 2017c. “REVISED SHEET NO. 90, Effective January 1-31, 2018.” 2017. https://www.hawaiianelectric.com/Documents/my_account/rates/hawaii_electric_light_rates/helco_rates_ppac.pdf.

———. 2017d. “REVISED SHEET NO. 91, Effective June 1, 2017.” 2017. https://www.hawaiianelectric.com/Documents/my_account/rates/hawaii_electric_light_rates/helco_rates_rba.pdf.

Henninger, Robert H, and Michael Witte. n.d. “EnergyPlus Testing with HVAC Equipment Component Tests,” 1–23.

Henninger, Robert H, and Michael J Witte. n.d. “EnergyPlus Testing with ASHRAE 1052-RP Toolkit – Building Fabric Analytical Tests.”

Henninger, Robert H, Michael J Witte, Drury B Crawley, and Case E Base. 2003. “EXPERIENCE TESTING ENERGYPLUS WITH THE IEA HVAC BESTEST E100-E200 SERIES,” 467–74.

Henze, Gregor P., and Moncef Krarti. 1999. “The Impact of Forecasting Uncertainty on the Performance of a Predictive Optimal Controller for Thermal Energy Storage Systems.” *ASHRAE Transactions* 105: 553.

Herter, K., and Y. Okuneva. 2014. “SMUD’s Residential Summer Solutions Study 2011-2012.” *Herter Energy Research Solutions. El Dorado Hills, CA*.

Hu, Maomao, Fu Xiao, and Lingshi Wang. 2019. “Investigation of Demand Response Potentials of Residential Air Conditioners in Smart Grids Using Grey-Box Room Thermal Model.” *Applied Energy* 207 (2017): 324–35. https://doi.org/10.1016/j.apenergy.2017.05.099.

Ice Energy. 2018a. “Ice Bear 20.” https://www.ice-energy.com/wp-content/uploads/2018/05/IB-20-ProductSheet-2017-US-D4.pdf.

———. 2018b. “Ice Bear 40.” https://www.ice-energy.com/wp-content/uploads/2018/05/IB-20-ProductSheet-2017-US-D4.pdf.

Im, Piljae. 2016. “Multi-Year Plan for Validation of EnergyPlus Multi-Zone HVAC System Modeling Using ORNL’s Flexible Research Platform,” no. August.

Janko, Samantha A., Michael R. Arnold, and Nathan G. Johnson. 2016. “Implications of High-Penetration Renewables for Ratepayers and Utilities in the Residential Solar

Photovoltaic (PV) Market." *Applied Energy* 180: 37–51. https://doi.org/10.1016/j.apenergy.2016.07.041.

Johra, Hicham, and Per Heiselberg. 2017. "In Fl Uence of Internal Thermal Mass on the Indoor Thermal Dynamics and Integration of Phase Change Materials in Furniture for Building Energy Storage : A Review." *Renewable and Sustainable Energy Reviews* 69 (November 2016): 19–32. https://doi.org/10.1016/j.rser.2016.11.145.

Keeney, Kevin R., and James E. Braun. 1997. "Application of Building Precooling to Reduce Peak Cooling Requirements." *ASHRAE Transactions* 103 (1): 463–69.

Kintner-Meyer, M., and A. F. Emery. 1995. "Optimal Control of an HVAC System Using Cold Storage and Building Thermal Capacitance." *Energy and Buildings* 23 (1): 19–31. https://doi.org/10.1016/0378-7788(95)00917-M.

Klaassen, C. J., John M. House, and Iowa Energy Center. 2002. "Demonstration of Load Shifting and Peak Load Reduction with Control of Building Thermal Mass." *Teaming for Efficiency: Commercial Buildings: Technologies, Design, Performance Analysis, and Building Industry Trends* 3: 55.

Krarti, Moncef, Gregor P. Henze, and Dagfinn Bell. 1999. "Planning Horizon for a Predictive Optimal Controller for Thermal Energy Storage Systems." *ASHRAE Transactions* 105: 543.

Lee, Kyoung-ho, and James E. Braun. 2008a. "Development of Methods for Determining Demand-Limiting Setpoint Trajectories in Buildings Using Short-Term Measurements." *Building and Environment* 43 (10): 1755–68.

———. 2008b. "Model-Based Demand-Limiting Control of Building Thermal Mass." *Building and Environment* 43 (10): 1633–46.

Lee, Kyoung-Ho, and James E. Braun. 2008. "A Data-Driven Method for Determining Zone Temperature Trajectories That Minimize Peak Electrical Demand." *ASHRAE Transactions* 114 (2).

Lee, Robert. n.d. "City of Los Angeles." Accessed January 1, 2018. http://www.uutinfo.org/uutinfo_city_info/los_angeles/uutinfo_los_angeles.htm.

Lizana, Jesús, Ricardo Chacartegui, Angela Barrios-Padura, and José Manuel Valverde. 2017. "Advances in Thermal Energy Storage Materials and Their Applications towards Zero Energy Buildings: A Critical Review." *Applied Energy* 203: 219–39. https://doi.org/10.1016/j.apenergy.2017.06.008.

Los Angeles Department of Water and Power. 2016. "Electric Rate Schedules." 2016. https://www.ladwp.com/ladwp/faces/wcnav_externalId/a-fr-elecrate-schel?_adf.ctrl-state=xogg89u6n_49&_afrLoop=350577774383580&_afrWindowMode=0&_afrWi

ndowId=gdatcyg8s_1#%40%3F_afrWindowId%3Dgdatcyg8s_1%26_afrLoop%3D350577774383580%26_afrWindowMode%3D0%26_ad.

Luerssen, Christoph, Oktoviano Gandhi, Thomas Reindl, Chandra Sekhar, and David Cheong. 2019. “Levelised Cost of Storage (LCOS) for Solar-PV-Powered Cooling in the Tropics.” *Applied Energy* 242 (March): 640–54. https://doi.org/10.1016/j.apenergy.2019.03.133.

Luo, Na, Tianzhen Hong, Hui Li, Ruoxi Jia, and Wenguo Weng. 2017. “Data Analytics and Optimization of an Ice-Based Energy Storage System for Commercial Buildings.” *Applied Energy* 204: 459–75. https://doi.org/10.1016/j.apenergy.2017.07.048.

Mammoli, Andrea, and Matthew Robinson. 2018. “Numerical Analysis of Heat Transfer Processes in a Low-Cost, High-Performance Ice Storage Device for Residential Applications.” *Applied Thermal Engineering* 128: 453–63. https://doi.org/10.1016/j.applthermaleng.2017.09.043.

McKane, Aimee. 2010. “Automated Demand Response: The Missing Link in the Electricity Value Chain.” *Lawrence Berkeley National Laboratory*. http://escholarship.org/uc/item/4kz048j2.pdf.

Muresan, Adela. 2016. “Who Lives Largest? The Growth of Urban American Homes in the Last 100 Years.” Real Estate Broad. 2016. https://www.propertyshark.com/Real-Estate-Reports/2016/09/08/the-growth-of-urban-american-homes-in-the-last-100-years/.

Musgrove, A. R.de L., H. J. Ehmke, and K. J. Stocks. 1989. “Optimum Design and Operation of Ice-Storage Air-Conditioning Systems under Australian TOU Tariffs.” *Energy* 14 (9): 525–35. https://doi.org/10.1016/0360-5442(89)90023-6.

National Renewable Energy Laboratory. 2016. “BEopt.” https://beopt.nrel.gov/.

Navarro, Lidia, Alvaro De Gracia, Shane Colclough, Maria Browne, Sarah J Mccormack, Philip Grif, and Luisa F Cabeza. 2016. “Thermal Energy Storage in Building Integrated Thermal Systems : A Review . Part 1 . Active Storage Systems” 88. https://doi.org/10.1016/j.renene.2015.11.040.

Navidbakhsh, Mahdi, Ali Shirazi, and Sepehr Sanaye. 2013. “Four e Analysis and Multi-Objective Optimization of an Ice Storage System Incorporating PCM as the Partial Cold Storage for Air-Conditioning Applications.” *Applied Thermal Engineering* 58 (1–2): 30–41. https://doi.org/10.1016/j.applthermaleng.2013.04.002.

Ohama, Raun. 2017. “Total Interior Area Hawaii.” Honolulu: Hawaii Information Services.

Oró, E., A. de Gracia, A. Castell, M. M. Farid, and L. F. Cabeza. 2012. “Review on Phase Change Materials (PCMs) for Cold Thermal Energy Storage Applications.” *Applied Energy* 99: 513–33. https://doi.org/10.1016/j.apenergy.2012.03.058.

Pacific Northwest National Laboratory, Oak Ridge National Laboratory. 2010. “Guide to Determining Climate Regions by County.” https://www1.eere.energy.gov/buildings/publications/pdfs/building_america/ba_climateguide_7_1.pdf.

Project, Salt River. 2015. “STANDARD PRICE PLAN FOR RESIDENTIAL TIME-OF-USE SERVICE.”

Rismanchi, B., R. Saidur, H. H. Masjuki, and T. M I Mahlia. 2012. “Energetic, Economic and Environmental Benefits of Utilizing the Ice Thermal Storage Systems for Office Building Applications.” *Energy and Buildings* 50: 347–54. https://doi.org/10.1016/j.enbuild.2012.04.001.

Ruan, Yingjun, Qingrong Liu, Zhengwei Li, and Jiazheng Wu. 2016. “Optimization and Analysis of Building Combined Cooling, Heating and Power (BCHP) Plants with Chilled Ice Thermal Storage System.” *Applied Energy* 179 (2016): 738–54. https://doi.org/10.1016/j.apenergy.2016.07.009.

Salt River Project. n.d. “How to Read a Residential Bill.” Accessed January 10, 2017. https://www.srpnet.com/billing/home/read.aspx.

Sanaye, Sepehr, and Mohammad Hekmatian. 2016. “Ice Thermal Energy Storage (ITES) for Air-Conditioning Application in Full and Partial Load Operating Modes.” *International Journal of Refrigeration* 66: 181–97. https://doi.org/10.1016/j.ijrefrig.2015.10.014.

Sanaye, Sepehr, and Ali Shirazi. 2013. “Thermo-Economic Optimization of an Ice Thermal Energy Storage System for Air-Conditioning Applications.” *Energy and Buildings* 60: 100–109. https://doi.org/10.1016/j.enbuild.2012.12.040.

Springer, David, and Davis Energy Group. 2007. *SMUD Off-Peak Over-Cooling Project: Final Project Report*. California Energy Commission.

Tang, Rui, and Shengwei Wang. 2019. “Model Predictive Control for Thermal Energy Storage and Thermal Comfort Optimization of Building Demand Response in Smart Grids.” *Applied Energy* 242 (March): 873–82. https://doi.org/10.1016/J.APENERGY.2019.03.038.

Turner, W. J.N., I. S. Walker, and J. Roux. 2015. “Peak Load Reductions: Electric Load Shifting with Mechanical Pre-Cooling of Residential Buildings with Low Thermal Mass.” *Energy* 82: 1057–67. https://doi.org/10.1016/j.energy.2015.02.011.

U.S. Department of Energy. n.d. “Tips on Saving Money and Energy in Your Home Contents.”

———. 2017. “EnergyPlus.” *U.S. Department of Energy’s*. https://energyplus.net/.

Units, Rooftop. 2017. “Landmark ® Rooftop Units.”

Venkata Rao, Ravipudi. 2018. *Jaya: An Advanced Optimization Algorithm and Its Engineering Applications*. *Jaya: An Advanced Optimization Algorithm and Its Engineering Applications*. https://doi.org/10.1007/978-3-319-78922-4.

Wijesuriya, Sajith, Matthew Brandt, and Paulo Cesar Tabares-Velasco. 2018. “Parametric Analysis of a Residential Building with Phase Change Material (PCM)-Enhanced Drywall, Precooling, and Variable Electric Rates in a Hot and Dry Climate.” *Applied Energy* 222 (March): 497–514. https://doi.org/10.1016/j.apenergy.2018.03.119.

Wilcox, S, and W Marion. 2008. “Users Manual for TMY3 Data Sets.” *Renewable Energy*, no. May: 51. https://doi.org/NREL/TP-581-43156.

Wilson, E, C Engebrecht Metzger, S Horowitz, and R Hendron. 2014. “2014 Building America House Simulation Protocols.”

Witte, Michael J, Robert H Henninger, and Drury B Crawley. 2004. “EXPERIENCE TESTING ENERGYPLUS WITH THE ASHRAE 1052-RP BUILDING FABRIC ANALYTICAL TESTS,” 1–8.

Xu, Peng. 2006. “Evaluation of Demand Shifting with Thermal Mass in Two Large Commercial Buildings.” Ernest Orlando Lawrence Berkeley National Laboratory, Berkeley, CA (US).

Xu, Yinliang, Kun Ji, Yan Lu, Yuebin Yu, and Wenxin Liu. 2013. “Optimal Building Energy Management Using Intelligent Optimization.” In *Automation Science and Engineering (CASE), 2013 IEEE International Conference On*, 95–99. IEEE.

Xue, Xue, and Wang Shengwei. 2012. “Interactive Building Load Management for Smart Grid.” In *Power Engineering and Automation Conference (PEAM), 2012 IEEE*, 1–5. IEEE.

Yau, Y. H., and Behzad Rismanchi. 2012. “A Review on Cool Thermal Storage Technologies and Operating Strategies.” *Renewable and Sustainable Energy Reviews* 16 (1): 787–97. https://doi.org/10.1016/j.rser.2011.09.004.

Zhao, Long, Zhiyong Yang, and Wei Jen Lee. 2017. “The Impact of Time of Use (TOU) Rate Structure on Consumption Patterns of The Residential Customers.” *IEEE*

Transactions on Industry Applications 9994 (c). https://doi.org/10.1109/TIA.2017.2734039.

CHAPTER 3

MODEL PREDICTIVE CONTROL OF MICROGRIDS FOR REAL-TIME ANCILLARY SERVICE MARKET PARTIPCATION

Authored by James R. Nelson, Nathan G. Johnson

Forthcoming Journal Submission in November 2019

Abstract

This study develops two model predictive control approaches to optimize microgrid dispatch, one with participation in real-time ancillary service markets and the other without participation. Results are compared to a baseline logic-based control with case study data taken from a grid-tied 326 kW solar photovoltaic, 634 kW/ 634 kWh battery, and 350 kW diesel generator microgrid portfolio designed to serve an office building. Annual performance evaluations show that model predictive control algorithms can reduce operating expenses by 13.73% when compared to logic-based controls, and through participation in ancillary service markets, model predictive control can reduce net operating expenses by up to 23.47%. Revenue from ancillary services accounted for up to 12.03% of operating costs from spinning reserve (7.52%) and non-spinning reserve (4.51%). Model predictive control with ancillary services maintained the battery state of charge an average of 38.78% higher than batteries dispatched by model predictive control without market participation. This reduced battery cycling losses, minimized battery O&M expenses, and improved battery lifetime. Sensitivity analyses indicate that more granular time steps and longer prediction horizons for model predictive control provide additional operating cost savings. Intraday simulations indicate that both model predictive control algorithms can adapt to differences in environmental conditions and pricing signals to

minimize operational costs. This generalizable finding suggests an inherent modularity, scalability, and robustness of the proposed algorithms to provide additional value to a variety of microgrid owners and operators.

3.1. Introduction

The increasing prevalence of distributed energy resources (DERs), societal interest in low-carbon energy, and added emphasis on resilience is creating rapid change in the electric power industry (Janko, Arnold, and Johnson 2016), (Grid Modernization Labortatory Consortium 2017). Utility revenue models, based traditionally on energy sales, are being disrupted by the adoption of DERs that offset customer energy purchases (Ceres 2015), (Small and Frantzis 2010). Higher amounts of variable, renewable power is also creating concerns for power stability and quality given that high-inertia, thermal generation may not as easily stabilize grid frequency and voltage (Sadamoto et al. 2018), (Chambers 2018), (Mazumder, Ghosh, and Zare 2013). Microgrids are one solution being implemented to address the technical and economic challenges of high-penetration distributed generation by providing advanced controls and coordination with higher-level centralized generation and transmission scheduling (Hirsch, Parag, and Guerrero 2018), (Goyal and Ghosh 2016), (Raquel, n.d.). Microgrids can provide low-cost energy while also increasing the reliability and resilience of energy supply by utilizing local generating resources in the event of a grid outage (Taft 2017b), (Amirioun et al. 2019), (Hussain, Bui, and Kim 2019), (Jiaren Wang et al. 2018). Potential customer segments include military, hospitals, health services, data centers, islands, and other critical public services and industries (Asmus, Forni, and Vogel 2018).

Traditional control methodologies for electric power systems implement hierarchical control architectures (Arafeh 1978) that typically consist of three control levels (primary, secondary, and tertiary) operating at different time scales to ensure supply meets demand and power quality is maintained (Undrill 2018), (NERC Resources Subcommittee 2011). This approach is common for managing power generation, transmission, and distribution within a service territory. Hierarchical control has also been implemented in microgrids to control assets internal to the microgrid and, in some instances, coordinate microgrid dispatch with the connected utility, regional transmission organization (RTO), or independent system operator (ISO) (Khongkhachat and Khomfoi 2015). Common classifications of microgrid controls include centralized, decentralized, and distributed controls (Sen and Kumar 2018). Each classification can be used for a variety of control functions similar to those of the main grid, such as droop control, voltage and frequency control, active and reactive power sharing, energy management, and market participation (Sen and Kumar 2018), (Zhou and Ho 2016). Each of these specific control functions is instantiated from a generic control methodology such as closed loop controls, open loop controls, logic-based controls, or optimization (Monesha, Kumar, and Rivera, n.d.), (Borazjani et al. 2014). Optimization techniques are an area of increasing research with example sub-fields including linear programming, non-linear programing, and metaheuristic optimization (e.g. genetic algorithms) (Fathima and Palanisamy 2015).

Model predictive control (MPC) has growing applications for dispatching energy assets with respect to uncertainty in renewable generation and loads (Rawlings and Mayne 2009). MPC techniques, also known as receding horizon optimization, have been shown to enhance economic and technical metrics for microgrids and similar energy systems (Gruber

et al. 2015), (Pereira, Munoz De La Pena, and Limon 2016), (Parisio, Rikos, Glielmo, et al. 2014), (J. Xu, Zou, and Niu 2014), (X. Zhang et al. 2017), (Prodan and Zio 2014), (Ghanbarian et al. 2017), (Morstyn et al. 2018), (Bruni et al. 2015), (Y. Zhang et al. 2015), (Mehleri et al. 2012), (Zachar and Daoutidis 2016). Parisio et al. demonstrated the viability of MPC through simulations and validated results with hardware testing in a lab environment (Parisio, Rikos, Tzamalis, et al. 2014). Continued work by the authors expanded the MPC methodology to account for uncertainty of loads and renewable generation using a two-stage stochastic approach that demonstrated reduced operational costs and emissions compared to a deterministic approach (Parisio, Rikos, and Glielmo 2016). A similar study by Zhang et al. showed that MPC was superior to a logic-based approach when forecast data are imperfect (Liu et al. 2016).

Prior work to minimize microgrid operating cost is now being advanced with research to increase revenue through wholesale market participation and further improve economics In 1992, the Federal Energy Regulatory Commission (FERC) issued The Restructuring Rule (Order No. 363) to create competitive markets that uncoupled the sale of energy services from transportation services (Tuttle et al. 2016). This order has helped motivate research of advanced microgrid control approaches that participate in energy markets and provide ancillary services (Gomes and Saraiva 2010), (Shi, Luo, and Tu 2014), (Ratnam and Weller 2018), (Gandhi et al. 2018), (Majzoobi and Khodaei 2017), (Chilipi et al. 2016). Wang et al. demonstrated that microgrids can increase revenue streams by 8%-25% by providing flexible ramping services and reserves to the electric grid in day-ahead markets (Jianxiao Wang et al. 2017). This improves project financials for the microgrid owner/operator while also providing flexibility and adequacy to the larger interconnected

power system. Few studies have explored the potential barriers to market entry and potential benefits of allowing distributed energy resources and microgrids to directly participate in wholesale markets (Studies, Applications, and Benefits 2019), (Cochran et al. 2013). Continued work is needed to explore the economic and operational potential of microgrids participating in real-time ancillary service markets.

This study develops microgrid control algorithms to schedule asset dispatch and participation in real-time energy markets. Contributions to literature include:

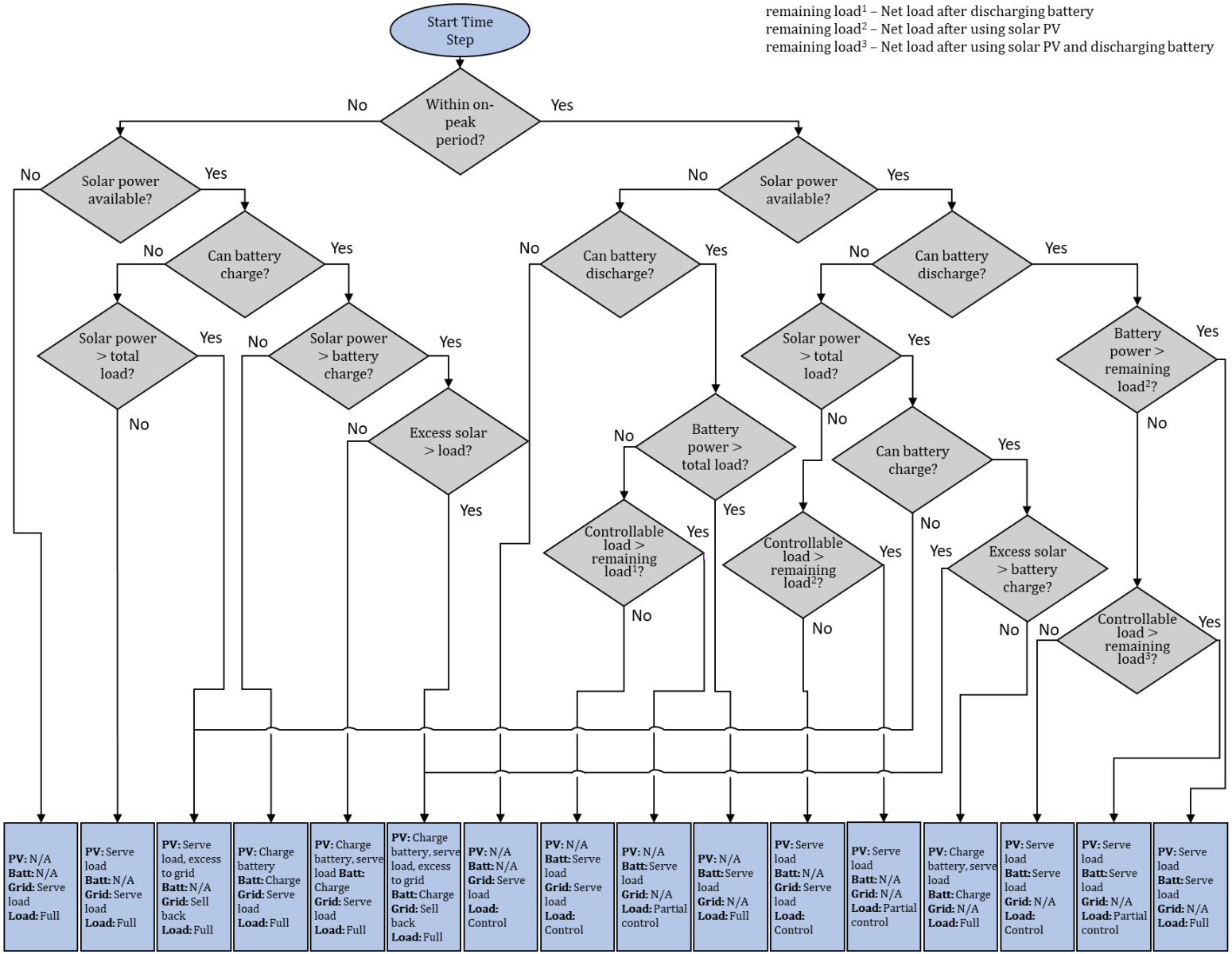
- Develops an MPC approach that optimally dispatches assets and participates in real-time energy markets to achieve cost-optimal operation.
- Designs a microgrid portfolio for a commercial building on Arizona State University's Tempe campus to serve local loads, exchange energy with the utility, and provide ancillary services to real-time energy markets.
- Quantifies the sensitivity of dispatch scheduling and operational cost to MPC time step size and prediction time horizon.
- Compares technical and economic performance of microgrid dispatch routines using logic-based controls, MPC without ancillary services, and MPC with ancillary services.

3.2. Microgrid Control Algorithms

Two model predictive control algorithms are developed and compared to a baseline algorithm using logic-based controls. Differences in operating behavior and cash flow are highlighted to identify opportunities for improving the technical and financial efficacy of grid-connected microgrids.

3.2.1. Logic-based Control

The logic-based control algorithm uses real-time information related to environmental conditions, pricing signals, and energy asset status to dispatch local energy assets to reduce current operational costs. Fig. 3.1 shows the process used to dispatch controllable energy assets.



3.1: Control process flow for the logic-based control algorithm.

3.2.2. Model Predictive Control

Model predictive control algorithms use historical data and real-time data to forecast future environmental conditions, pricing signals, and energy asset status over a specified time horizon. This information is input into an optimization formulation that schedules energy asset dispatch over a selected time horizon and executes dispatch choices in the first time step. With each time step, new forecasts are calculated and used to execute the optimal dispatch for the next time step. The optimization formulation consists of an objective function that describes microgrid operating costs and revenue streams, and constraints that ensure the microgrid and energy assets maintain proper operation within their limitations.

3.2.2.1. Objective Function

Microgrid operating cost is minimized using the objective function in Eq. 1 where T_h is the specified time horizon, $C_{f,a}^{dg}$ is the variable fuel cost of the distributed generator, C_{OM}^{dg} is the variable operation and maintenance cost of the distributed generator, P^{dg} is the power output of the distributed generator, t_{hf} is the time step hourly fraction, $C_{f,b}^{dg}$ is the no-load fuel cost of the distributed generator, B^{dg} is the binary variable that indicates if the distributed generator is on (1) or off (0), C_{OM}^{s} is the operation and maintenance cost of the energy storage, P_c^s is the charging power of energy storage, P_d^s is the discharging power of energy storage, $C_{e,buy}^{g}$ is the cost to buy energy from the grid, P_{buy}^{g} is the power purchased from the grid, $C_{e,sell}^{g}$ is the compensation price for selling energy to the grid, P_{sell}^{g} is the power sold to the grid, T_{bp} is the length of time of the billing period, $C_{dem,n}^{g}$ is the demand charge associated with the n^{th} time-of-use (TOU) period, and $P_{max,n}^{g}$ is the

maximum power demand seen by the grid during the n^{th} TOU period. Demand charges are imposed once per billing period while energy charges are imposed for every time step of the billing period. Stated differently, variables associated with energy charges are time dependent whereas variables associated with demand charges are not and only applied once per time horizon and scaled with the number of time horizons within each billing period.

$$J := \sum_{t=1}^{T_h} \left(\left(\left(C_{f,a}^{dg} + C_{OM}^{dg} \right) P^{dg}(t) + C_{f,b}^{dg} B^{dg}(t) \right) t_{hf} + \left(C_{OM}^{s} P_c^s(t) + C_{OM}^{s} P_d^s(t) \right) t_{hf} + \left(C_{e,buy}^{g}(t) P_{buy}^{g}(t) - C_{e,sell}^{g}(t) P_{sell}^{g}(t) \right) t_{hf} \right) + \frac{T_h}{T_{bp}} \sum_{n=1}^{N_{TOU}} C_{dem,n}^{g} P_{max,n}^{g} \quad \text{(Eq. 1)}$$

3.2.2.2. Constraints

Energy asset specifications, load forecasts, and renewable generation forecasts establish constraints to microgrid operation. Eq. 2 shows the energy balance that ensures electric load is served by a combination of power generated by distributed energy resources within the microgrid or power purchased from the grid, where P^{ren} is the power of renewable generation, P^{cont} is the power consumption of the controllable load, and P_{for}^{crit} is the forecasted power consumption of the critical load.

$$P^{dg}(t) + P^{ren}(t) + P_{buy}^{g}(t) - P_{sell}^{g}(t) - P_c^s(t) + P_d^s(t) - P^{cont}(t) - P_{for}^{crit}(t) = 0 \quad \text{for } t = 1, \dots, T_h \quad \text{(Eq. 2)}$$

Eq. 3 expresses the amount of renewable generation that can be curtailed, P^{ren}, and is limited by the forecasted future renewable generation, P_{for}^{ren}. Renewable generation is never curtailed in this case study but Eq. 3 is still included as part of a comprehensive

formulation to allow curtailment by request of the utility in an over-production scenario, or curtailment during a grid outage to balance power as described in Eq. 2.

$$0 \leq P^{ren}(t) \leq P^{ren}_{for} \quad \text{for } t = 1, \dots, T_h \tag{Eq. 3}$$

Eq. 4 constrains minimum generator loading, P^{dg}_{min}, to prevent wet stacking and damage to the generator (Clifford Power 1999). Eq. 5 sets the upper limit for generator operation using the maximum capacity, P^{dg}_{max}. Eqs. 6 and 7 ensure that the ramping limits of the distributed generator are followed when changing dispatch from one time step to the next, where $P^{dg}_{ramp,d}$ is the maximum hourly ramp down rate of the distributed generator and $P^{dg}_{ramp,u}$ is the maximum hourly ramp up rate of the distributed generator.

$$P^{dg}_{min} B^{dg}(t) \leq P^{dg}(t) \quad \text{for } t = 1, \dots, T_h \tag{Eq. 4}$$

$$P^{dg}(t) \leq P^{dg}_{max} B^{dg}(t) \quad \text{for } t = 1, \dots, T_h \tag{Eq. 5}$$

$$P^{dg}(t-1) - P^{dg}(t) \leq P^{dg}_{ramp,d} t_{hf} \quad \text{for } t = 2, \dots, T_h \tag{Eq. 6}$$

$$P^{dg}(t) - P^{dg}(t-1) \leq P^{dg}_{ramp,u} t_{hf} \quad \text{for } t = 2, \dots, T_h \tag{Eq. 7}$$

Eqs. 8 and 9 express energy storage constraints for minimum state of charge (SOC) and maximum SOC, where E^s_{min} and E^s_{max} are the minimum and maximum allowable energy levels in energy storage, respectively.

$$E^s_{min} \leq E^s(t) \quad \text{for } t = 1, \dots, T_h \tag{Eq. 8}$$

$$E^s(t) \leq E^s_{max} \quad \text{for } t = 1, \dots, T_h \tag{Eq. 9}$$

Eq. 10 defines the initial energy stored energy, E^s_{init}, at the start of the time horizon.

$$E^s(1) = E^s_{init} \quad \text{(Eq. 10)}$$

Eqs. 11 and 12 ensure that charging and discharging rates of energy storage remain within limits specified by the battery manufacturer's C-rating, where $P^s_{c,max}$ is the C-rating when charging and $P^s_{d,max}$ is the C-rating when discharging. Both $P^s_{c,max}$ and $P^s_{d,max}$ are positive by convention.

$$0 \le P^s_c(t) \le P^s_{c,max} \quad \text{for } t = 1, \dots, T_h \quad \text{(Eq. 11)}$$

$$0 \le P^s_d(t) \le P^s_{d,max} \quad \text{for } t = 1, \dots, T_h \quad \text{(Eq. 12)}$$

Eq. 13 balances energy flows for energy storage, where P^s_{self} is the self-discharge rate, η^s_c is the charging efficiency, and η^s_d is the discharging efficiency.

$$E^s(t) = E^s(t-1) + \left(\eta^s_c P^s_c(t-1) - \frac{1}{\eta^s_d} P^s_d(t-1) - P^s_{self} \right) t_{hf} \quad \text{for } t = 2, \dots, T_h \quad \text{(Eq. 13)}$$

The "Big M" method was used to ensure energy storage does not simultaneously charge and discharge in the same time step. A description of the "Big M" optimization technique can be found in (Zhenzhen 2015). Eqs. 14 and 15 show constraints that utilize the "Big M" method, where B^s is a binary variable that describes if the energy storage is charging (1) or discharging (0), and M is any large number, chosen to be 1,000,000 for this optimization formulation.

$$P^s_c(t) \le B^s(t) M \quad \text{for } t = 1, \dots, T_h \quad \text{(Eq. 14)}$$

$$P_d^s(t) \leq (1 - B^s(t))M \quad \text{for } t = 1, \dots, T_h \qquad \text{(Eq. 15)}$$

Eqs. 16 and 17 ensure that power purchased or sold from the grid remains below the interconnection limit to the microgrid, where P_{max}^g is the maximum power that can be exchanged through the point of common coupling.

$$0 \leq P_{buy}^g(t) \leq P_{max}^g(t) \quad \text{for } t = 1, \dots, T_h \qquad \text{(Eq. 16)}$$

$$0 \leq P_{sell}^g(t) \leq P_{max}^g(t) \quad \text{for } t = 1, \dots, T_h \qquad \text{(Eq. 17)}$$

Eqs. 18 and 19 show constraints used in the "Big M" method to ensure that power is not simultaneously bought and sold to the grid in the same time step. The binary variable B^g describes if power is being purchased (1) or sold (0).

$$P_{buy}^g(t) \leq B^g(t)M \quad \text{for } t = 1, \dots, T_h \qquad \text{(Eq. 18)}$$

$$P_{sell}^g(t) \leq (1 - B^g(t))M \quad \text{for } t = 1, \dots, T_h \qquad \text{(Eq. 19)}$$

Eq. 20 expresses the maximum power demand seen by the grid over specified TOU periods of the time horizon, where TOU_n^{start} is the start of the TOU period, TOU_n^{stop} is the end of the TOU period, and N_{TOU} is the total number of time-of-use periods.

$$P_{buy}^g(t) \leq P_{max,n}^g \quad \text{for } t = TOU_n^{start}, \dots, TOU_n^{stop} \quad \text{for } n = 1, \dots, N_{TOU} \qquad \text{(Eq. 20)}$$

Eqs. 21 and 22 constrain the dispatch of controllable loads. Eq. 21 ensures that only a specified amount of load can be added to any time step, where max_{shift} is the maximum load allowed to be added to any time step. The maximum load allowed to be shifted to any time step is defined in Eq. 22 in which the total amount of controllable load at any time in

the optimization horizon must be less than the forecasted maximum controllable load over the full timeframe of the simulation, T_{sim}. Eq. 23 ensures that the total amount of dispatched controllable load is equal to the total amount of the forecasted controllable load over the specified time horizon.

$$0 \leq P^{cont}(\mathrm{t}) \leq P_{for}^{cont}(t) + max_{shift}(t) \quad \text{for } t = 1, \dots, T_h \tag{Eq. 21}$$

$$max_{shift}(t) = \left(\max_{k=1,\dots,T_{sim}} P_{for}^{crit}(k)\right) - P_{for}^{cont}(t) \quad \text{for } t = 1, \dots, T_h \tag{Eq. 22}$$

$$\sum_{t=1}^{T} P^{cont}(\mathrm{t}) = \sum_{t=1}^{T} P_{for}^{cont}(t) \quad \text{for } t = 1, \dots, T_h \tag{Eq. 23}$$

3.2.3. Model Predictive Control with Ancillary Services

Model predictive control with ancillary services expands the mathematical development described in section 2.2 to include additional variables, constraints, and an expanded objective function that includes terms for revenue from ancillary services.

3.2.3.1. Objective Function

The objective function described in Eq. 24 includes ancillary services as an expansion to Eq. 1. Here, C_{spin}^{g} is the compensation price for supplying spinning reserve to the grid, P_{spin}^{g} is the capacity of the spinning reserve bid, C_{nspin}^{g} is the compensation price for supplying non-spinning reserve to the grid, P_{nspin}^{g} is the capacity of the non-spinning reserve bid, C_{rep}^{g} is the compensation price for supplying replacement reserve to the grid, and P_{rep}^{g} is the capacity of the replacement reserve bid. These ancillary services

provide revenue only, and hence are represented in Eq. 23 as reducing the objective function being minimized.

$$
\begin{aligned}
J: = \sum_{t=1}^{T_h} \Bigg(\Big(\Big(C_{f,a}^{dg} + C_{OM}^{dg} \Big) P^{dg}(t) + C_{f,b}^{dg} B^{dg}(t) \Big) t_{hf} \\
+ \big(C_{OM}^{s} P_c^{s}(t) + C_{OM}^{s} P_d^{s}(t) \big) t_{hf} \\
+ \Big(C_{e,buy}^{g}(t) P_{buy}^{g}(t) - C_{e,sell}^{g}(t) P_{sell}^{g}(t) \Big) t_{hf} \\
+ \Big(-C_{spin}^{g}(t) P_{spin}^{g}(t) - C_{nspin}^{g}(t) P_{nspin}^{g}(t) \\
- C_{rep}^{g}(t) P_{rep}^{g}(t) \Big) t_{hf} \Bigg) + \frac{T_h}{T_{bp}} \sum_{n=1}^{N_{TOU}} C_{dem,n}^{g} P_{max,n}^{g}
\end{aligned}
\qquad \text{(Eq. 24)}
$$

3.2.3.2. Constraints

Eqs. 25 and 26 ensure that the spinning reserve capacity bid can be met if called upon by imposing maximum limits, subject to physical operational limitations of each asset. Both equations are used to linearize a minimization function to select the lower value of the sum of the total energy stored in the energy storage and charging power (described in Eq. 25) and the maximum discharging rate of the energy storage (described in Eq. 26). This linearization is necessary to ensure that the classification of the optimization formation is maintained, and the optimization correctly solves. These equations ensure that the spinning reserve bid must be less that the maximum possible capacity provided by a combination of the energy storage, distributed generators, and controllable loads. Eqs. 27 and 28 constrain the capacity contribution of the distributed generator for the spinning reserve bid. Eq. 27 accounts for generator headroom and Eq. 28 accounts for generator ramp rate if the generator is online and able to provide spinning reserve. These equations reflect asset status using a binary variable, B^{dg}, indicating the generator must be online and synced with the grid to be eligible to bid into the spinning reserve market.

$$P_{spin}^{g}(t) \leq \left(\frac{E^{s}(t) - E_{min}^{s}}{t_{hf}} + P_{c}^{s}(t)\right) B_{spin}^{s}(t) + P_{spin}^{dg}(t) + P^{cont}(t) B_{spin}^{cont}(t) \quad \text{for } t = 1, \ldots, T_h \tag{Eq. 25}$$

$$P_{spin}^{g}(t) \leq \left(P_{d,max}^{s}\right) B_{spin}^{s}(t) + P_{spin}^{dg}(t) + P^{cont}(t) B_{spin}^{cont}(t) \quad \text{for } t = 1, \ldots, T_h \tag{Eq. 26}$$

$$0 \leq P_{spin}^{dg}(t) \leq \left(P_{max}^{dg} - P^{dg}(t)\right) B^{dg}(t) \quad \text{for } t = 1, \ldots, T_h \tag{Eq. 27}$$

$$P_{spin}^{dg}(t) \leq P_{ramp}^{dg} B^{dg}(t) \quad \text{for } t = 1, \ldots, T_h \tag{Eq. 28}$$

Eqs. 29 and 30 and Eqs. 32 and 33 are similar to Eqs. 25 and 26 but instead of constraining the capacity bids for spinning reserve Eqs. 29 and 30 constrain the capacity bids for non-spinning reserve and Eqs. 32 and 33 constrain the capacity bids for replacement reserve. Eq. 31 and 34 ensure that the capacity contribution of the distributed generator can only be provided for either non-spinning reserve or replacement reserve if the generator is offline and unsynchronized with the grid.

$$P_{nspin}^{g}(t) \leq \left(\frac{E^{s}(t) - E_{min}^{s}}{t_{hf}} + P_{c}^{s}(t)\right) B_{nspin}^{s}(t) + P_{nspin}^{dg}(t) B_{nspin}^{dg}(t) + P^{cont}(t) B_{nspin}^{cont}(t) \quad \text{for } t = 1, \ldots, T_h \tag{Eq. 29}$$

$$P_{nspin}^{g}(t) \leq \left(P_{d,max}^{s}\right) B_{nspin}^{s}(t) + P_{nspin}^{dg}(t) B_{nspin}^{dg}(t) + P^{cont}(t) B_{nspin}^{cont}(t) \quad \text{for } t = 1, \ldots, T_h \tag{Eq. 30}$$

$$0 \leq P_{nspin}^{dg}(t) \leq P_{\max}^{dg}\left(1 - B^{dg}(t)\right) \quad \text{for } t = 1, \ldots, T_h \tag{Eq. 31}$$

$$P_{rep}^{g}(t) \leq \left(\frac{E^{s}(t) - E_{min}^{s}}{t_{hf}} + P_{c}^{s}(t)\right) B_{rep}^{s}(t) + P_{rep}^{dg}(t) B_{rep}^{dg}(t) + P^{cont}(t) B_{rep}^{cont}(t) \quad \text{for } t = 1, \ldots, T_h \tag{Eq. 32}$$

$$P_{rep}^{g}(t) \leq \left(P_{d,max}^{s}\right) B_{rep}^{s}(t) + P_{rep}^{dg}(t) B_{rep}^{dg}(t) + P^{cont}(t) B_{rep}^{cont}(t) \quad \text{for } t = 1, \ldots, T_h \tag{Eq. 33}$$

$$0 \leq P_{rep}^{dg}(t) \leq P_{\max}^{dg}\left(1 - B^{dg}(t)\right) \quad \text{for } t = 1, \ldots, T_h \qquad \text{(Eq. 34)}$$

Eqs. 35 through 37 ensure that reserve capacity provided by each unique energy asset is not bid for multiple ancillary services by summing the binary variables for each type of reserve (e.g., B_{spin}^{s}, B_{nspin}^{s}, B_{rep}^{s}). Eq. 36 constrains distributed generator bids for each ancillary service but does not include a spinning binary variable because Eqs. 27, 28, 31, and 34 ensure that the distributed generator only provides spinning reserve if it is on (i.e. $B^{dg} = 1$) and non-spinning and replacement reserve if it is off (i.e. $B^{dg} = 0$).

$$B_{spin}^{s}(t) + B_{nspin}^{s}(t) + B_{rep}^{s}(t) \leq 1 \quad \text{for } t = 1, \ldots, T_h \qquad \text{(Eq. 35)}$$

$$B_{nspin}^{dg}(t) + B_{rep}^{dg}(t) \leq 1 \quad \text{for } t = 1, \ldots, T_h \qquad \text{(Eq. 36)}$$

$$B_{spin}^{cont}(t) + B_{nspin}^{cont}(t) + B_{rep}^{cont}(t) \leq 1 \quad \text{for } t = 1, \ldots, T_h \qquad \text{(Eq. 37)}$$

Eqs. 38 through 40 ensure that capacities of reserve bids are greater than the minimum threshold bid and below the maximum possible bid for each ancillary service, where $res_{spin,min}$, $res_{nspin,min}$, and $res_{rep,min}$ are the minimum capacity bids for spinning, non-spinning, and replacement reserve, respectively, and $res_{spin,max}$, $res_{nspin,max}$, and $res_{rep,max}$ are the maximum capacity bids for spinning, non-spinning, and replacement reserve, respectively. Binary variables, $B_{spin}^{g}(t)$, $B_{nspin}^{g}(t)$, and $B_{rep}^{g}(t)$ are used to allow the microgrid to not participate in each respective ancillary service market if it is uneconomical or the minimum capacity requirements cannot be met.

$$res_{spin,min}(t)B_{spin}^{g}(t) \leq P_{spin}^{g}(t) \leq res_{spin,max}(t)B_{spin}^{g}(t) \quad \text{for } t = 1, \ldots, T_h \qquad \text{(Eq. 38)}$$

$$res_{nspin,min}(t)B^{g}_{nspin}(t) \leq P^{g}_{nspin}(t) \leq res_{nspin,max}(t)B^{g}_{nspin}(t) \quad \text{for } t = 1, \dots, T_h \tag{Eq. 39}$$

$$res_{rep,min}(t)B^{g}_{rep}(t) \leq P^{g}_{rep}(t) \leq res_{rep,max}(t)B^{g}_{rep}(t) \quad \text{for } t = 1, \dots, T_h \tag{Eq. 40}$$

3.3. Evaluation Metrics

Six technical metrics and five economics metrics are used to evaluate performance of microgrid control algorithms. Technical metrics include the load factor, capacity bids of each ancillary service, energy throughput of energy storage, operating hours of the distributed generator, the maximum power sold to the grid, and the maximum power purchased from the grid. Economic metrics include revenue from selling energy, revenue from participation in ancillary service market, expenses from purchasing energy, expenses from demand charges, and net operation and maintenance costs.

Eqs. 41 and 42 show revenue from selling energy to the grid, R^{m}_{sell}, and revenue from participation in ancillary service markets, R^{m}_{as}, respectively, where m denotes microgrid and g denotes the main electric grid. These metrics are derived from the revenue terms within the objective function displayed in Eq. 24.

$$R^{m}_{sell} = \sum_{t=1}^{T_{sim}} C^{g}_{e,sell}(t)P^{g}_{sell}(t)t_{hf} \tag{Eq. 41}$$

$$R^{m}_{as} = \sum_{t=1}^{T_{sim}} C^{g}_{spin}(t)P^{g}_{spin}(t)t_{hf} + C^{g}_{nspin}(t)P^{g}_{nspin}(t)t_{hf} + C^{g}_{rep}(t)P^{g}_{rep}(t)t_{hf} \tag{Eq. 42}$$

Eqs. 43 and 44 calculate energy charges, C^{m}_{buy}, and demand charges, C^{m}_{dem}, associated to utility rate structures, where N_{bp} is the total number of billing periods within the simulation period.

$$C_{buy}^{m} = \sum_{t=1}^{T_{sim}} C_{e,buy}^{g}(t) P_{buy}^{g}(t) t_{hf} \quad \text{(Eq. 43)}$$

$$C_{dem}^{m} = \sum_{p=1}^{N_{bp}} \sum_{n=1}^{N_{TOU}} C_{dem,n}^{g} P_{max,n}^{g} \quad \text{(Eq. 44)}$$

Eq. 45 expresses the total operation and maintenance cost for all energy assets within the microgrid, C_{OM}^{m}, where C_{OM}^{ren} is the fixed operation and maintenance cost the solar PV generation.

$$C_{OM}^{m} = \sum_{t=1}^{T_{sim}} C_{OM}^{dg} P^{dg}(t) t_{hf} + \left(C_{OM}^{s} P_{c}^{s}(t) + C_{OM}^{s} P_{d}^{s}(t)\right) t_{hf} + C_{OM}^{ren} \quad \text{(Eq. 45)}$$

Eq. 46 represents the net operating expenses of the microgrid, C_{opex}^{m}. This is the primary economic metric used to evaluate finical benefits of the logic-based control and MPC algorithms. The fixed cost for being connected to the main grid is expressed as C_{fix}^{m}.

$$C_{opex}^{m} = C_{buy}^{m} + C_{dem}^{m} + C_{OM}^{m} + C_{fix}^{m} - R_{sell}^{m} - R_{as}^{m} \quad \text{(Eq. 46)}$$

Eqs. 47 through 55 show the technical evaluation metrics used to examine the operational behavior of the microgrid. Eqs. 47 and 48 calculate the load factor of the microgrid, LF^{m}, and the load factor for power exchange with the grid, LF^{g}, to express the utilization of distribution networks and service entrances.

$$LF^{m} = \frac{\frac{\sum_{t=1}^{T_{sim}} P^{cont}(t) + P_{for}^{crit}(t)}{T_{sim}}}{\max_{t=1,\ldots,T_{sim}} P^{cont}(t) + P_{for}^{crit}(t)} \quad \text{(Eq. 47)}$$

$$LF^{g} = \frac{\frac{\sum_{t=1}^{T_{sim}} P_{buy}^{g}(t)}{T_{sim}}}{\max_{t=1,\ldots,T_{sim}} P_{buy}^{g}(t)} \quad \text{(Eq. 48)}$$

Eqs. 49 through 51 describe capacity bids for each of the ancillary service types, where CB_{spin}^{m} is the sum of all spinning reserve capacity bids for, CB_{nspin}^{m} is the sum of all non-spinning reserve capacity bids, and CB_{rep}^{m} is the sum of all replacement reserve capacity bids.

$$CB_{spin}^{m} = \sum_{t=1}^{T_{sim}} P_{spin}^{g}(t) t_{hf} \quad \text{(Eq. 49)}$$

$$CB_{nspin}^{m} = \sum_{t=1}^{T_{sim}} P_{nspin}^{g}(t) t_{hf} \quad \text{(Eq. 50)}$$

$$CB_{rep}^{m} = \sum_{t=1}^{T_{sim}} P_{rep}^{g}(t) t_{hf} \quad \text{(Eq. 51)}$$

Eq. 52 calculates the total energy throughput of energy storage, $E_{T_{sim}}^{s}$. Reducing energy throughput reduces O&M costs and can increase usable lifetime of the system before replacement.

$$E_{T_{sim}}^{s} = \sum_{t=1}^{T_{sim}} \left(P_{c}^{s}(t) + P_{d}^{s}(t)\right) t_{hf} \quad \text{(Eq. 52)}$$

Eq. 53 calculates generator operating hours, OH_{sim}^{dg}. It is typically not economical to run the generator during normal grid-tied operation, however, a generator can gain revenue from non-spinning reserve when not operating, and could provide peak shaving, energy charge reduction, and spinning reserve when turned online.

$$OH_{sim}^{dg} = \sum_{t=1}^{T_{sim}} B^{dg}(t) t_{hf} \quad \text{(Eq. 53)}$$

Eqs. 54 and 55 describe the last two technical evaluations metrics, the maximum power sold to the grid, $P_{sell,max}^{g}$, and the maximum power purchased from the grid, $P_{buy,max}^{g}$.

$$P^{g}_{sell,max} = \sum_{t=1}^{T_{sim}} P^{g}_{sell}(t) \quad \text{(Eq. 54)}$$

$$P^{g}_{buy,max} = \sum_{t=1}^{T_{sim}} P^{g}_{buy}(t) \quad \text{(Eq. 55)}$$

3.4. Microgrid Portfolio

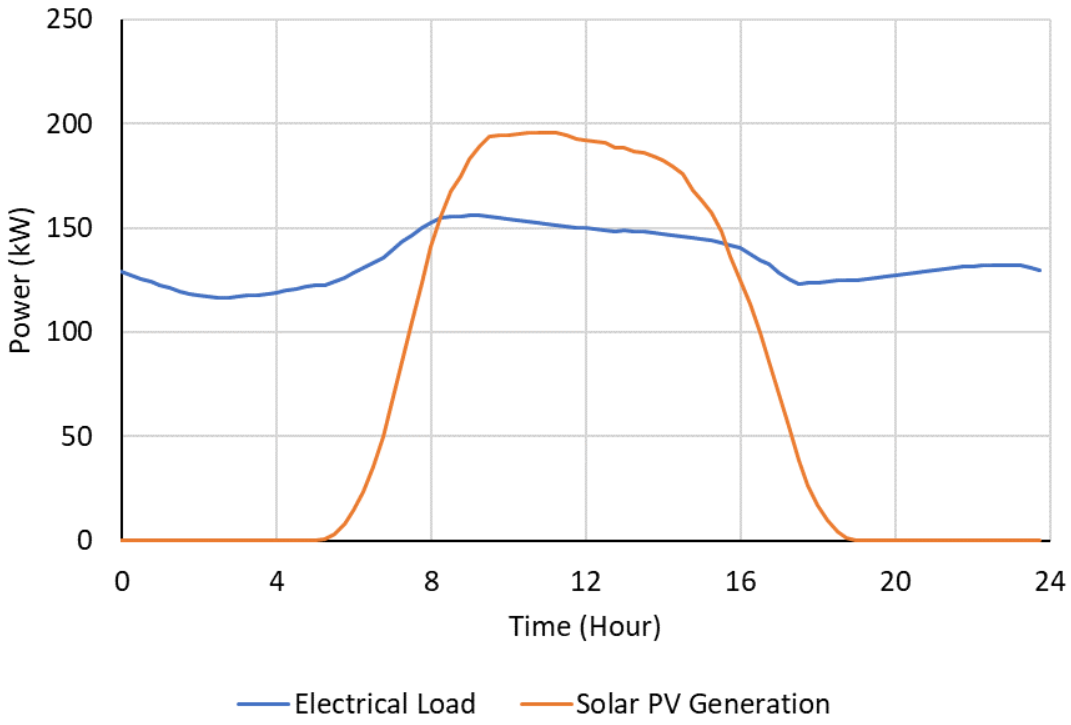
A microgrid was designed to serve an office building on the Arizona State University (ASU) campus with existing solar PV assets. A diesel generator and batteries were included in the simulation to ensure that critical loads could be served in the event of a grid outage. These assets can also participate in ancillary service markets.

3.4.1. Microgrid Specification Data

Electrical load and solar PV generation data for the ASU Fulton Center were collected from Campus Metabolism (Arizona State University, n.d.), a public resource including 15-minute data on over 400 buildings at ASU. Table 3.1 summarizes annual statistics with Fig. 3.2 showing the average annual 24-hour electrical load and solar PV generation profiles. The average annual load factor of the building is 0.43. This study assumes that 20% of the load can be controlled and shifted for building cooling and heating. Solar PV generates more power than the building consumes for 27.4% of time in a year, with the excess energy sold back to the grid at the wholesale rate.

Table 3.1: Annual statistics of electrical load and solar PV generation for the ASU Fulton Center.

Variable	Electrical Load	Solar PV
Peak (kW)	316	326 AC / 386 DC
Annual Total Energy (MWh)	1181.4	633.4



3.2: Average annual electrical load and on-site solar PV generation of the ASU Fulton Center.

The microgrid includes a lithium-ion (Li-ion) battery system that stores excess solar generation for local use to reduce energy and demand charges. The batteries can also participate in ancillary service markets to gain revenue according to FERC Order No. 841 (United States of America Federal Energy Regulatory Commission 2018). The 634-kWh battery system was sized to meet the max annual demand for a two-hour duration. Characteristics of a generic Li-ion battery technology were taken from (Lazard 2018) and (Few et al. 2018) for the following key parameters: $E^s_{min} = 10\%$, $E^s_{max} = 100\%$, $P^s_{c,max} = P^s_{d,max} = 1$ C (634 kW), $\eta^s_{self} = 0.001\%/\text{hr}$, $\eta^s_c = \eta^s_d = 94.9\%$, and $C^s_{OM} = 0.027917\$/\text{kWh}$.

A 350-kW diesel generator was selected to provide backup power to meet 110% of annual peak. This generator was included for illustration purposes; statistics from ASU

(Arizona State University, n.d.) and Arizona Public Service (APS) show negligible outages in the area (Office of Public Accountability/Ratepayer Advocate 2018). Generator variable operation and maintenance cost was 0.005 $/kWh (Power 2016) with additional cost for diesel fuel at 0.82 $/liter (The World Bank, n.d.). Manufacturer data on fuel consumption for the Generac SD350 (Generac Industrial Power 2012) were used in a linear-regression to calculate the following parameters with an R-squared value of 0.9987: $C_{f,a}^{dg} = 0.1998\$/\text{kWh}$, $C_{OM}^{dg} = 0.005\$/\text{kWh}$, and $C_{f,b}^{dg} = 9.307\$/\text{hr}$.

3.4.2. Electric Rate Structure

Table 3.2 summarizes the E-32TOU M time-of-use (TOU) electric rate structure for a medium customer (100-400 kW) in APS service territory. Energy prices and demand charges occur using two seasonal time periods, winter and summer, with different on-peak and off-peak rates applied to the same TOU periods. The rate structure uses tiered demand charges. However, only the first-tier price is used as the associated demand charge parameter to preserve the linearity of the optimization formulation.

Table 3.2: Charges for the APS E-32TOU M rate structure (Arizona Public Service 2017).

Charge Description	TOU Period	Value
Energy Price Off-Peak (Nov-Apr)	Weekdays: 8pm-3pm; Weekends: All day	0.04566 $/kWh
Energy Price On-Peak (Nov-Apr)	Weekdays: 3pm-8pm	0.05783 $/kWh
Energy Price Off-Peak (May-Oct)	Weekdays: 8pm-3pm; Weekends: All day	0.05953 $/kWh
Energy Price On-Peak (May-Oct)	Weekdays: 3pm-8pm	0.07170 $/kWh
Demand Charge Off-Peak, First 100 kW (Nov-Apr)	Weekdays: 8pm-3pm; Weekends: All day	6.742 $/kW
Demand Charge Off-Peak, All Additional KW (Nov-Apr)	Weekdays: 3pm-8pm	3.327 $/kW
Demand Charge Off-Peak, First 100 kW (May-Oct)	Weekdays: 8pm-3pm; Weekends: All day	18.190 $/kW
Demand Charge On-Peak, All Additional KW (May-Oct)	Weekdays: 3pm-8pm	11.744 $/kW
Service Charge	-	1.16 $/day
Country and City Tax	-	2.5%
County and State Tax	-	5.6%

3.4.3. Ancillary Service Market

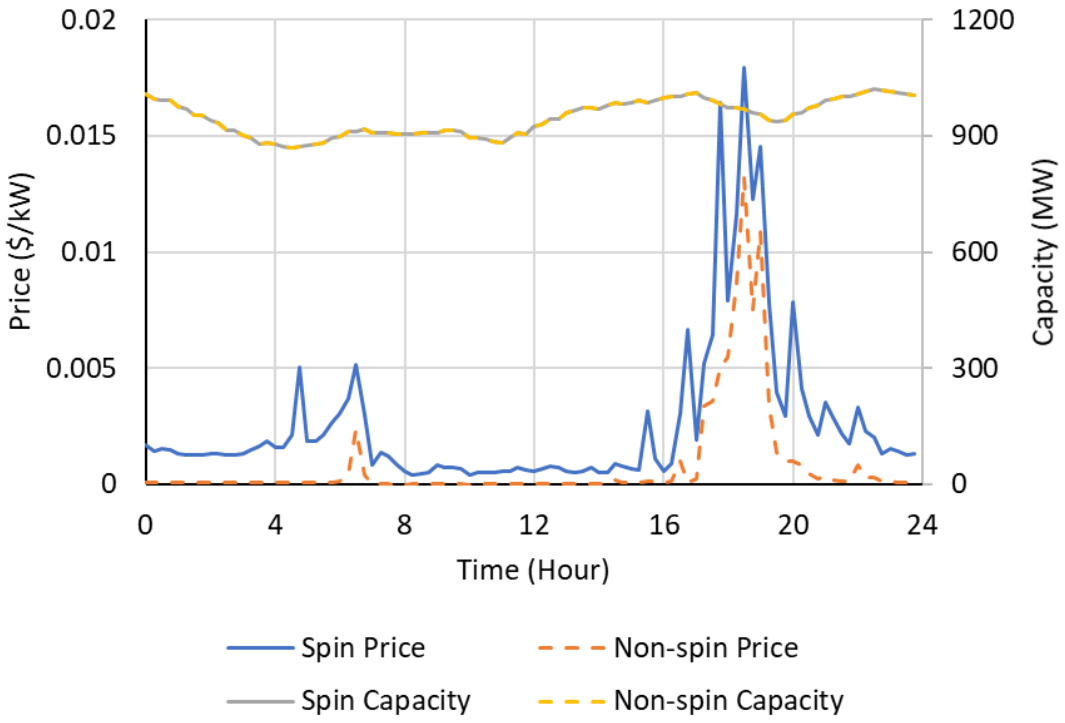
RTOs and ISOs administer regional wholesale electricity markets and provide reliability planning for regions within the three interconnection areas of North America (Hoffman and Streit 2015). These markets coordinate both day-ahead and real-time purchases of electric energy, electric power capacity, and ancillary services. In general, the RTOs/ISOs take bids in ascending order and stop accepting bids when the needed power or capacity is secured for a specified time interval (American Public Power Association 2018). All identified sellers within this time interval get compensated with the last bid price, also known as the clearing price.

Ancillary service clearing price and maximum capacity bid data for the California Independent System Operator (CAISO) territory were used to simulate participation in

spinning reserve and non-spinning reserve markets (California ISO, n.d.). In 2018, FERC issued Order 841 mandated that markets allow electric storage resources to participate in day-ahead and real-time markets for capacity, energy, and ancillary services (United States of America Federal Energy Regulatory Commission 2018). This additional technical capability and revenue stream can provide benefits to both customers/owners and utilities/regulatory organizations. Similar rules and regulations for generators, loads, and aggregated DERs are already in place in CAISO markets. This study assumes that minimum requirements are met for the aggregated generator, loads, and storage within the microgrid to participate in CAISO wholesale markets as detailed in (California ISO 2019). Participation in the replacement reserve market was omitted because replacement reserves in CAISO were suspended in 2002.

Fig. 3.3 shows the average annual 24-hour clearing price and capacity for CAISO's spinning reserve and non-spinning reserve markets. The maximum capacity bid for each market is nearly identical for all hours of the year because they are each calculated to ensure bids meet or exceed the minimum contingency operating reserve requirement in accordance with the North American Electric Reliability Corporation (NERC) and Western Electricity Coordination Council (WECC) reliability standards (California Independent System Operator 2018). However, the price for spinning reserve is almost always greater than the price for non-spinning reserve because assets providing spinning reserve are online and synchronized whereas assets providing non-spinning reserve are not. Prices peak in the late afternoon when the greatest reserves are required to compensate for the decline of renewables and coincident increase in load as customers are arriving home from work (California ISO 2012). Batteries and load control can provide spinning reserve because

they can be rapidly dispatched. The generator is primarily used to provide non-spinning reserve due to the relatively high cost of continuous operation but can provide spinning reserve when online. Solar PV can provide frequency and regulation reserves, but this functionality and market participation is outside the scope of this study. This study assumes that ancillary service bids are compensated on a capacity basis. It is also assumed that the spinning and non-spinning capacity bids are never called upon to be dispatched because these ancillary services are primarily used for contingency events that occur with relatively low frequency throughout a year (NERC 2019b). However, if these services were called upon and could not dispatch, the payment for the ancillary service would be rescinded as detailed in CAISO's Fifth Replacement Tariff (California Independent System Operator 2018).



3.3: Average annual required capacity and clearing price for the spinning and non-spinning reserve ancillary service markets in CAISO (California ISO, n.d.).

3.5. Annual Performance Evaluation and Sensitivity Analysis

Performance evaluations compare technical and financial metrics for logic-based control, MPC without ancillary services, and MPC with ancillary services. The efficacy of each control algorithm was evaluated and compared with respect to (i) the granularity of input data on 15 min., 30 min., and 60 min. time steps for load, solar PV generation, and pricing signals to quantify how model fidelity affects results, and (ii) the length of the prediction time horizon for both MPC methods including 24 hours, 48 hours, and 168 hours to quantify the value of forecasting and scheduling. Table 3.3 shows the total number of decision variables solved for each combination of time step size and prediction time horizon. As the total number of time steps increases so does the complexity of the optimization formulation. MPC without ancillary services algorithm and MPC with ancillary services algorithm use 13 and 30 decision variables per time step, respectively.

Table 3.3: Total number of decision variables solved in each iteration of MPC algorithms.

	Time Horizon		
Time Step Size	24 Hours (MPC without/with ancillary services)	48 Hours (MPC without/with ancillary services)	168 Hours (MPC without/with ancillary services)
15 min.	1,248 / 2,880	2,496 / 5,760	8,736 / 20,160
30 min.	624 / 1,440	1,248 / 2,880	4,368 / 10,080
60 min.	312 / 720	624 / 1,440	2,184 / 5,040

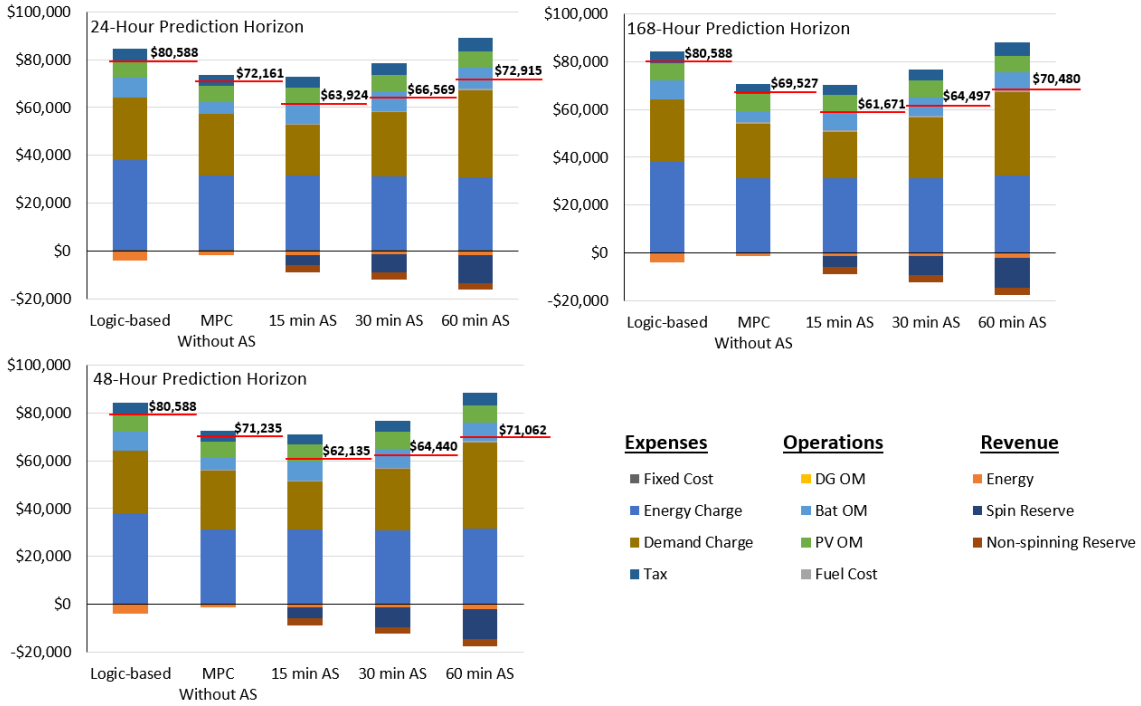
Demand charge components of electricity bills are traditionally applied using the maximum 15 min. average power draw over any 15 min. time period within a billing period. In this study, demand charges were applied to the maximum power draw over the specified time step size to maintain uniformity across all annual simulations (i.e., simulations using a time step size of 30 min. included demand charges for maximum monthly power draw over a 30 min. period).

Simulations of logic-based controls were conducted to provide baseline comparison data for the building microgrid. Logic-based control used real-time information to make dispatch decisions and therefore did not have a prediction time horizon. Resulting financial and technical metrics were found to be within ±2% for all time step sizes. This difference is primarily attributed to how demand charges are calculated for varying time step sizes, a difference that is negligible in the overall comparison to MPC methods. Therefore, average metrics for the three logic-based simulations are used throughout for comparison against MPC algorithms. A similar outcome was observed in annual metrics for MPC without ancillary services simulations with only a ±0.5% variation regardless of the duration of the specified time step size, however, results varied appreciably with the prediction time horizon. Therefore, the average metrics for MPC without ancillary services are used for each specified time horizon.

Fig. 3.4 compares annual operating expenses for each of the three control algorithms using a 24-hour, 48-hour, and 168-hour prediction time horizon. Compared to the baseline logic-based control, MPC without ancillary services can reduce net operating expenses by 10.46% to 13.73% across all three prediction time horizons, with a modest improvement observed for longer time horizons. If ancillary services are included in the MPC algorithm, operating expenses can be reduced by up to 23.47% using a 168-hour prediction time horizon with 15 min. time steps. These savings are attributed to reductions in demand charges and additional revenue from ancillary services.

Both MPC algorithms optimize dispatch of on-site assets to reduce grid energy expenditures by an average of 17.35% across all time steps and prediction time horizons when compared to the logic-based control algorithm. This is accomplished through better

utilization of the battery at storing excess solar for use rather than selling back to utility. Revenue generated from energy sell back is reduced by an average of 61.46%, but the 17.35% reduction in energy expenditures greatly outweigh the reduced revenue from selling excess solar. Shorter duration time steps always result in lower net operating expenses regardless of the length of the prediction time horizon. This indicates that more granular input data allow the MPC control algorithms to improve economic operation. Longer prediction time horizons resulted in lower net operating expenses for MPC algorithms with and without ancillary services. This suggests that longer duration forecasts improve the efficacy of the MPC algorithms due to the ability to optimize current operations with respect to future events.



3.4: Annual operating expenses for each of the logic-based, MPC without ancillary services, and MPC with ancillary services control algorithms using a 24-hour, 48-hour, and 168-hour prediction time horizon.

Longer duration time steps result in additional revenue being gained through participation in ancillary service markets when compared to shorter duration time steps. Tables 3.4 through 3.6 show that 60 min. time step simulations resulted in a 70.07% and 23.20% increase in spinning reserve bids and non-spinning reserve bids, respectively, when compared to the 15 min time steps. Tables 3.4 through 3.6 also show that the 60 min. time step simulations result in a 104.49% average increase in the maximum off-peak power bought from the gird when compared to the 15 min. time step simulations. This indicates longer time step simulations show tendencies to shift energy use to off-peak times to maximize participation in ancillary service markets. However, this behavior results in increased total operating expenses due to increased off-peak demand charges despite the fact that larger on-peak demand charges are avoided. High demand charges for 60 min. time step simulations for MPC with ancillary services also increase expenses beyond that of logic-based control, although the net operating expenses are lower than logic-based control due to additional revenue gained from ancillary services.

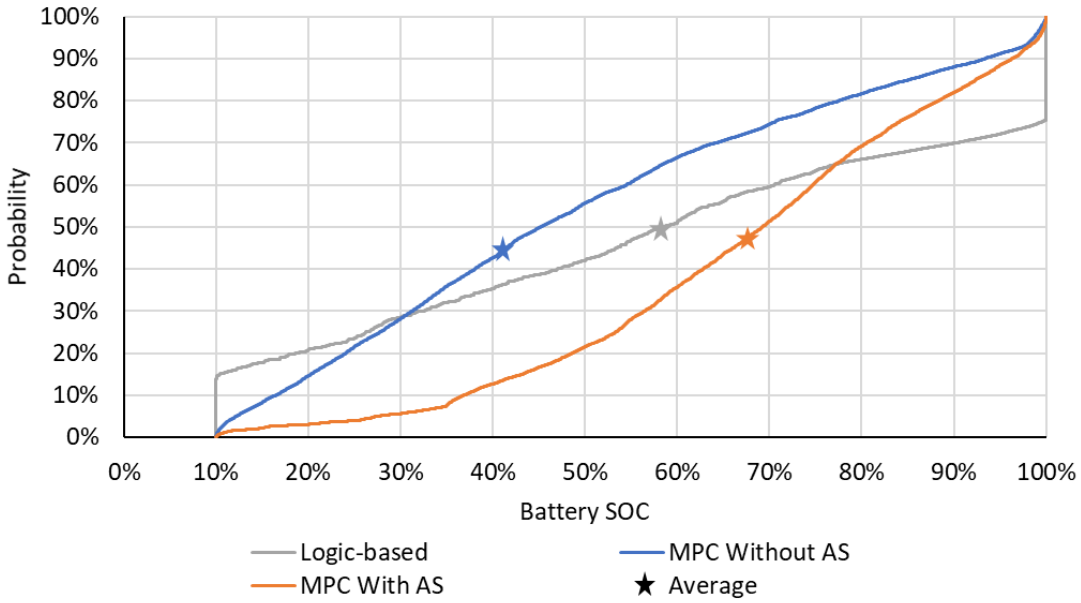
The microgrid load factor and grid load factor describe the utilization of the internal microgrid distribution network and the utilization of the interconnection between the microgrid and grid, respectively. The microgrid load factor increases modestly as the prediction time horizon increases, suggesting that the distribution network internal to the microgrid is more fully utilized when the control algorithms use longer prediction horizons. Logic-based control and MPC without ancillary services result in similar grid load factors but MPC with ancillary services algorithm reduces the grid load factor. This trend is intensified as the time step duration is increased to 60 min. time steps, due to the relatively large maximum power bought from the grid and results in an average reduction of 69.02%

in the grid load factor across all prediction time horizons. This indicates that the interconnection or point of common coupling (PCC) between the microgrid and the grid is less utilized for a microgrid using the MPC with ancillary service control algorithm.

3.5 shows the cumulative distribution function of the battery SOC and average battery SOC over the annual simulation for each algorithm using 15 min. time steps and a 168-hour time horizon for each of the MPC approaches. MPC without AS maintains the battery at a lower SOC than logic-based control, and cycles 41.09% and 37.77% less energy through the batteries when compared to the logic-based and MPC with ancillary services algorithms, respectively. This indicates that battery operation and maintenance terms within the objective function play a more dominate role in asset dispatch when ancillary service market participation is not considered. This behavior results in a 61.00% decrease in battery operation and maintenance costs when comparing the MPC without ancillary service algorithm to MPC with ancillary service algorithm. 3.5 shows that MPC with ancillary services maintains a higher battery SOC than either of the other two algorithms to gain more revenue through spinning and non-spinning reserve markets.

Both MPC algorithms use the generator to perform peak shaving and minimize demand charges for a modest amount in the year. An average of 93% of the total generator operating hours were during on-peak times when using the MPC with ancillary service algorithms to minimize energy expenditures and demand charges. However, the remaining 7% of the operating hours were during off-peak times when spikes in the spinning reserve price resulted in substantial revenue potential. Enabling market participation creates additional economic incentive to operate traditional stand-by generators as shown in the

greater total generator operating hours when participation in ancillary service markets is considered.



3.5: Annual cumulative distribution and average battery SOC for the logic-based, MPC without ancillary services, and MPC with ancillary services control algorithms using a 15 min. time step and 168-hour prediction time horizon.

Table 3.4: Statistics for annual simulation using 24-hour prediction time horizon.

Control Strategy	Microgrid Load Factor (%)	Grid Load Factor (%)	Total Spinning Bids (MWh)	Total Non-spinning Bids (MWh)	Battery Energy Throughput (MWh)	Generator Operating Time (Hours)	Max Grid Sell (kW)	Max Grid Buy (kW) (On-peak/Off-peak)
Logic-based	43.19	26.12	0	0	292	0.00	221	319/312
Without AS	45.16	26.39	0	0	173	5.00	227	230/266
15 min. AS	44.92	16.54	610	1,336	290	18.75	233	122/434
30 min. AS	44.72	12.03	12,919	1,415	303	19.00	229	122/587
60 min. AS	44.48	7.95	19,649	1,656	317	25.00	224	123/878

Table 3.5: Statistics for annual simulation using 48-hour prediction time horizon.

Control Strategy	Microgrid Load Factor (%)	Grid Load Factor (%)	Total Spinning Bids (MWh)	Total Non-spinning Bids (MWh)	Battery Energy Throughput (MWh)	Generator Operating Time (Hours)	Max Grid Sell (kW)	Max Grid Buy (kW) (On-peak/Off-peak)
Logic-based	43.19	26.12	0	0	292	0.00	221	319/312
Without AS	46.27	27.67	0	0	177	6.50	228	230/252
15 min. AS	44.85	16.31	773	1,230	283	20.00	233	57/434
30 min. AS	45.62	11.98	1,449	1,425	284	20.50	220	51/587
60 min. AS	45.39	8.17	2,417	1,735	282	29.00	222	74/881

Table 3.6: Statistics for annual simulation using 168-hour prediction time horizon.

Control Strategy	Microgrid Load Factor (%)	Grid Load Factor (%)	Total Spinning Bids (MWh)	Total Non-spinning Bids (MWh)	Battery Energy Throughput (MWh)	Generator Operating Time (Hours)	Max Grid Sell (kW)	Max Grid Buy (kW) (On-peak/Off-peak)
Logic-based	43.19	26.12	0	0	292	0.00	221	319/312
Without AS	48.60	31.76	0	0	173	22.00	222	214/221
15 min. AS	48.27	16.46	669	1,340	278	27.75	228	66/434
30 min. AS	46.71	12.20	1,422	1,469	275	29.00	219	51/587
60 min. AS	48.95	8.16	2,498	1,700	266	33.00	221	51/901

3.6. Intraday Dispatch

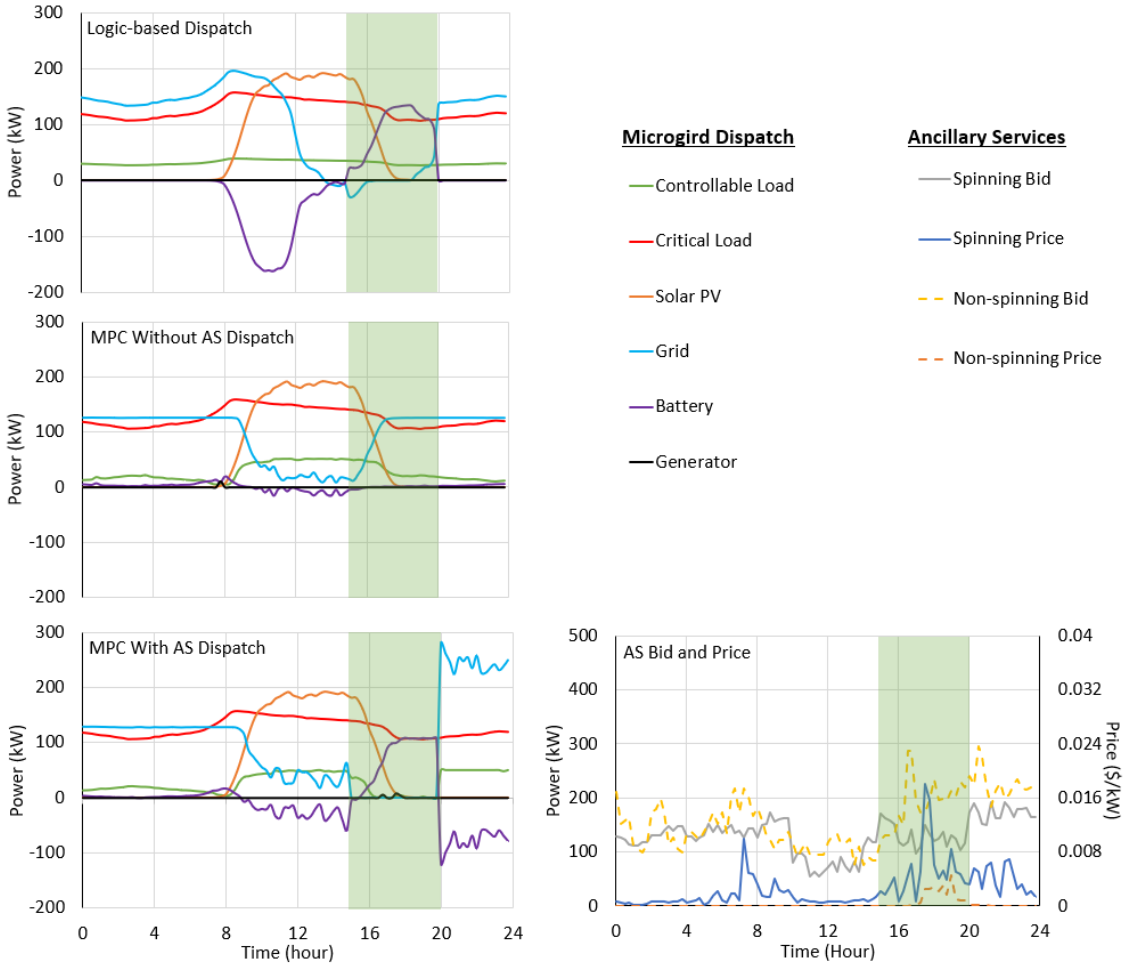
Causes of annual trends are explored in detail through examining intraday dispatch behavior. Examples shown use a 15 min. time step and both MPC algorithms use a 168-hour prediction time horizon because those conditions provided the lowest net annual operating expenses. Simulations were performed for the months of January and July to illustrate the effects of different environmental conditions, load profile, and pricing signals for each control algorithm.

Fig. 3.6 shows intraday dispatch for an average weekday in January with Table 3.7 providing a quantitative summary of results from all three control algorithms. The logic-based control algorithm charges the battery as soon as there is solar PV generation available and discharges the battery during on-peak times to reduce energy expenses and demand charges. This results in 88.38% and 9.64% more energy cycled through the batteries when compared to the MPC without ancillary services and MPC with ancillary service algorithms, respectively, for the average weekday in January.

MPC without ancillary services periodically charges the battery during off-peak times when there is solar PV generation and shifts controllable load to times of the day when solar PV generation is greater than the critical load. However, any excess solar PV beyond the critical load is diverted to controllable load rather than being used to charge batteries, and as solar PV declines, the controllable load is reduced to maintain a constant peak demand as shown in Fig. 3.6. This behavior can be attributed to the relatively short length of PV generation (approximately 9 hours) and the battery operation and maintenance terms within the objective function that dissuades cycling the battery. Unlike the logic-based dispatch, MPC without ancillary services regulates the controllable load throughout

the day to achieve load leveling and reduce demand charges. This results in a relatively consistent microgrid load factor and grid load factor across.

MPC with ancillary service shows some similarities to the logic-based dispatch in that the battery is charged with solar PV and the battery is discharged during on-peak times to minimize energy and demand charges. The controllable load is shifted to times of day with excess solar PV and off-peak times, similar to MPC without ancillary services. However, after on-peak times conclude for a day, the dispatch algorithm charges batteries with low price energy and thereby increases state of charge to gain more revenue through ancillary service bids. This creates a 30.09% and 55.00% percent increase in off-peak demand when compared to the logic-based and MPC without ancillary service algorithms, respectively. Yet, the optimization solver calculates that the additional revenue off sets the resulting additional demand charges.



3.6: January weekday dispatch of microgrid using logic-based, MPC without ancillary services, and MPC with ancillary services control algorithms. Green shaded region indicates the on-peak time of the TOU rate structure.

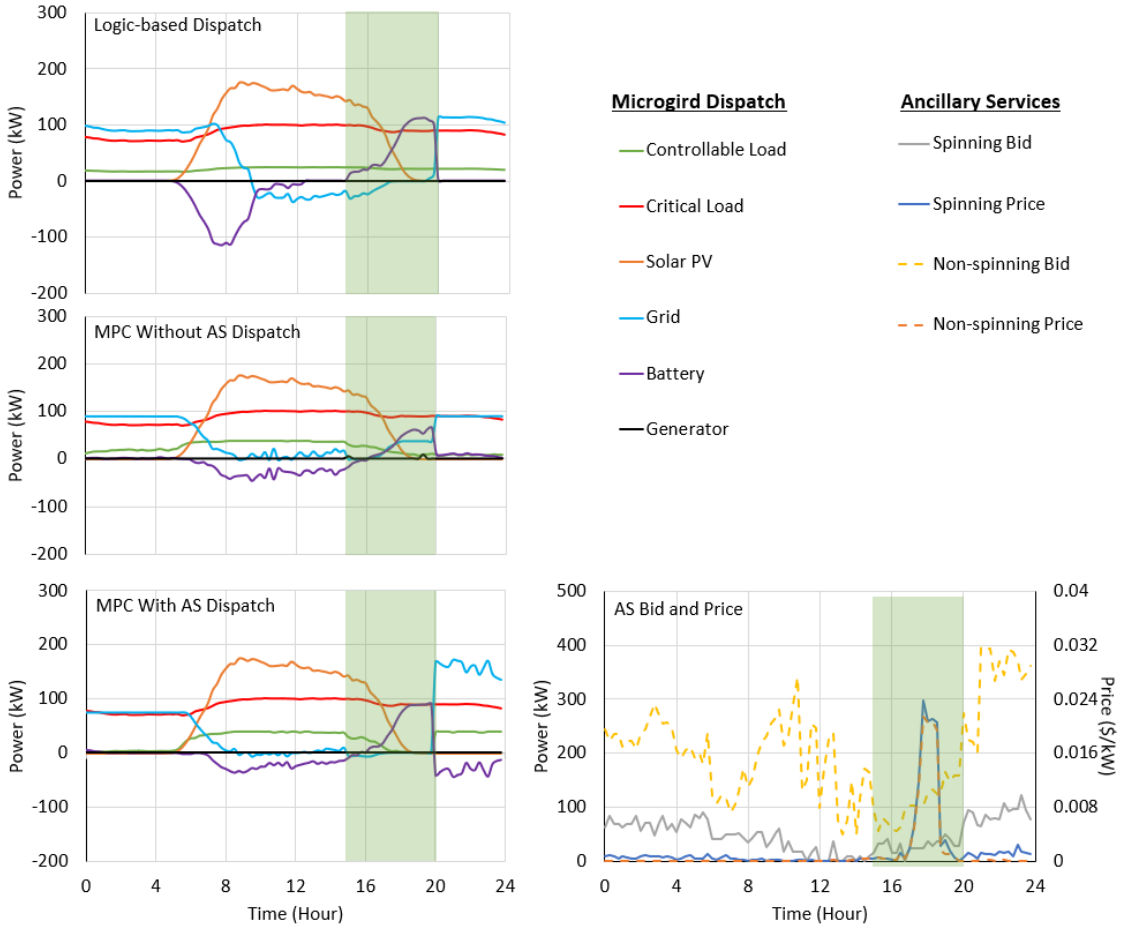
Table 3.7: Statistics for average weekday in January for a 168-hour prediction time horizon.

Control Strategy	Microgrid Load Factor (%)	Grid Load Factor (%)	Total Spinning Bids (kWh)	Total Non-spinning Bids (kWh)	Battery Energy Throughput (kWh)	Generator Operating Time (Hours)	Max Grid Sell (kW)	Max Grid Buy (kW) (On-peak/Off-peak)
Logic-based	80.02	54.95	0	0	3,960	0.00	29	43/196
15 min. Without AS	76.08	77.03	0	0	464	0.25	12	126/126
15 min. With AS	76.95	35.89	12,514	15,505	3,578	0.25	4	0/280

Fig. 3.7 shows intraday dispatch for an average weekday in July with Table 3.8 providing a quantitative summary of results from all three control algorithms. Similar trends from January remain in July. All three algorithms reduce on-peak energy use and peak demand by discharging batteries during on-peak times. Both MPC algorithms charge batteries at a slower rate and over a longer duration when compared to the logic-based algorithm.

MPC without ancillary services shows similar off-peak behavior in July and January, but the on-peak behavior in July more closely resembles the logic-based and MPC with ancillary service while in January the battery was not dispatched during on-peak hours. For July, the controllable load is reduced and batteries are discharged during on-peak times to minimize energy charges and reduce on-peak demand by 59.03% relative to off-peak demand. This behavior shows that the optimization-based control algorithms adapts to differences in environmental conditions (e.g. solar PV available for 4 additional hours when compared to January) and pricing signals (e.g. greater on-peak energy charges when compared to January). The behavior of the MPC with ancillary services algorithm in July is similar to the behavior exhibited in January but the off-peak demand seen after the

on-peak TOU period is reduced by 38.90% because the battery achieves a greater SOC with excess solar during the afternoon. In July, total spinning bids are reduced by 170.79% and total non-spinning bids are increased by 18.86% when compared to ancillary service market participation in January. This occurs because the average price for spinning reserve is smaller in July whereas the average price for non-spinning reserve is greater in July, creating different battery and generator dispatch behavior.



3.7: July weekday dispatch of microgrid using logic-based, MPC without ancillary services, and MPC with ancillary services control algorithms. Green shaded region indicates the on-peak time of the TOU rate structure.

Table 3.8: Statistics for average weekday in July for a 168-hour prediction time horizon.

Control Strategy	Microgrid Load Factor (%)	Grid Load Factor (%)	Total Spinning Bids (kWh)	Total Non-spinning Bids (kWh)	Battery Energy Throughput (kWh)	Generator Operating Hours (Hours)	Max Grid Sell (kW)	Max Grid Buy (kW) (On-peak/Off-peak)
Logic-based	86.91	49.36	0	0	2,609	0.00	41	12/113
15 min. Without AS	80.37	55.44	0	0	1,886	0.25	15	37/89
15 min. With AS	79.65	29.21	4,621	19,110	2,245	0.25	12	0/171

3.7. Conclusions

This study developed a logic-based control algorithm and two optimization-based control algorithms to minimize operational expenses of microgrids. The model predictive control approach optimally dispatch microgrid assets with respect to asset characteristics, pricing signals, environmental conditions, loads, and uncertainty in the underlying data. Expansions to existing model predictive control research enabled participation in ancillary service markets. A commercial building on the Arizona State University (ASU) campus was selected as the case study with to compare technical and financial results. Significant findings include:

- Model predictive controls can reduce net operating expenses for a microgrid by up to 13.73% when compared to logic-based controls. Expanding the formulation to include participation in real-time ancillary service markets can further reduce net operating expenses by up to 23.47%.
- The MPC algorithms can reduce grid energy expenditures and demand charges by up to 17.58% and 25.89%, respectively, when compared to a logic-based algorithm. The MPC operational behavior reduces total annual operating expenses

by optimally using on-site generation to meet local loads instead of exporting back to the grid.

- The MPC without ancillary service reduces energy sale revenue by up to 66.57% when compared to the logic-based algorithm. The MPC with ancillary service reduces energy sale revenue by up to 67.01% when compared to the logic-based algorithm but can increase the total operational revenue by up to 354.34% through participation in real-time energy markets.
- MPC algorithms with longer duration time steps provide additional revenue through ancillary service markets when compared to shorter duration time steps. The longer duration time steps display tendencies to arbitrage energy during off-peak times to maximize participation in ancillary service markets.
- MPC with ancillary services increased off-peak demand by 118.59% and 308.40% when compared to the logic-based and MPC without ancillary service algorithms, respectively. This behavior resulted in the grid load factor being decreased by 68.78% and 74.31%, respectively. This behavior could potentially require upgrades to the interconnection between the microgrid and the grid to accommodate the larger power exchange.
- For an average weekday in January, a logic-based algorithm cycles 88.38% and 9.64% more energy through the batteries when compared to the MPC without ancillary services and MPC with ancillary service algorithms, respectively. This behavior increases the associated O&M expenses and can potentially negatively affect battery longevity.

- MPC with ancillary services maintained the battery state of charge an average of 38.78% higher than a battery dispatched by MPC without ancillary services. This behavior minimizes O&M expense associated with battery cycling and increased revenue through participation in spinning and non-spinning reserve markets.
- Both MPC algorithms sparingly dispatch the generator to perform peak shaving and minimize demand charges. Enabling market participation creates additional economic incentive and increased generator operating hours by average of 13.5 hours per year.
- Simulations for an average weekday in July showed that the MPC with ancillary services algorithm reduced participation in the spinning reserve market and increases participation in non-spinning reserve market by 170.79% and 18.86%, respectively, when comparing an average weekday in January. This operational behavior shows that the MPC algorithm can adapt to different market signals to optimize operational cost because the average price for spinning reserve is greater in January and the average price for non-spinning reserve being greater in July.

The MPC algorithms were shown to adapt to differences in environmental conditions and pricing signals to minimize operational expenses. Generalized findings show that more granular time steps and longer prediction horizons used in MPC algorithms provide lower net operating expenses. Enabling ancillary service market participation in the MPC algorithm provides significant revenue enhancement when compared to a logic-based algorithm, with up to a 300% increase in revenue demonstrated in this study. The combined cost savings and increased revenue can reduce microgrid project payback

periods and help accelerate the adoption of reliable, low-cost, and low-carbon energy solutions.

Future work can examine the economic and operational effects of participation in additional real-time markets such as energy markets and frequency regulation. Adding thermal considerations into the control formulation is another area to explore the benefits of co-optimizing electrical systems, thermal systems, and market participation.

3.8. Acknowledgements

This study was funded in part by the United States Office of Naval Research (ONR) Defense University Research-to-Adoption (DURA) Initiative under award N00014-18-1-2393.

3.9. References

American Public Power Association. 2018. "Wholesale Electricity Markets and Regional Transmission Organizations," no. 888. https://web.archive.org/web/20180412151454/https://www.publicpower.org/policy/wholesale-electricity-markets-and-regional-transmission-organizations.

Amirioun, M H, F Aminifar, H Lesani, and M Shahidehpour. 2019. "Electrical Power and Energy Systems Metrics and Quantitative Framework for Assessing Microgrid Resilience against Windstorms." *Electrical Power and Energy Systems* 104 (January 2018): 716–23. https://doi.org/10.1016/j.ijepes.2018.07.025.

Arafeh, Samir A. 1978. "Hierarchical Control of Power Distribution Systems." *IEEE TRANSACTIONS ON AUTOMATIC CONTROL* AC-23 (2): 333–43.

Arizona Public Service. 2017. "RATE SCHEDULE E-32 M MEDIUM GENERAL SERVICE (101 KW - 400 KW)."

Arizona State University. n.d. "Campus Metabolism." https://cm.asu.edu/.

Asmus, Peter, Adam Forni, and Laura Vogel. 2018. "Microgrid Analysis and Case Studies Report."

Borazjani, Pouya, Noor Izzri Abdul Wahab, Hashim b. Hizam, and Azura Bt Che Soh. 2014. "A Review on Microgrid Control Techniques." *2014 IEEE Innovative Smart Grid Technologies - Asia (ISGT ASIA)*, 749–53. https://doi.org/10.1109/ISGT-Asia.2014.6873886.

Bruni, G., S. Cordiner, V. Mulone, V. Rocco, and F. Spagnolo. 2015. “A Study of Energy Management in Domestic Micro-Grids Based on Model Predictive Control Strategies.” *Energy Procedia* 102: 1012–16. https://doi.org/10.1016/j.egypro.2014.11.1013.

California Independent System Operator. 2018. “California Independent System Operator Corporation Fifth Replacement Electronic Tariff.”

California ISO. n.d. “California ISO OASIS.” http://oasis.caiso.com/mrioasis/logon.do.

———. 2012. “What the Duck Curve Tells Us about Managing a Green Grid.” *California ISO, Shaping a Renewed Future*. Vol. Fact Sheet. https://doi.org/CommPR/HS/10.2013.

———. 2019. “Entering the Energy Market.” 2019. http://www.caiso.com/participate/Pages/default.aspx.

Ceres. 2015. “Pathway to a 21st Century Electric Utility,” no. November.

Chambers, Tom. 2018. “Distributed Energy Resources and Power Quality.” *IEEE Rural Electric Power Conference*, 37–41. https://doi.org/10.1109/REPC.2018.00015.

Chilipi, Rajasekharareddy, Naji Al Sayari, Khalifa Al Hosani, and Abdul Rahiman Beig. 2016. “Control Scheme for Grid-Tied Distributed Generation Inverter under Unbalanced and Distorted Utility Conditions with Power Quality Ancillary Services” 10: 140–49. https://doi.org/10.1049/iet-rpg.2015.0095.

Cochran, Jaquelin, Mackay Miller, Michael Milligan, Erik Ela, Douglas Arent, Aaron Bloom, Matthew Futch, et al. 2013. “Market Evolution: Wholesale Electricity Market Design for 21st Century Power Systems.” *Contract*, no. October 2013. https://doi.org/10.2172/1260327.

Fathima, A. Hina, and K. Palanisamy. 2015. “Optimization in Microgrids with Hybrid Energy Systems - A Review.” *Renewable and Sustainable Energy Reviews* 45: 431–46. https://doi.org/10.1016/j.rser.2015.01.059.

Few, Sheridan, Oliver Schmidt, Gregory J. Offer, Nigel Brandon, Jenny Nelson, and Ajay Gambhir. 2018. “Prospective Improvements in Cost and Cycle Life of Off-Grid Lithium-Ion Battery Packs: An Analysis Informed by Expert Elicitations.” *Energy Policy* 114 (May 2017): 578–90. https://doi.org/10.1016/j.enpol.2017.12.033.

Gandhi, Oktoviano, Carlos D. Rodríguez-Gallegos, Wenjie Zhang, Dipti Srinivasan, and Thomas Reindl. 2018. “Economic and Technical Analysis of Reactive Power Provision from Distributed Energy Resources in Microgrids.” *Applied Energy* 210 (August 2017): 827–41. https://doi.org/10.1016/j.apenergy.2017.08.154.

Generac Industrial Power. 2012. “Generac SD350 Industrial Diesel Generator Set Spec Sheet.” Vol. 156.

Ghanbarian, Mohammad Mehdi, Majid Nayeripour, Amir Hosein Rajaei, Fatemeh

Jamshidi, and Eberhard Waffenschmidt. 2017. “Model Predictive Control of Distributed Generation Micro-Grids in Island and Grid Connected Operation under Balanced and Unbalanced Conditions.” *Journal of Renewable and Sustainable Energy* 9 (4): 0–17. https://doi.org/10.1063/1.4990823.

Gomes, Mário Helder, and João Tomé Saraiva. 2010. “Allocation of Reactive Power Support, Active Loss Balancing and Demand Interruption Ancillary Services in MicroGrids.” *Electric Power Systems Research* 80 (10): 1267–76. https://doi.org/10.1016/j.epsr.2010.04.013.

Goyal, Megha, and Arindam Ghosh. 2016. “Sustainable Energy , Grids and Networks Microgrids Interconnection to Support Mutually during Any Contingency.” *Sustainable Energy, Grids and Networks* 6: 100–108. https://doi.org/10.1016/j.segan.2016.02.006.

Grid Modernization Labortatory Consortium. 2017. “Grid Modernization: Metrics Analysis (GMLC1.1),” no. May.

Gruber, J. K., F. Huerta, P. Matatagui, and M. Prodanović. 2015. “Advanced Building Energy Management Based on a Two-Stage Receding Horizon Optimization.” *Applied Energy* 160: 194–205. https://doi.org/10.1016/j.apenergy.2015.09.049.

Hirsch, Adam, Yael Parag, and Josep Guerrero. 2018. “Microgrids : A Review of Technologies , Key Drivers , and Outstanding Issues” 90 (March): 402–11. https://doi.org/10.1016/j.rser.2018.03.040.

Hoffman, Patricia, and Devon Streit. 2015. “United States Electricity Industry Primer.” *Office of Electricity Delivery and Energy Reliability U.S. Department of Energy, DOE/OE-0017*, no. July: 1–94. https://doi.org/DOE/OE-0017.

Hussain, Akhtar, Van-hai Bui, and Hak-man Kim. 2019. “Microgrids as a Resilience Resource and Strategies Used by Microgrids for Enhancing Resilience.” *Applied Energy* 240 (February): 56–72. https://doi.org/10.1016/j.apenergy.2019.02.055.

Janko, Samantha A., Michael R. Arnold, and Nathan G. Johnson. 2016. “Implications of High-Penetration Renewables for Ratepayers and Utilities in the Residential Solar Photovoltaic (PV) Market.” *Applied Energy* 180: 37–51. https://doi.org/10.1016/j.apenergy.2016.07.041.

Khongkhachat, Somkiart, and Surin Khomfoi. 2015. “Hierarchical Control Strategies in AC Microgrids.” *ECTI-CON 2015 - 2015 12th International Conference on Electrical Engineering/Electronics, Computer, Telecommunications and Information Technology*, 1–6. https://doi.org/10.1109/ECTICon.2015.7206968.

Lazard. 2018. “Lazard’s Levelized Cost of Storage Analysis - Version 4.0.”

Liu, Yajie, Bo Guo, Tao Zhang, Rui Wang, and Yan Zhang. 2016. “Model Predictive Control-Based Operation Management for a Residential Microgrid with Considering Forecast Uncertainties and Demand Response Strategies.” *IET Generation, Transmission & Distribution* 10 (10): 2367–78. https://doi.org/10.1049/iet-

gtd.2015.1127.

Majzoobi, Alireza, and Amin Khodaei. 2017. “Application of Microgrids in Providing Ancillary Services to the Utility Grid.” *Energy* 123: 555–63. https://doi.org/10.1016/j.energy.2017.01.113.

Mazumder, Sumit, Arindam Ghosh, and Firuz Zare. 2013. “Improving Power Quality in Low-Voltage Networks Containing Distributed Energy Resources.” *International Journal of Emerging Electric Power Systems* 14 (1): 67–78. https://doi.org/10.1515/ijeeps-2013-0022.

Mehleri, E. D., L. G. Papageorgiou, N. C. Markatos, and H. Sarimveis. 2012. *A Model Predictive Control Framework for Residential Microgrids*. *Computer Aided Chemical Engineering*. Vol. 30. Elsevier B.V. https://doi.org/10.1016/B978-0-444-59519-5.50066-6.

Monesha, S, S Ganesh Kumar, and M Rivera. n.d. “Microgrid Energy Management and Control : Technical Review.” *2016 IEEE International Conference on Automatica (ICA-ACCA)*, 1–7. https://doi.org/10.1109/ICA-ACCA.2016.7778452.

Morstyn, Thomas, Branislav Hredzak, Ricardo P. Aguilera, and Vassilios G. Agelidis. 2018. “Model Predictive Control for Distributed Microgrid Battery Energy Storage Systems.” *IEEE Transactions on Control Systems Technology* 26 (3): 1107–14. https://doi.org/10.1109/TCST.2017.2699159.

NERC. 2019. “State of Reliability 2019.” *Nerc*, no. June.

NERC Resources Subcommittee. 2011. “Balancing and Frequency Control.” Princeton. https://www.nerc.com/docs/oc/rs/NERC Balancing and Frequency Control 040520111.pdf.

Office of Public Accountability/Ratepayer Advocate. 2018. “Measuring Electric Service Reliability.”

Parisio, Alessandra, Evangelos Rikos, and Luigi Glielmo. 2016. “Stochastic Model Predictive Control for Economic/Environmental Operation Management of Microgrids: An Experimental Case Study.” *Journal of Process Control* 43: 24–37. https://doi.org/10.1016/j.jprocont.2016.04.008.

Parisio, Alessandra, Evangelos Rikos, Luigi Glielmo, and Senior Member. 2014. “A Model Predictive Control Approach to Microgrid Operation Optimization” 22 (5): 1813–27.

Parisio, Alessandra, Evangelos Rikos, George Tzamalis, and Luigi Glielmo. 2014. “Use of Model Predictive Control for Experimental Microgrid Optimization.” *Applied Energy* 115: 37–46. https://doi.org/10.1016/j.apenergy.2013.10.027.

Pereira, M., D. Munoz De La Pena, and D. Limon. 2016. “Robust Economic Model Predictive Control of a Community Micro-Grid.” *2016 IEEE 55th Conference on Decision and Control, CDC 2016* 100: 2739–44. https://doi.org/10.1109/CDC.2016.7798676.

Power, Generac Industrial. 2016. “Total Cost of Ownership Diesel vs . Natural Gas Generators,” 1–5.

Prodan, Ionela, and Enrico Zio. 2014. “A Model Predictive Control Framework for Reliable Microgrid Energy Management.” *International Journal of Electrical Power and Energy Systems* 61: 399–409. https://doi.org/10.1016/j.ijepes.2014.03.017.

Raquel, Parks. n.d. “Microgrids : Legal and Regulatory Hurdles for a More Resilient Energy Infrastructure,” 173–202.

Ratnam, Elizabeth L., and Steven R. Weller. 2018. “Receding Horizon Optimization-Based Approaches to Managing Supply Voltages and Power Flows in a Distribution Grid with Battery Storage Co-Located with Solar PV.” *Applied Energy* 210 (August 2017): 1017–26. https://doi.org/10.1016/j.apenergy.2017.08.163.

Rawlings, James B, and David. Q Mayne. 2009. *Model Predictive Control: Theory and Design*. Madison: Nob Hill Publishing.

Sadamoto, Tomonori, Aranya Chakrabortty, Takayuki Ishizaki, and Jun-ichi Imura. 2018. “Dynamic Modeling , Stability , and Control of Power Systems with Distributed Energy Resources.” *ArXiv E-Prints*, 1–36.

Sen, Sachidananda, and Vishal Kumar. 2018. “Microgrid Control: A Comprehensive Survey.” *Annual Reviews in Control* 45 (March): 118–51. https://doi.org/10.1016/j.arcontrol.2018.04.012.

Sheet, Information, and Wet Stacking. 1999. “Wet Stacking of Generator Sets and How to Avoid It.”

Shi, L., Y. Luo, and G. Y. Tu. 2014. “Bidding Strategy of Microgrid with Consideration of Uncertainty for Participating in Power Market.” *International Journal of Electrical Power and Energy Systems* 59: 1–13. https://doi.org/10.1016/j.ijepes.2014.01.033.

Small, Forrest, and L Frantzis. 2010. “The 21st Century Electric Utility: Positioning for a Low-Carbon Future.” *Ceres - Igniting 21st Century Solutions for a Sustainable Economy*, no. July.

Studies, Case, Emerging Applications, and Their Benefits. 2019. “PUTTING DISTRIBUTED ENERGY RESOURCES TO WORK IN WHOLESALE Case Studies of Emerging Applications and Their,” no. September.

Taft, J D. 2017. “Electric Grid Resilience and Reliability for Grid Architecture,” no. November.

The World Bank. n.d. “Pump Price for Diesel Fuel (US$ per Liter).” https://data.worldbank.org/indicator/ep.pmp.desl.cd.

Tuttle, David P., Gurcan Gulen, Robert Hebner, Carey W. King, David B. Spence, Juan Andrade, Jason A. Wible, Ross Baldick, and Roger Duncan. 2016. “The History and Evolution of the U.S. Electricity Industry,” 24. http://energy.utexas.edu/.

Undrill, John. 2018. “Primary Frequency Response and Control of Power System Frequency,” no. February. https://www.ferc.gov/industries/electric/indus-act/reliability/frequency-control-requirements/primary-response.pdf.

United States of America Federal Energy Regulatory Commission. 2018. *Electric Storage Participation in Markets Operated by Regional Transmission Organizations and Independent System Operators*. *18 CFR Part 35*. https://doi.org/10.1017/CBO9781107415324.004.

Wang, Jianxiao, Haiwang Zhong, Wenyuan Tang, Ram Rajagopal, Qing Xia, Chongqing Kang, and Yi Wang. 2017. “Optimal Bidding Strategy for Microgrids in Joint Energy and Ancillary Service Markets Considering Flexible Ramping Products.” *Applied Energy* 205: 294–303. https://doi.org/10.1016/j.apenergy.2017.07.047.

Wang, Jiaren, Ning Xie, Wenxian Wu, Dong Han, Chengmin Wang, and Binruo Zhu. 2018. “Resilience Enhancement Strategy Using Microgrids in Distribution Network.” *Global Energy Interconnection* 1 (5): 537–43. https://doi.org/10.14171/j.2096-5117.gei.2018.05.002.

Xu, Jun, Yuanyuan Zou, and Yugang Niu. 2014. “Multi-Time Scale Hierarchical Predictive Control for Energy Management of Microgrid System with Smart Users.” *26th Chinese Control and Decision Conference, CCDC 2014*, 3055–60. https://doi.org/10.1109/CCDC.2014.6852699.

Zachar, Michael, and Prodromos Daoutidis. 2016. “Nonlinear Economic Model Predictive Control for Microgrid Dispatch.” *IFAC-PapersOnLine* 49 (18): 778–83. https://doi.org/10.1016/j.ifacol.2016.10.260.

Zhang, Xinan, Jie Bao, Ruigang Wang, Chaoxu Zheng, and Maria Skyllas-Kazacos. 2017. “Dissipativity Based Distributed Economic Model Predictive Control for Residential Microgrids with Renewable Energy Generation and Battery Energy Storage.” *Renewable Energy* 100: 18–34. https://doi.org/10.1016/j.renene.2016.05.006.

Zhang, Yan, Tao Zhang, Rui Wang, Yajie Liu, and Bo Guo. 2015. “Optimal Operation of a Smart Residential Microgrid Based on Model Predictive Control by Considering Uncertainties and Storage Impacts.” *Solar Energy* 122: 1052–65. https://doi.org/10.1016/j.solener.2015.10.027.

Zhenzhen, Song. 2015. “The Evaluation of Parameter M in the Big M Method of Linear Programming Song Zhenzhen,” no. Meita: 37–40.

Zhou, Yang, and Carl Ngai-man Ho. 2016. “A Review on Microgrid Architectures and Control Methods.” *2016 IEEE 8th International Power Electronics and Motion Control Conference (IPEMC-ECCE Asia)*, 3149–56. https://doi.org/10.1109/IPEMC.2016.7512799.

CHAPTER 4

STATISTICAL DEVLOPMENT OF MICROGRID RESILIENCE DURING ISLANDING OPERATIONS

Authored by James R. Nelson, Nathan G. Johnson, Kelsey Fahy, Timothy A. Hansen

Forthcoming Journal Submission in November 2019

Abstract

This study develops a statistical framework to quantify the resilience of grid-connected microgrids to meet critical load requirements during islanding events. The primary metric of resilience is microgrid survivability, and is expressed as the probability for a microgrid to meet critical load requirements during a grid outage. Probabilities are evaluated using a Markov chain that describes microgrid operating states each hour for a 7-day time horizon. This system-level metric uses asset-level reliability data on prominent failure modes (i.e., up-time, failure to start, failure to run). A military microgrid with an existing 5,250 kW diesel generators is contrasted to a hybrid microgrid that contains 2,250 kW generators, 3,450 kW / 13,800 kWh storage, and 16,479 kW solar photovoltaics (PV). Sensitivity analyses identify control parameters that improve survivability while also reducing fuel usage and curtailed load. The hybrid microgrid requires 37.5% less on-site fuel reserves to meet these same metrics and increases survivability by 10% when compared to a generator-only microgrid. If solar PV drops by 50%, the survivability of the hybrid microgrid falls below the generator-only microgrid. Increasing critical load by 30% above the designed value decreases autonomy and survivability by 58.76% and 79.07%, respectively, for the hybrid microgrid. At the onset of a grid outage, the battery starting state-of-charge must be at least 70% to exceed the survivability of a generator-only

microgrid and serve the full critical load without curtailment over the duration of the islanding event. Starting with a lower SOC diminishes the survivability of the microgrid because of insufficient capacity in storage to supplement failure to a generator or battery stack. Methods and findings from this study can inform the design and operation of resilient microgrids for critical grid-connected loads or off-grid applications.

4.1. Introduction

Multiple large-scale blackouts have originated due to severe weather (Bryan 2012), (Fischer and Knutti 2015), (Kerr 2011), (Stott 2016), physical and cyber-attacks (T. M. Chen et al. 2011), (Zhu and Yan 2014), mitigating forest fires risks (sunrun 2019), (Stelloh 2019), equipment failure (Venkatasubramanian and Li 2004), human error (Abraham and Efford 2004), anthropogenic attacks (Rebecca 2014), or a combination of these stressors (Hines and Balasubramaniam 1977), (Schossig and Schossig 2013). These blackouts can begin with a localized problem that resolves into voltage and/or frequency disturbances that cascade to affect larger regions. Similar disturbances are thought possible due to the rapid growth in uncontrolled distributed energy resources (DERs) (Abd-rabou, Soliman, and Mokhtar 2015), (Mahmud, Hossain, and Pota 2011), (Ogunjuyigbe, Ayodele, and Akinola 2016), (Khani, Sadeghi, and Madadi 2012), (Dulau, Abrudean, and Bica 2014), though approaches in distributed control, fast-response power electronics for stability, and longer-duration storage are helping reduce this concern (H. Lee et al. 2016), (M. Braun et al. 2016), (Ayar et al. 2017), (Yu et al. 2018).

Customers requiring more reliable power have begun implementing grid-connected microgrids to maintain power to critical operations in the event of a grid outage. The Department of Energy (DOE) defines a microgrid as “a group of interconnected loads and

distributed energy resources within clearly defined electrical boundaries that acts as a single controllable entity with respect to the grid. A microgrid can connect and disconnect from the grid to enable it to operate in both grid-connected or island-mode.'' (Ton and Smith 2012). Microgrids have been used to increase reliability and decrease operational costs for a variety of customer types including utility, military, health service, education, data centers, aviation, and agriculture (Martin-martínez and Rivier 2016), (Asmus, Forni, and Vogel 2018). Recent work has also indicated that microgrids enhance resilience through increased flexibility to handle grid disturbances (Hussain, Bui, and Kim 2019), (Jiaren Wang et al. 2018), (Raquel, n.d.).

Historically, the reliability of electrical systems has been modeled using contingency analyses (Müller et al. 2013), (Jamei et al., n.d.), (Miller 2008), (Momoh 2012). This type of analysis simulates failures to generation and transmission infrastructure to determine the impact on system capacity, stability, and the ability to serve load. Similar analyses have been conducted on microgrids and groups of microgrids during islanding contingencies (Aghdam, Salehi, and Ghaemi 2018), (Goyal and Ghosh 2016), (Mashayekh et al. 2017). Metrics of reliability are well-established and include the system average interruption duration index (SAIDI), system average interruption frequency index (SAIFI), and customer average interruption duration index (CAIDI) (Eto and Lacommare 2008). These metrics represent the duration and frequency of system interruptions (i.e. how often and how long customers lose power) but do not express the resilience of a system. Resilience does not have a standard definition, parameters, or metrics despite receiving significant recent attention (The Gridwise Alliance 2013), (Electric Power Research Institute 2016), (Ji et al. 2016), (Lammers 2017).

The definition of resilience used in this work is "… the ability to withstand grid stress events without suffering operational compromise or to adapt to the strain so as to minimize compromise via graceful degradation." (Taft 2017b). Grid stresses include, but are not limited to, congestion, imbalances, extreme weather, cyber-attacks, and device or system failure (Widergren et al. 2018). These stresses can cause power quality issues, equipment failure, outages, and the loss of property, life, or finances. Current research is developing metrics, indexes, and frameworks to evaluate the resilience of power systems and microgrids (Naja, Peiravi, and Guerrero 2018), (Vugrin, Castillo, and Silva-monroy 2017), (Roege et al. 2014). Amirioun et al. introduces survivability as an indicator of a power systems resilience (Amirioun et al. 2019). Lawder et al. analyze the autonomy of microgrids with respect to solar power and battery storage capacity (Lawder, Viswanathan, and Subramanian 2015). Rodrigues et al. use survival time to evaluate the autonomy of an islanded microgrid (Rodrigues et al. 2020). Molyneaux et al. use fuel consumption, loss of load, and other metrics to compare the resilience of different power systems around the world (Molyneaux et al. 2012).

Recent research is developing new concepts and models to simulate the resilience of energy systems and other critical infrastructure (Y. Lin and Bie 2016), (Jing Wang et al. 2020). Shen et al. statistically showed resilience improvements in the Northeast Power Coordinating Council (NPCC) using data on electrical disturbance events throughout U.S. power grid and a custom combined measure of resilience (Shen, Cassottana, and Tang 2018). Optimization routines have been formulated to calculate resilience-based recovery, restoration, and operations of power distribution systems (Figueroa-candia, Felder, and Coit 2018), (Lau et al. 2018). Saleh et al. developed an optimal protection coordination

scheme during N-1 contingencies for microgrids and showed that the protection equipment and operation can be optimally designed to accommodate multiple network topologies and contingency scenarios (Saleh, Zeineldin, and El-saadany 2017). Cattaneo et al. developed optimal operation dispatch and control for an islanded microgrid to survive generator contingencies while considering system dynamics, voltages, and line flows (Cattaneo, Chalil, and Backhaus 2018). Cagnano et al. developed and physically tested a cooperative control scheme for islanded microgrids to maximize generation reserves and share the regulation burden between the distributed energy resources (Cagnano, Bugliari, and Tuglie 2018). These studies are beginning to add structure to the growing field of resilience research. Further work is needed to statistically describe how specific assets, asset combinations, and asset reliability affects microgrid resilience.

Military microgrids are primarily designed and implemented for energy security (Hirsch, Parag, and Guerrero 2018). An MIT Lincoln Laboratory study on energy security for Department of Defense (DoD) defines energy security as "… the ability of an installation to access reliable supplies of electricity and fuel and the means to use them to protect and deliver sufficient energy to meet critical operations during an extended outage of the local electric grid." (Nguyen 2012). A military microgrid is analyzed in this study to understand the potential resilience benefits and resulting effects on energy security.

This study provides the following contributions to literature:

- Develops a statistical framework using Markov chains to describe the ability of microgrids to "survive" and meet critical load during islanding operations.
- Demonstrates use of XENDEE for optimal sizing of microgrid assets that minimizes operating expenses without sacrificing resilience.

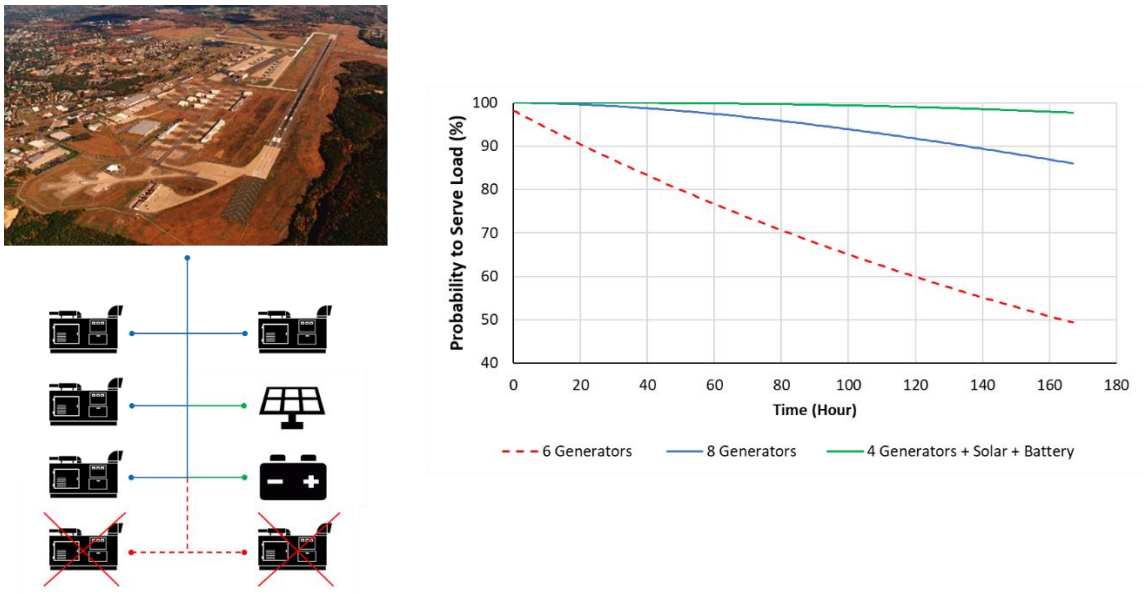
- Develops an optimized dispatch control algorithm to operate microgrids for improved resilience during a grid outage.
- Completes sensitivity analyses to select control parameters that improve microgrid autonomy and survivability.
- Compares performance of a generator-only microgrid portfolio to a hybrid microgrid portfolio that includes generators, battery storage, and solar PV.
- Evaluates microgrid resilience on four metrics including survivability, autonomy, fuel consumption, and unserved load.

4.2. Statistical Development of Microgrid Survivability

Microgrid survivability is the probability that critical load will be served over the duration of an islanding event. This definition parallels a common definition of system reliability that describes the ability of a system to provide its intended function and the probability that it will not fail (Hecht 2003). A variety of approaches have been used to model system reliability including fault trees (Biswal, Maheshwari, and Dewal 2012), Monte Carlo simulations (Billinton and Li 1994), (Ramakrishnan 2016), and Markov chains (Prowell and Poore 2004), (P. O. T. Lin et al. 2014). Fault trees are a subset of analytical logic techniques used in operations research and are commonly used for modeling fixed probability systems (HBM Prenscia 2019). Monte Carol simulations use random variables and statistical sampling techniques to calculate a distribution of possible outcomes (U.S. Environmental Protection Agency 1997). Markov chains are mathematical tools used to describe random phenomena evolving through time using knowledge of a system's current state and a set of probabilities to express transitions to future states (Norris 1998). Markov chains have been used to statistically model natural processes (He and Jiang

2018), (Mei and Gong 2018) and the performance and reliability of built systems and infrastructure (Ye et al. 2018), (Miao et al. 2018). This study uses a Markov chain to model microgrid survivability due to the inherent capability to compute long-term behavior with a "memoryless" feature using only the current state of the system and no data on the history of events to that point in time. The knowledge on system history is implicit in the probability to transition back to certain operating states over time (e.g. if an asset fails, the system can't transition back to a state where that asset is operational). These attributes of Markov chains enable calculations to be completed with a relatively low computation cost.

This study equates microgrid's survivability using a critical load profile, energy asset operating states, and a Markov matrix to evolve states through time. Survivability of the microgrid is primarily dependent on the combined generator, battery, and solar PV generation capacity available at any given time. The greater the available capacity, the more likely the microgrid can continue serving the load in the event of a component or subsystem failure. 4.1 shows a generic model of microgrid survivability with various microgrid portfolios. If two generators fail, the microgrid is less likely to be able to serve the load over the outage duration. However, microgrid survivability improves if battery and solar PV generation capacity is added to the microgrid portfolio.



4.1: Survivability of a generic microgrid containing various energy assets.

Statistical development of survivability is demonstrated for a generic microgrid consisting of multiple generators, multiple battery stacks, solar PV, a critical load, and a controllable load. Electric loads are assumed to use the exact quantity of power modeled, a perfect forecast. Potential failures in diesel generators and battery stacks are represented statistically. Generator reliability is expressed as failure to start and failure to run (failure rate) (Ericson 2019) (Mrowca 2011). Generators up-time is also expressed to account for maintenance schedules. Eq. 1 shows how these two metrics are combined to calculate generator availability, α^g, where γ_{up}^g is generator up-time and γ_{start}^g is failure to start.

$$\alpha^g = \gamma_{up}^g - \gamma_{start}^g \quad \text{(Eq. 1)}$$

Eq. 2 expresses battery stack availability, α^b, as equivalent to up-time, γ_{up}^b, because battery stacks do not typically have failure to start issues (EOS, n.d.).

$$\alpha^b = \gamma_{up}^b \quad \text{(Eq. 2)}$$

Solar PV arrays are traditionally assumed to have high availability and operate with minimal downtime (Collins et al. 2009), (Hunt et al. 2015). The main source of failure is inverter failure (Colli 2015), (Golnas 2013), which can be localized by implementing many smaller string inverters that each have minimal impact to total solar PV production. This study assumes power generated from the solar PV array is 100% reliable and always provides capacity of the modeled generation profile (i.e. $\alpha^{sol} = 1$).

The initial state of the microgrid is expressed using the availability of generators and battery stack. The availability of solar PV is not directly modeled because it is assumed to 100% reliable. After the initial state of the system is calculated, the failure rate of the generators and battery stacks are used to describe reliability of each asset class. Eq. 3 shows the relationship between generator mean time between failure, $MTBF^g$, and generator failure rate,λ^g. The reliability function for the exponential distribution shown in Eq. 4 was used to calculate the failure rate of the battery stacks where λ^g is the failure rate, d is an assumed duration of the specified outage (168 hours), and γ_{up}^b is the up-time of the battery stacks. The exponential distribution was used to model battery failure rate given the absence of data on mean time between failure for battery storage.

$$\lambda^g = \frac{1}{MTBF^g} \quad \text{(Eq. 3)}$$

$$\lambda^b = -\frac{\ln(\gamma_{up}^b)}{d} \quad \text{(Eq. 4)}$$

Assuming that generator availability and battery stack availability are uncorrelated, the binomial distribution in Eq. 5 can be used to model the initial state of the microgrid where N^g is the total number of generators, g is a subset of generators, α^g is the availability

of generators, N^b is the total number of battery stacks, b is a subset of battery stacks, and α^b is the availability of battery stacks.

$$P(0,g,b) = \binom{N^g}{g}(1-\alpha^g)^g(\alpha^g)^{N^g-g}\binom{N^b}{b}(1-\alpha^b)^b(\alpha^b)^{N^b-b} \qquad \text{(Eq. 5)}$$

Eq. 6 calculates the probability of having g' generators and b' battery stacks available during the next system state, given that g generators and b battery stacks are available in the current system state. This equation is similar to the formulation in Eq. 5 with modifications to express transition states between time steps.

$$p(g,g',b,b') = \binom{g}{g'}(1-\lambda^g)^{g'}(\lambda^g)^{g-g'}\binom{b}{b'}(1-\lambda^b)^{b'}(\lambda^b)^{b-b'} \qquad \text{(Eq. 6)}$$

Eq. 6 is calculated for every combination of generators and battery stacks and placed into the Markov matrix shown in Eq. 7. This $(N^g \times N^b + N^g + N^b + 1) \times (N^g \times N^b + N^g + N^b + 1)$ Markov matrix, also known as the transition matrix represents the probability to transition between all possible operating states of a microgrid. Any future state of the system can be calculated by multiplying the current state with the transition matrix and specifying the number of time steps over which the transition occurs, d.

$$\begin{bmatrix} 1 & p(1,0,0,0) & \dots & p(N^g,0,N^b,0) \\ 0 & p(1,1,0,0) & \dots & p(N^g,1,N^b,0) \\ \vdots & \vdots & \ddots & \vdots \\ 0 & \dots & 0 & p(N^g,N^g,N^b,N^b) \end{bmatrix}^d \qquad \text{(Eq. 7)}$$

The microgrid survives the islanding event if the total available generating capacity is greater than the critical load for the duration of the grid outage. This condition is checked each time step. Load is curtailed if there is insufficient generation capacity. The survival criteria for the initial state of the microgrid is shown in Eq. 8 where s_t is the chance of survival, V_{av}^g is the available on-site fuel, μ_{fuel}^g is the generator fuel consumption

coefficient, P_{max}^{g} is the maximum power of the generators, E^{b} is the energy stored in the battery stacks, E_{min}^{b} is the minimum allowable energy capacity of the battery stacks, $P_{d,max}^{b}$ is the maximum discharge rate of the battery stacks, P_{crit}^{load} is the power consumption of the critical load, and P^{sol} is the power produced by the solar PV array. The chance of survival is set to zero if the combination of g generators and b battery stacks does not provide sufficient generation to serve the load. However, if the combination of g generators and b battery stacks does provide sufficient generation, the chance of survival is set equal to the probability that g generators and b battery stacks are available to use as the start of an islanding event. Minimum functions in the inequality equations ensure that generators and battery stacks can provide power subject to available on-site fuel reserves and available stored energy, respectively. The maximum function in the inequality ensures that the right side of the equation is always greater than or equal to zero, even if there is more solar PV generation than critical load.

$$s_t(0,g,b) = \begin{cases} 0 & g \times \min\left(\frac{V_{av}^{g}/g}{\mu_{fuel}^{g}}, P_{max}^{g}\right) + b \times \min\left(\sum_{b=0}^{N^b}\left(E^b(0,b) - E_{min}^{b}\right), P_{d,max}^{b}\right) < \max\left(P_{crit}^{load}(0) - P^{sol}(0), 0\right) \\ P(0,g,b) & g \times \min\left(\frac{V_{av}^{g}/g}{\mu_{fuel}^{g}}, P_{max}^{g}\right) + b \times \min\left(\sum_{b=0}^{N^b}\left(E^b(0,b) - E_{min}^{b}\right), P_{d,max}^{b}\right) \geq \max\left(P_{crit}^{load}(0) - P^{sol}(0), 0\right) \end{cases} \quad \text{(Eq. 8)}$$

The chance of microgrid survival for the next time step, $d+1$, is calculated using Eqs. 9 and 10. The probability that the microgrid is operating with a specific quantity of diesel generators and battery stacks is first calculated for timestep $d+1$ using Eq. 9. The resulting vector is the probability of all microgrid states. Then, the survival probability of all possible system states which have less than the required amount of total generation capacity is set to zero using Eq. 10, similar to the process described for Eq. 8. This process

is repeated for each time step of the islanding event, with results yielding the probability of all system states over the full duration of the islanding event.

$$\begin{bmatrix} 1 & p(1,0,0,0) & \dots & p(N^g,0,N^b,0) \\ 0 & p(1,1,0,0) & \dots & p(N^g,1,N^b,0) \\ \vdots & \vdots & \ddots & \vdots \\ 0 & \dots & 0 & p(N^g,N^g,N^b,N^b) \end{bmatrix} \begin{bmatrix} s_t(d,0,0) \\ s_t(d,1,0) \\ \vdots \\ s_t(d,N^g,N^b) \end{bmatrix} = \begin{bmatrix} s'_t(d+1,0,0) \\ s'_t(d+1,1,0) \\ \vdots \\ s'_t(d+1,N^g,N^b) \end{bmatrix} \quad \text{(Eq. 9)}$$

$$s_t(d+1,g,b) = \begin{cases} 0 & g \times \min\left(\frac{V_{av}^g/g}{\mu_{fuel}^g}, P_{max}^g\right) + b \times \min\left(\sum_{b=0}^{N^b}\left(E^b(d+1,b) - E_{min}^b\right), P_{d,max}^b\right) < \max\left(P_{crit}^{load}(d+1) - P^{sol}(0),0\right) \\ s'_t(d+1,g,b) & g \times \min\left(\frac{V_{av}^g/g}{\mu_{fuel}^g}, P_{max}^g\right) + b \times \min\left(\sum_{b=0}^{N^b}\left(E^b(d+1,b) - E_{min}^b\right), P_{d,max}^b\right) \geq \max\left(P_{crit}^{load}(d+1) - P^{sol}(0),0\right) \end{cases} \quad \text{(Eq. 10)}$$

The survivability of a microgrid can be equated by taking the summation of the state vector at any time of the islanding event. Eq. 11 expresses the survivability of a microgrid, $S_t(D)$, starting in hour t and lasting for D hours, where $s_t(D,g,b)$ is the chance of survival, ending with g diesel generators and b battery stacks. The sum of all possible system states of the resulting vector in Eq. 9 is used to calculate the total probability that the microgrid can meet the critical load. This summation typically sums to one but because states that cannot meet the critical load are zeroed out as described in Eq. 10 the resulting survivability degrades with time.

$$S_t(D) = \sum_{g=0}^{N^g}\sum_{b=0}^{N^b} s_t(D,g,b) \quad \text{(Eq. 11)}$$

4.3. Asset Dispatch During an Islanding Event

The dispatch routine for islanded operation was developed to improve microgrid resilience by (i) maximizing generation capacity to improve microgrid survivability despite an increasing probability of asset failure over time, (ii) minimizing fuel consumption to increase autonomy and extend the duration the microgrid can operate without fuel resupply,

and (iii) permitting load shedding as a last resort if there is insufficient generation. Total dispatchable generation, generators and battery stacks, is reduced if there is generator failure, battery stack failure, insufficient fuel, or insufficient energy in the battery stacks. A microgrid with lower generation capacity is less capable of meeting the critical load and hence is less resilient.

4.3.1. Objective Function

The objective function in Eq. 12 is maximized and matches the intent of the dispatch routine with three components that (i) maximize microgrid reserve capacity using battery storage where E^b is the energy stored in the battery stacks and ω_{bat} is the corresponding weighting factor for battery storage, (ii) minimize fuel consumption where F^g is the fuel consumption of the diesel generators, ω_{fuel} is the corresponding weighting factor for fuel, and Δt is the duration of each simulated time step, and (iii) minimize curtailed load where P_{us}^{load} is the unserved load, ω_{load} is the corresponding weighting factor, and d is the hour of the islanding event. The sum of all three weighting factors is equal to one, a common approach for multi-objective optimization (R T Marler and Arora 2004), (R Timothy Marler and Arora 2010). Weights can be adjusted to evaluate the effect on microgrid resilience metrics. The weighting factor for unserved load is set equal to nearly one (0.999999999) to heavily disincentivize load shedding for use as a last resort to maintain solution feasibility if there are insufficient generation sources to serve load.

$$J = \sum_{d=0}^{D}\left[\omega_{bat}\frac{P_{d,max}^{b}}{E_{max}^{b}}\left(\sum_{b=0}^{N^b}\left(E^b(d,b)\right)\right) - \omega_{fuel}\frac{P_{max}^{g}}{P_{max}^{g}\Delta t}\left(\sum_{g=0}^{N^g}\left(F^g(d,g)F_{LHV}^{g}\right)\right) - \omega_{load}\frac{\left(P_{us}^{load}(d)\right)}{d}\right] \quad \text{(Eq. 12)}$$

4.3.2. Constraints

Constraints were developed using equipment specifications, load data, and renewable generation data. Eq. 13 shows the microgrid energy balance solved in each time step. Terms include the critical load, unserved load, power from diesel generators, P^g, power from charging battery stacks, P_c^b, and power from discharging battery stacks, P_d^b.

$$\sum_{g=0}^{N^g} P^g(d,g) + P^{sol}(d) + \sum_{b=0}^{N^b} \left(-P_c^b(d,b) + P_d^b(d,b)\right) - P_{crit}^{load}(d) + P_{us}^{load}(d) = 0 \quad \text{for } d = 0, \dots, D \tag{Eq. 13}$$

Eq. 14 expresses the amount of solar PV that can be curtailed, P^{sol}, limited by an upper bound for the forecasted future solar PV generation, P_{for}^{sol}. Solar PV is curtailed if the critical load is served and battery stacks are fully charged.

$$0 \le P^{sol}(d) \le P_{for}^{sol}(d) \quad \text{for } d = 0, \dots, D \tag{Eq. 14}$$

Eq. 15 sets the minimum generator power output, P_{min}^g, to prevent wet stacking, the incomplete combustion of fuel and buildup of carbon in exhaust that can damage the generator (Clifford Power 1999). A binary variable, B^g, describes if the generator is on (1) or off (0). Eq. 16 sets the maximum generator power output equivalent to the rated capacity, P_{max}^g.

$$P_{min}^g B^g(d,g) \le P^g(d,g) \quad \text{for } d = 0, \dots, D \text{ and } g = 1, \dots, N^g \tag{Eq. 15}$$

$$P^g(d,g) \le P_{max}^g B^g(d,g) \quad \text{for } d = 0, \dots, D \text{ and } g = 1, \dots, N^g \tag{Eq. 16}$$

Eq. 17 express the generator fuel consumption, F^g, as a linear regression of power output and constant fuel efficiency.

$$F^g(d,g) = \mu^g_{fuel} \times P^g(d,g) \quad \text{for } d = 0,\dots,D \text{ and } g = 1,\dots,N^g \tag{Eq. 17}$$

Eq. 18 constrains total fuel use during the islanding event to be less than or equal to the fuel stored on-site, F^g_{os}.

$$\sum_{d=0}^{D}\left[\sum_{g=0}^{N^g} F^g(d,g)\right] \leq F^g_{os} \tag{Eq. 18}$$

Eqs. 19 and 20 express constraints on battery minimum state-of-charge (SOC) and maximum SOC, where E^b_{min} and E^b_{max} are the minimum and maximum allowable energy stored in each battery stack, respectively.

$$E^b_{min} \leq E^b(d,b) \quad \text{for } d = 0,\dots,D \text{ and } b = 1,\dots,N^b \tag{Eq. 19}$$

$$E^b(d,b) \leq E^b_{max} \quad \text{for } d = 0,\dots,D \text{ and } b = 1,\dots,N^b \tag{Eq. 20}$$

Eq. 21 defines the initial energy stored in each battery stack, E^b_{init}, at the start of the islanding event.

$$E^b(0,b) = E^b_{init} \quad \text{for } b = 1,\dots,N^b \tag{Eq. 21}$$

Eqs. 22 and 23 ensure charging and discharging rates of battery stacks remain within the specified C-rating of the battery stacks, where P^b_c is the charging rate of the battery stack, $P^b_{c,max}$ is the maximum charging rate, P^b_d is the discharging rate of the battery stack, and $P^b_{d,max}$ is the maximum discharging rate.

$$0 \leq P^b_c(d,b) \leq P^b_{c,max} \quad \text{for } d = 0,\dots,D \text{ and } b = 1,\dots,N^b \tag{Eq. 22}$$

$$0 \leq P_d^b(d,b) \leq P_{d,max}^b$$
$$\text{for } d = 0, \dots, D \text{ and } b = 1, \dots, N^b \quad \text{(Eq. 23)}$$

Eq. 24 balances energy flows for the battery stacks, where η_{self}^b is the self-discharge loss of the battery stacks, η_c^b is the charging efficiency of the battery stacks, and η_d^b is the discharging efficiency of the battery stacks.

$$E^b(d,b) = E^b(d-1,b) \times \left(1 - \eta_{self}^b\right) + \left(\eta_c^b P_c^b(d-1,b) - \frac{1}{\eta_d^b} P_d^b(d-1,b)\right) \times d \quad \text{(Eq. 24)}$$
$$\text{for } d = 1, \dots, D \text{ and } b = 1, \dots, N^b$$

The "Big M" method (Zhenzhen 2015) was used to ensure battery stacks did not simultaneously charge and discharge in the same time step. Eqs. 25 and 26 show constraints that utilize the "Big M" method, where B^b is a binary variable that describes if the battery is charging (1) or discharging (0) and M is any large number (chosen to be 1,000,000 for this optimization formulation).

$$P_c^b(d,b) \leq B^b(d,b)M$$
$$\text{for } d = 0, \dots, D \text{ and } b = 1, \dots, N^b \quad \text{(Eq. 25)}$$

$$P_d^b(d,b) \leq (1 - B^b(d,b))M$$
$$\text{for } d = 0, \dots, D \text{ and } b = 1, \dots, N^b \quad \text{(Eq. 26)}$$

4.4. Microgrid Resilience Metrics

Four metrics describe microgrid resilience during an islanding event: survivability, autonomy, fuel consumption, and unserved load.

Section 2 provided mathematical development of microgrid survivability over the duration of a single islanding event. However, the ability of a microgrid to survive an

islanding event can be dependent on when the event starts and the hourly variability of loads and solar PV generation. The average probability of surviving an islanding event over the course of a year is shown in Eq. 27, where Q is a probability density function and q_t is the probability of an outage starting in hour t. A uniform distribution is assumed for q_t to indicate an islanding event has equal probability to start at any of the 8760 hours in a year.

$$\bar{S_t}(D,Q) = \sum_{t=0}^{8760} q_t S_t(D) \quad \text{(Eq. 27)}$$

Autonomy, A, represents the duration of time in hours that the microgrid can serve 100% of the critical load as described in Eq. 28, where B_{loss}^{load} is a binary variable that is equal to one if 100% of the critical load is served in that time step and zero if the critical load is not fully served.

$$A = \sum_{d=0}^{D} B_{loss}^{load}(d) \quad \text{where} \quad \begin{cases} B_{loss}^{load}(d) = 1 & P_{loss}^{load}(d) = 0 \\ B_{loss}^{load}(d) = 0 & P_{loss}^{load}(d) \neq 0 \end{cases} \quad \text{(Eq. 28)}$$

Eq. 29 calculates generator fuel consumption, F_{con}^{g}, during an islanding event to identify minimum fuel requirements to meet the critical load. This formulation can be modified to identify how much longer critical loads can continue to be served before fuel tanks are depleted.

$$F_{con}^{g} = \sum_{d=0}^{D} \left[\sum_{g=0}^{N^g} F^g(d,g) \right] \quad \text{(Eq. 29)}$$

The unserved load over the duration of the islanding event, equated in Eq. 30, quantifies how much load will need to be curtailed to maintain microgrid operation at a reduced capacity.

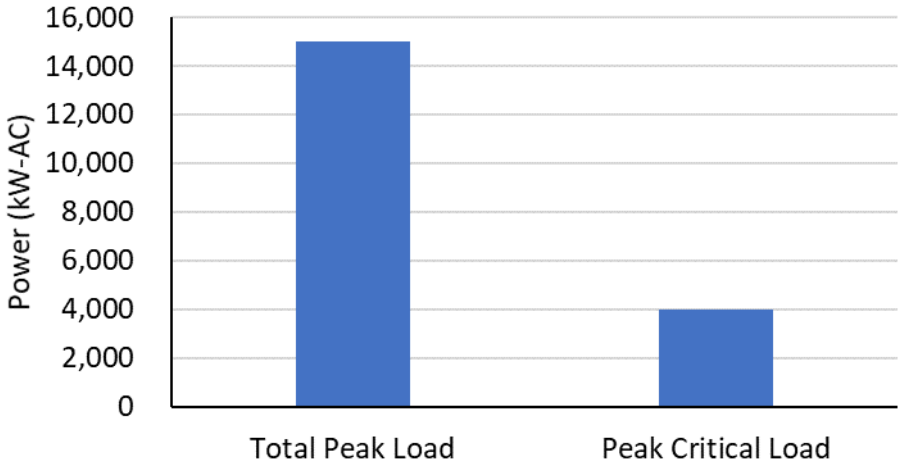
$$P_{us}^{load,D} = \sum_{d=0}^{D} P_{us}^{load}(d) \quad \text{(Eq. 30)}$$

4.5. Microgrid Site Data

A military microgrid was chosen as the case study given increasing interest from the USA Office of the Secretary of Defense (OSD) to maintain resilience and power critical loads during a grid outage (Department of Defense 2014), (Department of the Navy, n.d.), (Department of Defense 2017). Sensitive information has been anonymized.

4.5.1. Installation Loads

4.2 shows the total peak load and peak critical load of the military microgrid over the duration of a year (ESTCP 2019).



4.2: Summary of on-site electrical load.

4.5.2. Microgrid Assets

Two microgrid portfolios were designed: a generator-only microgrid portfolio, and a hybrid microgrid portfolio with generators, energy storage, and solar PV. The 750-kW diesel generators were assumed to have a constant fuel efficiency of 0.0727 gal/kW-hr

calculated from a linear regression (R-squared = 0.9962) of manufacturer fuel consumption data (MQ Power 2007). Multiple generators are capable of operating in parallel. Metrics for up-time, failure to start, and mean time between failure were assumed to be 99.9%, 99.8% and 1700 hours, respectively (ESTCP 2019). The power profile of the solar PV array was generated by scaling the power output of a measured smaller array adjacent to the installation (ESTCP 2019). Operating characteristics for the considered EOS zinc aqueous battery (EOS, n.d.) are provided in Table 4.1.

Table 4.1: Operational characteristics of EOS battery storage considered in the hybrid microgrid portfolio (EOS, n.d.).

Round-trip Efficiency (%)	Decay (fraction of battery capacity lost per hour)	C-Rate	Min/Max SOC (fraction of battery capacity)	Unit Size (kWh)	Lifetime (cycles)	Up-time (%/year)
75	0.01	C/4	0.00 / 1.00	600	5000+	98

Economic data for capital cost, operation and maintenance cost, and incentives are provided in Table 4.2 for all asset types. A diesel fuel price of 2.97 $/gal was assumed (ESTCP 2019). A 2.2% annual inflation rate and 6.0% nominal investment discount rate for a 20-year investment horizon was also assumed (ESTCP 2019). The investment tax credit (ITC) is a mechanism in federal tax code that enables a portion of energy-related investments to be credited towards the developer's or operator's taxes (Sherlock 2018). The Modified Accelerated Cost Recovery System (MARCS) is a depreciation mechanism in federal tax code that allows a business to deduct the cost of an asset with more than one year of lifetime (Dorn, n.d.). Both a 30% ITC and a 5-year MACRS schedule incentive were applied to the capital investment costs of the solar PV system and battery systems. To be eligible for the full 30% of the ITC, the battery system was only permitted to be charged from renewable sources of generation during on-grid operations.

Table 4.2: Generator, solar PV, and battery economic data used to calculate the optimal microgrid portfolio.

Technology	Capital Cost ($/kW or $/kWh)	Annual Fixed O&M Cost ($/year)	Variable O&M Cost ($/kW/month or $/kWh/month)	Investment Tax Credit (%)	MARCS Depreciation (%)	MARCS Years
Generator (750 kW)	750 (ESTCP 2019)	7000 (ESTCP 2019)	NA	NA	NA	NA
Solar PV	2,100 (Fu et al. 2018)	NA	1.42 (Fu et al. 2018)	30	85	5
EOS Battery (600 kWh)	436 (EOS, n.d.)	NA	0.33 (EOS, n.d.)	30	85	5

4.5.3. Microgrid Portfolios

The baseline generator-only microgrid included 5,250 kW of back-up generator capacity (seven 750 kW units). This provided N+1 reliability to ensure peak critical load could be met if one unit is unavailable due to maintenance, failure to start, or failure to run (Hedman et al. 2010).

The hybrid microgrid portfolio was optimized using XENDEE ("BankableEnergy" 2018), (Stadler and Nasle 2019), (Pencenak, Stadler, and Fahy 2019). XENDEE is a cloud computing software that jointly performs techno-economic optimization and power systems analysis. XENDEE's economic optimization tool selects, sizes, places, and dispatches energy assets within a microgrid portfolio using a Mixed Integer Linear Programing (MILP) approach. The optimization tool minimizes total annual costs (or emissions) of providing energy services to a microgrid considering system energy demand, regulatory requirements, and energy procurement costs including monthly fixed utility costs, volumetric electricity purchases, demand charges, annualized technology investment costs, and technology operation and maintenance (O&M) costs during grid-connected and

islanding operations. Optimization accounts for technical operating constraints of the considered technologies (e.g. charging/discharging limits of battery stacks) and environmental conditions that influence the capacity of on-site renewable generation. The cost-optimal sizing of microgrid assets for on-grid operation in XENDEE was then evaluated for off-grid operation using dispatch routines presented in this study.

On-grid economic dispatch in XENDEE was completed using a local utility tariff for the defense installation service territory, which consisted of monthly fixed charges, distribution energy charges, on-peak energy charges, mid-peak energy charges, off-peak energy charges, monthly peak demand charges, and taxes. Energy costs differed for summer (June through September) and winter (October through May) months. Table 4.3 compares the baseline generator-only case with the cost-optimal (hybrid) microgrid portfolio calculated from XENDEE. Four fewer generators can be installed if solar PV and battery stacks are included in the microgrid portfolio while still meeting energy balance requirements at each hour of the optimization. Peak capacity of the dispatchable generation (generator + battery storage) of the hybrid microgrid portfolio (5,700 kW) exceeds the peak capacity of the generator-only microgrid (5,250 kW), indicating the hybrid system can provide additional capacity reserve when battery storage is full. Table 4.4 shows that the hybrid microgrid reduces the levelized cost of electricity (LCOE) and operating expenses by 17.2% and 46.5%, respectively, by reducing both energy and demand charges paid to the utility during normal grid-tied operation.

Table 4.3: Capacity of energy assets included in military microgrid portfolios.

Microgrid Portfolio	Generator Units	Total Generator Capacity (kW)	Solar PV Area (m^2)	Total Solar PV Capacity (kW)	Battery Units	Total Battery Capacity (kWh)
Generator-only	7	5,250	0	0	0	0
Hybrid	3	2,250	109,862	16,479	23	13,800

Table 4.4: Economics of generator-only and hybrid military microgrid portfolios.

Microgrid Portfolio	Levelized Cost of Electricity ($/kWh)	Operating Expenses ($)	Annualized Investment Costs ($)	20-year Net Present Value ($)
Generator-only	0.0884	7,312,209	343,289	41,165,000
Hybrid	0.0732	3,915,299	2,000,145	49,359,000

4.6. Control Parameter Sensitivity Analysis

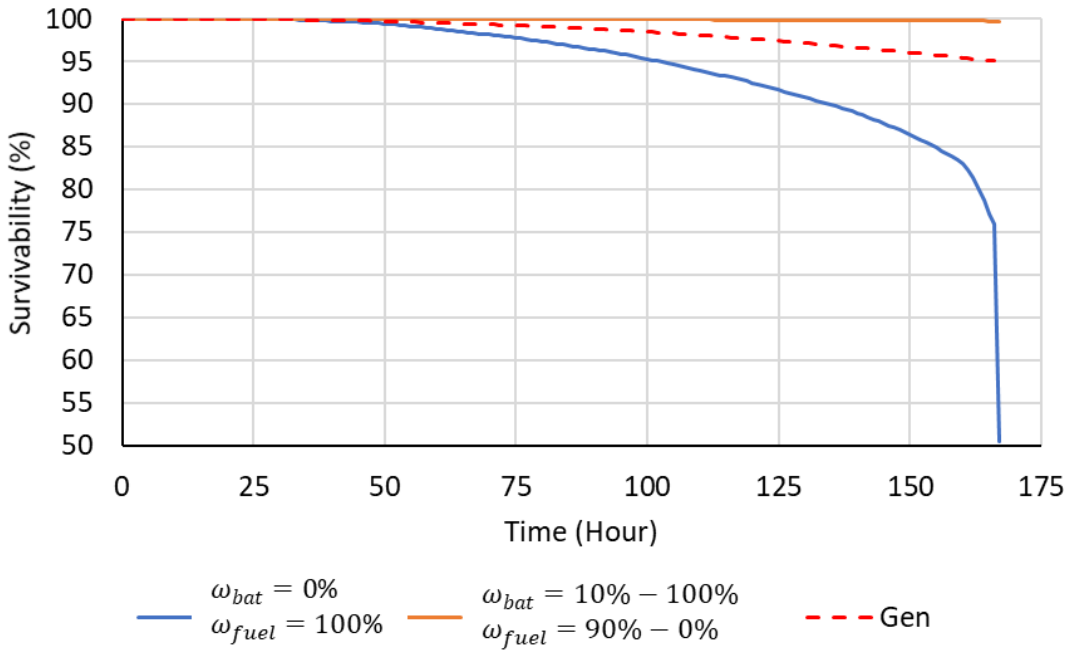
A sensitivity analysis was performed for weighting factors in the objective function (Eq. 12) to evaluate the effect on resilience metrics. The summation of the three weighting factors (ω_{bat}, ω_{fuel}, and ω_{load}) was constrained to one as described in Section 3.1. The unserved load weighting factor, ω_{load}, was set near to one (0.999999999) to heavily disincentive load shedding unless on-site generation cannot meet the critical load. Eqs. 31 and 32 show how the remaining unused weight was shared between the weighting factor for batteries, ω_{bat}, and the weighting factor for fuel, ω_{fuel}, where γ is a scaling factor between 0 and 1.

$$\omega_{bat} = (1 - \omega_{load}) \times \gamma \quad \text{(Eq. 31)}$$

$$\omega_{fuel} = (1 - \omega_{load}) \times (1 - \gamma) \quad \text{(Eq. 32)}$$

Battery stacks are assumed to be fully charged at the beginning of an islanding event, an assumption that is later relaxed and explored. 50,000 gallons of fuel is assumed to be on-site (ESTCP 2019). Simulations were performed with an outage starting in each hour of the year, with results combined to calculate average annual performance

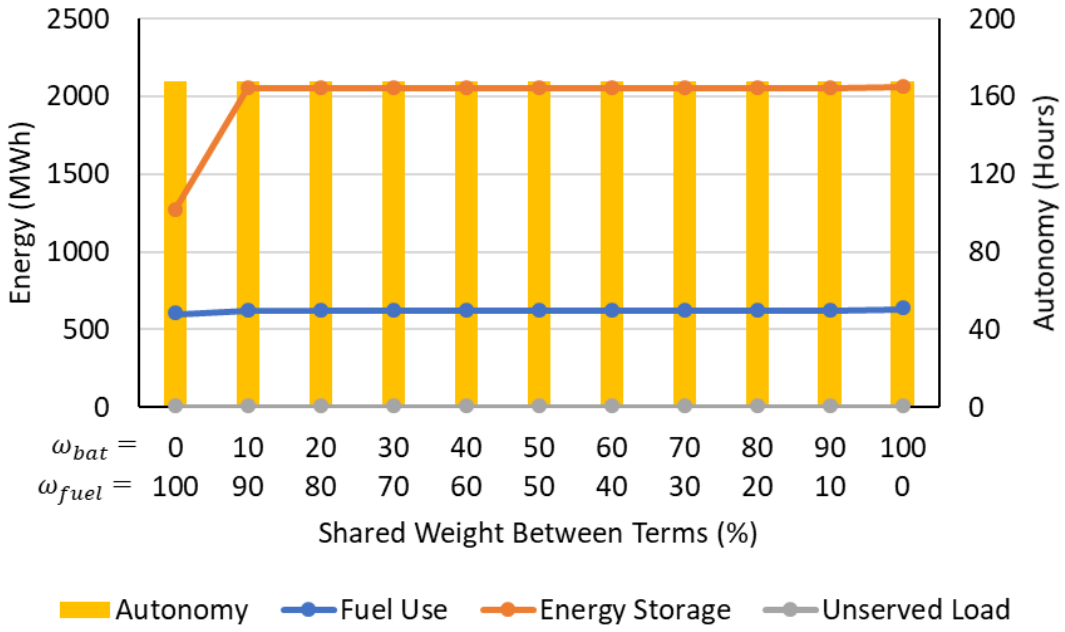
characteristics that incorporate the hourly variability of loads and solar PV generation over a year. 4.3 shows survivability of the microgrid over a 168-hour grid outage. The survivability curve for the baseline generator-only microgrid reduces over time as likelihood for asset failure increases due to the generator mean time between failure. This effect is reduced in the hybrid microgrid with fewer generators due to the addition of storage and solar PV in the microgrid portfolio. The hybrid microgrid shows a significant improvement in survivability over 168-hours to 99.72%, as compared to the generator-only microgrid at 95.03% over the same time period. This demonstrates the hybrid microgrid improves the probability to meet critical loads and extends autonomy to provide continuity of operations during even longer outages beyond 7 days. The last survivability curve in Fig. 4.3 shows the effect of removing the battery weighting factor (i.e. $\omega_{bat} = 0$), which simplifies the objective function to reduce fuel and dispatches batteries instead of saving battery storage for capacity reserve. Batteries provide 3,450 kW of the 5,700 kW total on-site peak generation capacity and the absence of that generation capacity significantly affects microgrid survivability. This critical finding indicates that an optimization routine working to minimize fuel consumption could worsen the probability to meet critical load for hybrid microgrids.



4.3: Survivability of microgrids with various values of the resilience weighting factor control parameter.

4.4 shows three of the four resilience metrics, and the total energy stored in battery stacks for the duration of the outage. The microgrid is autonomous for the full duration of the islanding event (168 hours) and is capable of meeting all critical load regardless of the battery weighting factor and analogous change in the fuel weighting factor. A battery weighting factor between 10% and 100% results in nearly identical performance metrics. However, when the battery weighting factor is set equal to zero, the optimization formulation dispatches battery storage to minimize fuel use, leading to 3.5% less fuel consumed over an outage and 62.2% less energy stored in battery stacks when compared to the other sensitivity scenarios with near-equal results. Although this creates a modest decrease in fuel consumption, microgrid survivability is reduced by 49.25% at the end of a 168-hour islanding event because the total energy stored in the battery stacks during the

outage is decreased, resulting in scenarios when the battery stacks cannot provide capacity to displace failure of a generation source.



4.4: Resilience metrics of control parameters sensitivity analysis.

This finding indicates that battery terms dominate the objective function whereas fuel terms have no effect or a negative effect on microgrid survivability, the primary performance metric. Therefore, the remaining sensitivity analyses and performance evaluations use values of 0.000000001 and 0 for the battery and fuel weighting factors, respectively. This promotes energy security by maintaining a higher battery state of charge to provide capacity in the event of a failed generator or battery stack.

4.7. Performance Evaluations

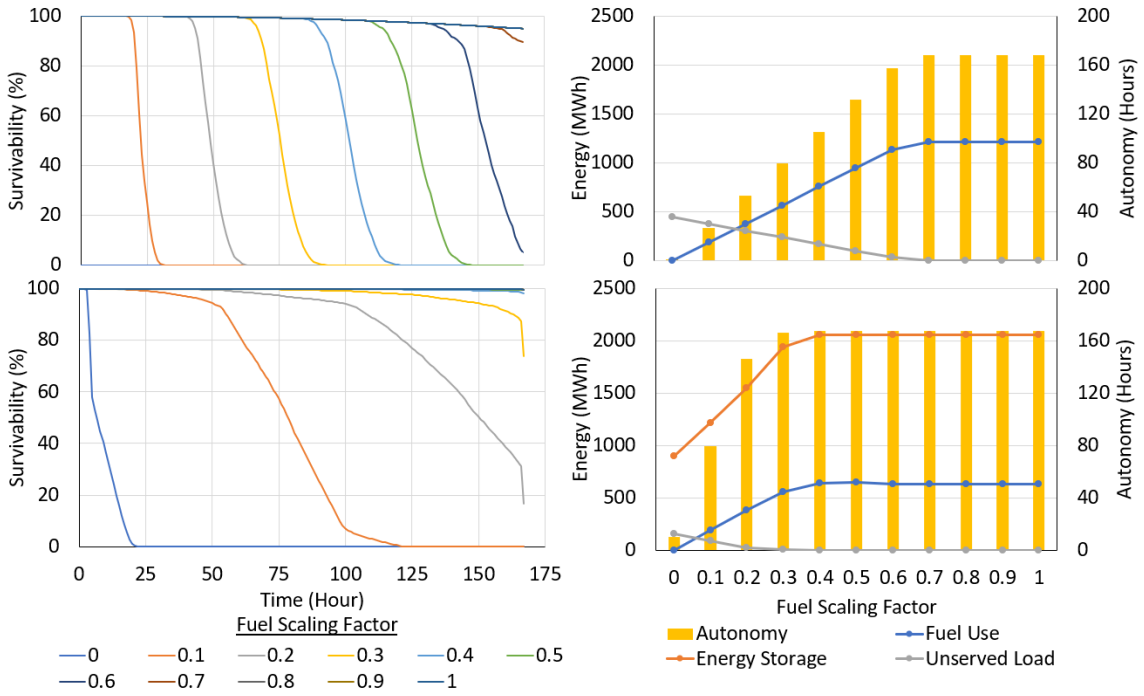
Performance evaluations compare a hybrid microgrid to a generator-only microgrid to quantify potential benefits of adding solar PV and energy storage, and reducing the number of generators, to meet critical load during an islanding event. Four resilience metrics were evaluated through sensitivity analyses of operational parameters including the amount of on-site fuel reserves, critical load intensity, solar PV generation, and battery SOC at the start of an islanding event.

4.7.1. On-site Fuel Reserves

On-site fuel reserve availability was varied between 0% and 100% of the nominal 50,000 gallons. 4.5 displays evaluation metrics for a generator-only and a hybrid microgrid. Once fuel reserves are exhausted, survivability for the generator-only microgrid decreases rapidly until it reaches zero. The hybrid microgrid has slower degradation in survivability because solar PV and battery stacks displace generator use and slow consumption of fuel reserves. If there is no fuel on-site or if fuel is depleted, the hybrid microgrid is still able to provide autonomy to meet the critical load for 10 hours, on average over the year, by using solar PV generation and storage energy in battery stacks.

The generator-only microgrid requires a minimum of 40,000 gallons (80%) of on-site fuel reserves to ensure 100% of the critical load will be served and 89.50% survivability at the end of a 168-hour islanding event. However, the hybrid microgrid requires only 25,000 gallons (50%) of on-site fuel reserves to meet 100% of the critical load and increases survivability to 99.56% at the end of a 168-hour islanding event. Similar survivability results occur when the generator-only microgrid has 70% fuel reserves and the hybrid microgrid has only 30% fuel reserves. Exploring this in more detail indicates

that the generator-only microgrid uses 47.80% more fuel than the hybrid microgrid to meet the critical load. These findings illustrate that a microgrid with solar plus storage is much less dependent on fuel availability and resupply when compared to a generator-only microgrid.



4.5: Sensitivity analysis of on-site fuel reserves on performance metrics for generator-only microgrid (top) and hybrid microgrid (bottom).

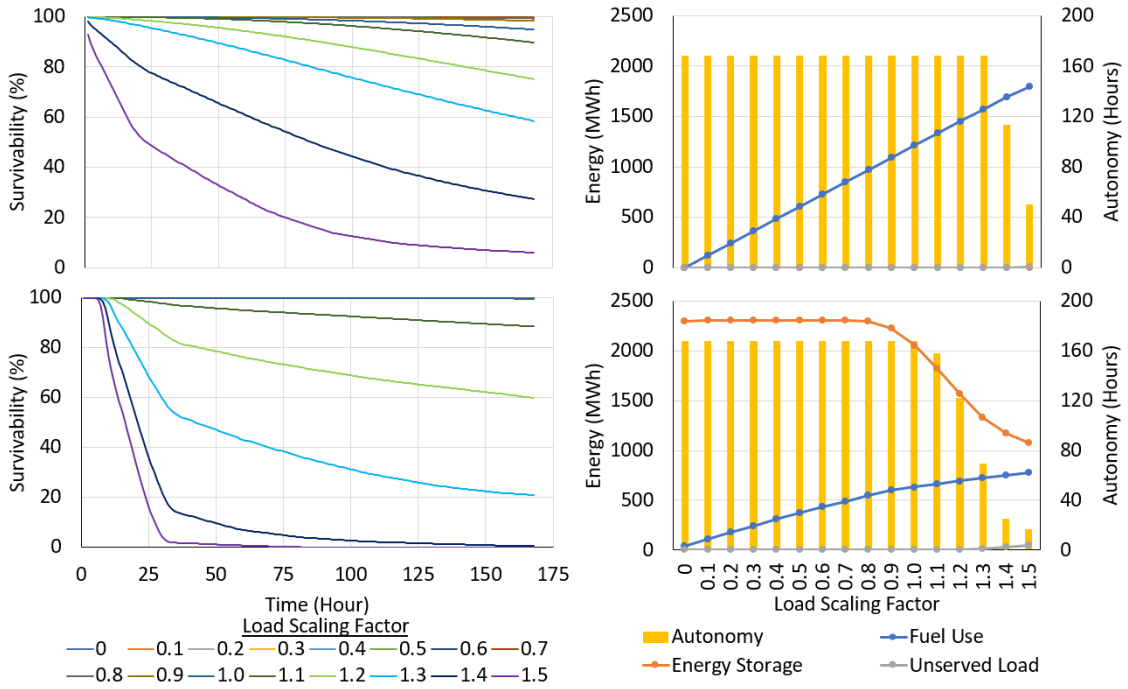
4.7.2. Critical Load

Both microgrid portfolios were designed to meet peak critical load observed at the military installation. Sensitivity analysis of the critical load intensity provides insights into how the installed equipment could meet changes to installation infrastructure or assignments, or address real-time changes in mission objectives. 4.6 displays resilience metrics of a generator-only and hybrid microgrid when varying the critical load from 0% to 150%.

Survivability of the generator-only microgrid and hybrid microgrid is similar for 110% critical loads suggesting that both portfolios are equally adept at serving slightly increased loads than originally designed for. However, for greater intensities of critical load, the survivability of the hybrid microgrid is affected more significantly than the generator-only microgrid because the total generation capacity of the hybrid microgrid was optimally determined while the total generation capacity of the generator-only microgrid considered a N+1 reliability constraint.

Fuel use increases linearly with critical load from 0% to 150% in the generator-only microgrid. This linear trend is similar for the hybrid microgrid as critical load increases from 0% to 100%, but becomes sub-linear from 110% to 150% because loads exceed the combined capacity of all generators and therefore battery stacks must be dispatched in combination with generators to meet greater loads, resulting in a modest reduction in the amount of fuel used per kWh of load served. The amount of energy stored in battery stacks remains nearly constant as critical load increases from 0% to 80% because the dispatch optimization prioritizes stored energy over saving fuel. However, once the critical load is increased above 80%, battery stacks must be dispatched to ensure the microgrid can achieve 168-hour autonomy. Once the critical load is increased above 100%, the autonomy of the microgrid is negatively affected with a large decrease between 120% (122 hours autonomy) and 140% (25 hours autonomy). This occurs because the combined capacity of the battery stacks, diesel generators, and solar PV are insufficient to meet the increased demand, creating circumstances in which the autonomy of the hybrid microgrid is less than the generator-only microgrid. Although the hybrid microgrid can meet 150% of the critical load for a shorter duration, the reduction of fuel use by 57.05% means the

hybrid system can operate at reduced capacity for a longer period of time. At 150% critical load the hybrid microgrid curtails 51.3 MWh of critical load.



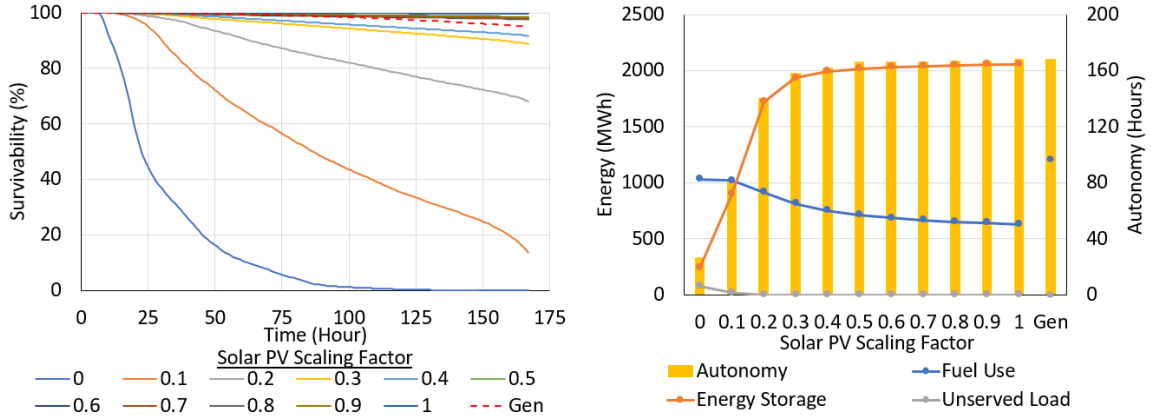
4.6: Sensitivity analysis of critical load intensity on performance metrics for generator-only microgrid (top) and hybrid microgrid (bottom).

4.7.3. Solar PV Generation

Solar PV generation is typically viewed as a non-dispatchable resource with high variability due to intermittent environmental conditions. Performance evaluations here vary solar PV generation between 0% and 100% to quantify how solar intermittency affects resilience metrics. 4.7 shows evaluation metrics for a hybrid microgrid and a generator-only microgrid.

Reducing solar PV generation by 50% has limited impact on autonomy (-1.04%) and a modest increase on fuel use (+11.20%) because generators must be dispatched to keep batteries charged when excess solar PV generation is not available. When solar PV generation decreases below 50%, there is insufficient solar to maintain batteries at full

charge and therefore autonomy and survivability are negatively affected. If there is an extended period with no solar PV generation (i.e. 0% solar PV scaling factor), autonomy reduces by 83.98% and the critical load must be curtailed by 17.54%. This modest reduction in serving the critical load shows that the hybrid microgrid can still dispatch generators and battery stacks to maintain operations at reduced levels.



4.7: Sensitivity analysis of solar PV generation on performance metrics for hybrid microgrid.

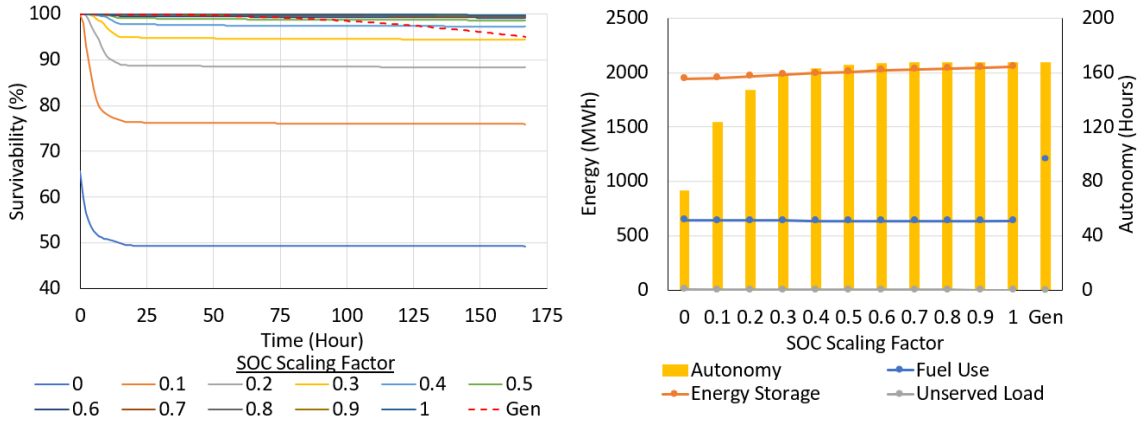
4.7.4. Battery Stack Starting State of Charge

The starting SOC of battery stacks at the onset of an islanding event can vary if on-grid dispatch routines discharge batteries to improve economics, such as during peak shaving. This effect is explored by varying the starting SOC between 0% and 100% with results shown in 4.8 for a hybrid microgrid and a generator-only microgrid.

The survivability of the microgrid decreases appreciably if the starting SOC is below 40%, dropping down to 49.24% if batteries are fully depleted. A hybrid microgrid portfolio must begin an islanding event with batteries above 40% SOC to surpass the 7-day survivability of the generator-only microgrid. However, if the hybrid portfolio starts with a battery stack SOC of 40%, than it is more likely than the generator-only microgrid

portfolio to serve the critical load for outages lasting longer than 130 hours. This is because the probability of a generator failure for the generator-only microgrid is more probable than the combined probability of a generator failure or battery stack failure once the batteries are fully charge for the hybrid microgrid.

The hybrid portfolio uses an average 47.80% less fuel than the generator-only portfolio but needs to start with at least 70% SOC to achieve 168-hour autonomy. However, even if battery stacks are fully depleted at the beginning of an islanding event, the microgrid can achieve an average autonomy of 74 hours over the simulated year when the initial critical load is low enough to be met with generators, allowing solar PV generation to charge batteries for capacity reserve later in the islanding event. That behavior produces the flattening of the survivability curve shown in Fig. 4.8. Fuel use is slightly increased for lower battery starting SOC because generators charge battery stacks at the beginning of an outage if there is insufficient solar for charging. These findings indicate that on-grid economic dispatch should impose a minimum 70% SOC operational constraint if 168-hour autonomy is mission critical. However, if the hybrid portfolio starts with less than 70% SOC a modest 0.23% of the critical load can be curtailed over the duration of the islanding event to reach 168-hour autonomy.



4.8: Sensitivity analysis of battery starting SOC on performance metrics for hybrid microgrid.

4.8. Conclusions

This study developed a statistical approach to model microgrid resilience and formulated an optimization algorithm for microgrid control during islanding events. A hybrid military microgrid portfolio with solar PV, storage, and generators was optimally designed to minimize on-grid operational expenses using XENDEE. For off-grid operation, the survivability of that hybrid system to meet mission critical loads was modeled using a Markov chain model with probabilities reflected for generator reliability and battery stack reliability. Sensitivity analyses and performance evaluations compared resilience metrics for a hybrid microgrid and generator-only microgrid: survivability, autonomy, fuel usage, and unserved load. Significant findings include:

- Optimization control algorithms that solely minimize fuel consumption can significantly reduce the survivability of hybrid microgrids. Case studies demonstrated that survivability could be reduced by up to 49.25% if minimizing fuel was the sole operational goal.

- The hybrid microgrid requires 37.5% less on-site fuel reserves than the generator-only microgrid to ensure autonomy for 168 hours, 100% of the critical load will be served, and 99.56% survivability at the end of a 168-hour islanding event. However, the generator-only microgrid can only ensure 89.50% survivability at the end of a 168-hour islanding event.
- The hybrid microgrid portfolio uses 47.80% less fuel than the generator-only microgrid portfolio for 168-hour islanding events under nominal conditions.
- If there is no fuel on-site and the battery stacks start with 100% SOC, the hybrid microgrid can provide autonomy to meet the critical load for 10 hours by using a combination of stored energy and solar PV generation.
- For intensities of critical load above 110%, the survivability of the hybrid microgrid is reduced more drastically than the generator-only microgrid due to N+1 reliability design considerations that resulted in excess on-site generation capacity in the generator-only microgrid portfolio.
- The survivability at the end of a 168-hour islanding event of a hybrid microgrid serving 150% of the nominal critical load is reduced by 5.96% when compared to a generator-only microgrid. However, the hybrid microgrid uses 57.05% less fuel to meet 88.40% of the critical load. This fuel savings can be used to extend operations at reduced capacity for a longer period of time than the generator-only microgrid.
- The hybrid microgrid portfolio is dependent on the full solar PV generation to achieve autonomy for 168 hours but can still serve 99.95% of the critical load with just 50% of solar PV generation.

- Battery starting SOC at the beginning of an islanding event must be above 70% to ensure autonomy for 168 hours. However, if batteries are fully depleted, excess solar PV and generators can recharge the batteries to maintain microgrid survivability with only 0.23% of the critical load being curtailed.
- The hybrid microgrid portfolio is statistically more likely to survive a 168-hour islanding event than a generator-only microgrid portfolio if the battery stack starting SOC is above 50%.
- On-grid economic dispatch should maintain batteries with sufficient contingency reserve capacity to reach 168-hour autonomy in the event of a grid outage. A minimum 70% battery SOC was identified for the case study analyzed.

Generalized findings indicate that a hybrid microgrid that minimizes fuel use by dispatching batteries is less likely to survive an islanding event than a generator-only microgrid. Batteries in the hybrid microgrid are crucial to providing capacity reserve in case of generator failure or battery stack failure. If the batteries are depleted to save fuel, the hybrid microgrid is less capable of surviving an islanding event. The hybrid microgrid is less reliant on fuel and therefore can potentially increase mission autonomy for extended duration islanding events when compared to a generator-only microgrid. The diversity and increased quantity of generation assets within the hybrid microgrid portfolio results in a more resilient system to provide local power over the duration of an islanding event.

Further work can explore the reliability of all subsystems including but not limited to solar PV, electrical distribution network, communication networks, and switch gear. Modifying the Markov chain to account for real-time maintenance of energy assets is another area for investigation. Lastly, the assumption that an islanding event can occur with

equal probability over the year can be revaluated to accurately depict risk to seasonal issues such as hurricanes, forest fires, extreme heat events, flooding, etc.

4.9. Acknowledgements

This study was funded in part by the US Department of Defense Environmental Security Technology Certification Program (ESTCP) under contract number W912HQ19P0012 / ESTCP Project Number EW19-5277. Support from XENDEE Corporation, Southern Research, and 350Solutions is greatly appreciated.

4.10. References

Abd-rabou, A M, A M Soliman, and A S Mokhtar. 2015. "Impact of DG Different Types on the Grid Performance" 2: 149–60.

Abraham, S., and R. Efford. 2004. "Final Report on the August 14, 2003 Blackout in the United States and Canada." *," US-Canada Power System Outage Task Force*.

Aghdam, Farid Hamzeh, Javad Salehi, and Sina Ghaemi. 2018. "Contingency Based Energy Management of Multi-Microgrid Based Distribution Network." *Sustainable Cities and Society* 41 (January): 265–74. https://doi.org/10.1016/j.scs.2018.05.019.

Amirioun, M H, F Aminifar, H Lesani, and M Shahidehpour. 2019. "Electrical Power and Energy Systems Metrics and Quantitative Framework for Assessing Microgrid Resilience against Windstorms." *Electrical Power and Energy Systems* 104 (January 2018): 716–23. https://doi.org/10.1016/j.ijepes.2018.07.025.

Asmus, Peter, Adam Forni, and Laura Vogel. 2018. "Microgrid Analysis and Case Studies Report."

Ayar, Muharrem, Student Member, Serhat Obuz, Student Member, Rodrigo D Trevizan, Student Member, Arturo S Bretas, Senior Member, Haniph A Latchman, and Senior Member. 2017. "A Distributed Control Approach for Enhancing Smart Grid Transient Stability and Resilience" 8 (6): 3035–44.

"BankableEnergy." 2018. 2018. https://www.bankableenergy.com/.

Billinton, Li, and Wenyuan Li. 1994. *Reliability Assessment of Electric Power Systems Using Monte Carlo Methods*. New York: Plenum.

Biswal, Gyan Ranjan, R. P. Maheshwari, and M. L. Dewal. 2012. "System Reliability and Fault Tree Analysis of SeSHRS-Based Augmentation of Hydrogen: Dedicated for Combined Cycle Power Plants." *IEEE Systems Journal* 6 (4): 647–56. https://doi.org/10.1109/JSYST.2012.2192065.

Braun, Martin, Chenjie Ma, Paul Kaufmann, and J T. 2016. “Optimal Generation Dispatch of Distributed Generators Considering Fair Contribution to Grid Voltage Control” 87: 946–53. https://doi.org/10.1016/j.renene.2015.07.083.

Bryan, W. 2012. “Emergency Situation Reports: Hurricane Sandy.”

Cagnano, A, A Caldarulo Bugliari, and E De Tuglie. 2018. “A Cooperative Control for the Reserve Management of Isolated Microgrids.” *Applied Energy* 218 (March): 256–65. https://doi.org/10.1016/j.apenergy.2018.02.142.

Cattaneo, Alessandro, Sreenath Chalil, and Scott Backhaus. 2018. “Integration of Optimal Operational Dispatch and Controller Determined Dynamics for Microgrid Survivability Consortium for Electric Reliability Technology Solutions.” *Applied Energy* 230 (August): 1685–96. https://doi.org/10.1016/j.apenergy.2018.08.127.

Chen, Thomas M, Senior Member, Juan Carlos Sanchez-aarnoutse, John Buford, and Senior Member. 2011. “Petri Net Modeling of Cyber-Physical Attacks on Smart Grid.” *IEEE Transactions on Smart Grid* 2 (4): 741–49. https://doi.org/10.1109/TSG.2011.2160000.

Clifford Power. 1999. “Wet Stacking of Generator Sets and How to Avoid It.”

Colli, Alessandra. 2015. “Failure Mode and Effect Analysis for Photovoltaic Systems.” *Renewable and Sustainable Energy Reviews* 50: 804–9. https://doi.org/10.1016/j.rser.2015.05.056.

Collins, Elmer, Michael Dvorack, Jeff Mahn, Michael Mundt, and Michael Quintana. 2009. “RELIABILITY AND AVAILABILITY ANALYSIS OF A FIELDED PHOTOVOLTAlC,” 2316–21.

Department of Defense. 2014. “Department of Defense Directive 4180.01.”

———. 2017. “Army Directive 2017-07.”

Department of the Navy. n.d. “Department of the Navy’s Energy Program for Security and Independence.” https://doi.org/10.1016/0010-4485(78)90081-7.

Dorn, Derek. n.d. “MACRS Depreciation and Renewable Energy Finance.”

Dulau, Lucian Ioan, Mihail Abrudean, and Dorin Bica. 2014. “Effects of Distribution Generation on Electric Power Systems.” *Procedia Technology* 12: 681–86. https://doi.org/10.1016/j.protcy.2013.12.549.

Electric Power Research Institute. 2016. “Electric Power System Resiliency Challenges and Opportunities.”

EOS. n.d. “Eos Aurora Product Description.” http://www.eosenergystorage.com/wp-content/uploads/2017/01/eos_product_brouchure011817.pdf.

———. n.d. “EOS Energy Storage.” https://eosenergystorage.com/.

Ericson, Sean. 2019. “Calculating the Reliability of a Backup System,” 1–6.

ESTCP. 2019. “Environmental Security Technology Certification Program (ESTCP).”

Eto, Joseph H, and Kristina Hamachi Lacommare. 2008. “Tracking the Reliability of the U . S . Electric Power System : An Assessment of Publicly Available Information Reported to State Public Utility Commissions,” no. October.

Figueroa-candia, Marcelo, Frank A Felder, and David W Coit. 2018. “Resiliency-Based Optimization of Restoration Policies for Electric Power Distribution Systems.” *Electric Power Systems Research* 161: 188–98. https://doi.org/10.1016/j.epsr.2018.04.007.

Fischer, E M, and R Knutti. 2015. “Anthropogenic Contribution to Global Occurrence of Heavy-Precipitation and High-Temperature Extremes” 5 (June). https://doi.org/10.1038/NCLIMATE2617.

Fu, Ran, David Feldman, Robert Margolis, Ran Fu, David Feldman, and Robert Margolis. 2018. “U . S . Solar Photovoltaic System Cost Benchmark : Q1 2018 U . S . Solar Photovoltaic System Cost Benchmark : Q1 2018,” no. November.

Golnas, Anastasios. 2013. “PV System Reliability : An Operator ’ s Perspective” 3 (1): 416–21.

Goyal, Megha, and Arindam Ghosh. 2016. “Sustainable Energy , Grids and Networks Microgrids Interconnection to Support Mutually during Any Contingency.” *Sustainable Energy, Grids and Networks* 6: 100–108. https://doi.org/10.1016/j.segan.2016.02.006.

HBM Prenscia. 2019. “Fault Tree Analysis.” 2019. https://www.weibull.com/basics/fault-tree/index.htm.

He, Zichang, and Wen Jiang. 2018. “A New Belief Markov Chain Model and Its Application in Inventory Prediction.” *International Journal of Production Research* 7543: 1–18. https://doi.org/10.1080/00207543.2017.1405166.

Hecht, Herbert. 2003. *Systems Reliability and Failure Prevention*. Artech House. https://ebookcentral-proquest-com.ezproxy1.lib.asu.edu/lib/asulib-ebooks/detail.action?docID=227632.

Hedman, Kory W, Student Member, Michael C Ferris, Richard P O Neill, Emily Bartholomew Fisher, Student Member, and Shmuel S Oren. 2010. “Co-Optimization of Generation Unit Commitment and Transmission Switching With N-1 Reliability” 25 (2): 1052–63.

Hines, Paul, and Karthikeyan Balasubramaniam. 1977. “Cascading Failures in Power Grids.”

Hirsch, Adam, Yael Parag, and Josep Guerrero. 2018. “Microgrids : A Review of Technologies , Key Drivers , and Outstanding Issues” 90 (March): 402–11. https://doi.org/10.1016/j.rser.2018.03.040.

Hunt, Kirby, Anthony Blekicki, Robert Callery, and First Solar. 2015. “Availability of

Utility-Scale Photovoltaic Power Plants," 0–2.

Hussain, Akhtar, Van-hai Bui, and Hak-man Kim. 2019. "Microgrids as a Resilience Resource and Strategies Used by Microgrids for Enhancing Resilience." *Applied Energy* 240 (February): 56–72. https://doi.org/10.1016/j.apenergy.2019.02.055.

Jamei, Mahdi, Eran Schweitzer, Anna Scaglione, and Kory W Hedman. n.d. "Gas and Electric Grid Unit Commitment with Coordinated N-1 Generator Contingency Analysis." *2018 Power Systems Computation Conference (PSCC)*, 1–7. https://doi.org/10.23919/PSCC.2018.8442863.

Ji, Chuanyi, Yun Wei, Henry Mei, Jorge Calzada, Matthew Carey, and Steve Church. 2016. "Large Scale Data Analysis of Power Grid Resilience across Multiple US Service Regions," no. April 2018. https://doi.org/10.1038/nenergy.2016.52.

Kerr, Richard A. 2011. "Humans Are Driving Extreme Weather ; Time to Prepare." https://doi.org/10.1126/science.334.6059.1040.

Khani, Davood, Ahmad Sadeghi, and Hossein Madadi. 2012. "Electrical Power and Energy Systems Impacts of Distributed Generations on Power System Transient and Voltage Stability" 43: 488–500. https://doi.org/10.1016/j.ijepes.2012.06.007.

Lammers, Imke. 2017. "Grid Resilience Governance of the Future : Analyzing the Role of Associations in Experimental Smart Grid Projects in The Netherlands Grid Resilience Governance of the Future : Analyzing the Role of Associations in Experimental Smart Grid Projects in The N," no. August. https://doi.org/10.1007/978-3-319-61813-5.

Lau, Eng Tseng, Kok Keong Chai, Yue Chen, and Jonathan Loo. 2018. "Efficient Economic and Resilience-Based Critical Infrastructures," 1–20. https://doi.org/10.3390/en11123418.

Lawder, Matthew T, Vilayanur Viswanathan, and Venkat R Subramanian. 2015. "Balancing Autonomy and Utilization of Solar Power and Battery Storage for Demand Based Microgrids" 279: 645–55. https://doi.org/10.1016/j.jpowsour.2015.01.015.

Lee, Hyojong, Shwetha Niddodi, Anurag Srivastava, and David Bakken. 2016. "Decentralized Voltage Stability Monitoring and Control in the Smart Grid Using Distributed Computing Architecture." *2016 IEEE Industry Applications Society Annual Meeting*, 1–9. https://doi.org/10.1109/IAS.2016.7731871.

Lin, P. O.Ting, Y. U.Cheng Chou, Yung Ting, Shian Shing Shyu, and Chang Kuo Chen. 2014. "A Robust System Reliability Analysis Using Partitioning and Parallel Processing of Markov Chain." *Artificial Intelligence for Engineering Design, Analysis and Manufacturing: AIEDAM* 28 (4): 311–22. https://doi.org/10.1017/S0890060414000493.

Lin, Yanling, and Zhaohong Bie. 2016. "Study on the Resilience of the Integrated Energy System." *Energy Procedia* 103 (April): 171–76.

https://doi.org/10.1016/j.egypro.2016.11.268.

Mahmud, M A, M J Hossain, and H R Pota. 2011. *Analysis of Voltage Rise Effect on Distribution Network with Distributed Generation*. *IFAC Proceedings Volumes*. Vol. 44. IFAC. https://doi.org/10.3182/20110828-6-IT-1002.01305.

Marler, R T, and J S Arora. 2004. "Survey of Multi-Objective Optimization Methods for Engineering" 395: 369–95. https://doi.org/10.1007/s00158-003-0368-6.

Marler, R Timothy, and Jasbir S Arora. 2010. "The Weighted Sum Method for Multi-Objective Optimization : New Insights," 853–62. https://doi.org/10.1007/s00158-009-0460-7.

Martin-martínez, F, and M Rivier. 2016. "A Literature Review of Microgrids : A Functional Layer Based Classi Fi Cation" 62: 1133–53. https://doi.org/10.1016/j.rser.2016.05.025.

Mashayekh, Salman, Michael Stadler, Gonçalo Cardoso, Miguel Heleno, Sreenath Chalil Madathil, Harsha Nagarajan, Russell Bent, Marc Mueller-stoffels, Xiaonan Lu, and Jianhui Wang. 2017. "Security-Constrained Design of Isolated Security-Constrained Design of Isolated Multi-Energy Microgrids," no. September.

Mei, Xiong, and Guangcai Gong. 2018. "Predicting Airborne Particle Deposition by a Modi Fi Ed Markov Chain Model for Fast Estimation of Potential Contaminant Spread" 185 (October 2017): 137–46. https://doi.org/10.1016/j.atmosenv.2018.04.050.

Miao, Shuwei, Guangtao Ning, Yingzhong Gu, Jiahao Yan, and Botao Ma. 2018. "Markov Chain Model for Solar Farm Generation and Its Application to Generation Performance Evaluation" 186. https://doi.org/10.1016/j.jclepro.2018.03.173.

Miller, Stephen S. 2008. "Extending Traditional Planning Methods to Evaluate the Potential for Cascading Failures in Electric Power Grids," 1–7.

Molyneaux, Lynette, Liam Wagner, Craig Froome, and John Foster. 2012. "Resilience and Electricity Systems : A Comparative Analysis" 47: 188–201. https://doi.org/10.1016/j.enpol.2012.04.057.

Momoh, James. 2012. *Smart Grid: Fundamentals of Design and Analysis*. IEEE. https://ieeexplore-ieee-org.ezproxy1.lib.asu.edu/document/6183637.

MQ Power. 2007. "750kW Containerized Diesel Generator Set." Carson.

Mrowca, B. 2011. "Emergency Diesel Generator Failure Review 1999 - 2001." *EDG Failure Review*. http://www.nrc.gov/NRR/OVERSIGHT/ASSESS/faqs_by_id.pdf.

Müller, Sven C, Marc Osthues, Christoph Rekowski, Ulf Häger, and Christian Rehtanz. 2013. "Techno-Economic Evaluation of Corrective Actions for Efficient Attainment of (N-1) -Security in Operation and Planning." https://doi.org/10.1109/PESMG.2013.6672676.

Naja, Javad, Ali Peiravi, and Josep M Guerrero. 2018. “Power Distribution System Improvement Planning under Hurricanes Based on a New Resilience Index” 39 (December 2017): 592–604. https://doi.org/10.1016/j.scs.2018.03.022.

Nguyen, S V T. 2012. “Microgrid Study : Energy Security for DoD Installations,” no. June.

Norris, J.R. 1998. *Markov Chains*. Illustrate. Cambridge University Press.

Ogunjuyigbe, A S O, T R Ayodele, and O O Akinola. 2016. “Impact of Distributed Generators on the Power Loss and Voltage Profile of Sub-Transmission Network.” *Journal of Electrical Systems and Information Technology* 3 (1): 94–107. https://doi.org/10.1016/j.jesit.2015.11.010.

Pencenak, Z. K., M. Stadler, and K. Fahy. 2019. “Efficient Multi-Year Economic Energy Planning in Microgrids.” *Applied Energy* 255.

Prowell, S. J., and J. H. Poore. 2004. “Computing System Reliability Using Markov Chain Usage Models.” *Journal of Systems and Software* 73 (2): 219–25. https://doi.org/10.1016/S0164-1212(03)00241-3.

Ramakrishnan, M. 2016. “Integration of Functional Reliability Analysis and System Hardware Reliability through Monte Carlo Simulation.” *Annals of Nuclear Energy* 95: 54–63. https://doi.org/10.1016/j.anucene.2016.04.032.

Raquel, Parks. n.d. “Microgrids : Legal and Regulatory Hurdles for a More Resilient Energy Infrastructure,” 173–202.

Rebecca, Smith. 2014. “Assault on California Power Station Raises Alarm on Potential for Terrorism; April Sniper Attack Knocked Out Substation, Raises Concern for Country’s Power Grid.” *Wall Street Journal*, 2014.

Rodrigues, Yuri, Maíra Monteiro, Morad Abdelaziz, Liwei Wang, Antonio Z De Souza, and Paulo Ribeiro. 2020. “Electrical Power and Energy Systems Improving the Autonomy of Islanded Microgrids through Frequency Regulation.” *Electrical Power and Energy Systems* 115 (August 2019): 105499. https://doi.org/10.1016/j.ijepes.2019.105499.

Roege, Paul E, Zachary A Collier, James Mancillas, John A Mcdonagh, and Igor Linkov. 2014. “Metrics for Energy Resilience” 72: 249–56. https://doi.org/10.1016/j.enpol.2014.04.012.

Saleh, Khaled A, Hatem H Zeineldin, and Ehab F El-saadany. 2017. “Optimal Protection Coordination for Microgrids Considering N − 1 Contingency” 13 (5): 2270–78.

Schossig, Thomas, and Walter Schossig. 2013. “DISTURBANCES AND BLACKOUTS – LESSONS LEARNED TO MASTER THE ENERGY TURNAROUND,” no. October.

Shen, Lijuan, Beatrice Cassottana, and Loon Ching Tang. 2018. “Statistical Trend Tests for Resilience of Power Systems.” *Reliability Engineering and System Safety* 177

(April): 138–47. https://doi.org/10.1016/j.ress.2018.05.006.

Sherlock, Molly F. 2018. “The Energy Credit : An Investment Tax Credit for Renewable Energy,” 7–8.

Stadler, Michael, and A Nasle. 2019. “Planning and Implementation of Bankable Microgrids.” *The Electricty Journal*.

Stelloh, Tim. 2019. “California Braces for More Fires, Blackouts as Part of State’s New ‘Normal.’” NBC News. 2019. https://www.nbcnews.com/news/us-news/california-braces-more-fires-blackouts-wind-comes-roaring-back-state-n1073136.

Stott, By Peter. 2016. “How Climate Change Affects Extreme Weather Events” 352 (6293).

sunrun. 2019. “Building a More Resilient Grid.”

Taft, J D. 2017. “Electric Grid Resilience and Reliability for Grid Architecture,” no. November.

The Gridwise Alliance. 2013. “Improving Electric Grid Reliablity and Resilience: Lessons Learned from Superstorm Sandy and Other Extreme Events.”

Ton, Dan, and Merrill Smith. 2012. “The U.S. Department of Energy’s Microgrid Initiative.”

U.S. Environmental Protection Agency. 1997. “Guiding Principles for Monte Carlo Analysis.” *Us Epa*, no. March: 1–35. https://doi.org/EPA/630/R-97/001.

Venkatasubramanian, Vaithianathan, and Yuan Li. 2004. “Analysis of 1996 Western American Electric Blackouts.” *Bulk Power System Dynamics and Control* 4: 22–27.

Vugrin, Eric, Anya Castillo, and Cesar Silva-monroy. 2017. “Resilience Metrics for the Electric Power System : A Performance-Based Approach,” no. February.

Wang, Jiaren, Ning Xie, Wenxian Wu, Dong Han, Chengmin Wang, and Binruo Zhu. 2018. “Resilience Enhancement Strategy Using Microgrids in Distribution Network.” *Global Energy Interconnection* 1 (5): 537–43. https://doi.org/10.14171/j.2096-5117.gei.2018.05.002.

Wang, Jing, Wangda Zuo, Landolf Rhode-barbarigos, Xing Lu, Jianhui Wang, and Yanling Lin. 2020. “Literature Review on Modeling and Simulation of Energy Infrastructures from a Resilience Perspective.” *Reliability Engineering and System Safety* 183 (November 2017): 360–73. https://doi.org/10.1016/j.ress.2018.11.029.

Widergren, S, A Shankar, B Kelley, J Taft, and R Melton. 2018. “Toward a Practical Theory of Grid Resilience,” no. April.

Ye, Yixin, Ignacio E Grossmann, Jose M Pinto, and Sivaraman Ramaswamy. 2018. “Markov Chain MINLP Model for Reliability Optimization of System Design and Maintenance,” no. 2002: 1–6. https://doi.org/10.1016/B978-0-444-64241-7.50242-1.

Yu, Moduo, Wentao Huang, Nengling Tai, Xiaodong Zheng, Pan Wu, and Weidong Chen. 2018. “Transient Stability Mechanism of Grid-Connected Inverter-Interfaced Distributed Generators Using Droop Control Strategy.” *Applied Energy* 210 (March 2017): 737–47. https://doi.org/10.1016/j.apenergy.2017.08.104.

Zhenzhen, Song. 2015. “The Evaluation of Parameter M in the Big M Method of Linear Programming Song Zhenzhen,” no. Meita: 37–40.

Zhu, Yihai, and Jun Yan. 2014. “Revealing Cascading Failure Vulnerability in Power Grids Using Risk-Graph.” *IEEE Transactions on Parallel and Distributed Systems* 25 (12): 3274–84. https://doi.org/10.1109/TPDS.2013.2295814.

CHAPTER 5

DISSCUSION

The following discusses and compares findings from Chapters 2, 3, and 4 and presents opportunities for future research.

5.1. Implications for Scientific and Electrical Power and Energy Communities

Chapter 2 developed residential cooling strategies that provide customers and electric utilities with improved operational and financial outcomes. Six cooling strategies were evaluated and compared to a baseline logic-based controls strategy for a standard Building America B10 Benchmark residential home. Case studies completed for Phoenix, AZ, Los Angeles, CA, and Kona, HI demonstrate applicability of methods to locations with different environmental conditions and cooling needs. Each location also had unique time of use rate structure.

EnergyPlus was used to model the building envelope, heating ventilation and cooling system, thermal energy storage (TES) system, and annual energy costs. Control algorithms for dispatching of cooling systems were developed and coded into the EnergyPlus environment. An adaptive precooling strategy implemented thermostat control using a feedback loop to dispatch a heating ventilation and cooling system based on the intraday outdoor air temperature as a proxy for thermal losses to the environment. The controller automatically regulated cooling provided to the building based on expected thermal loads. This corrected potential issues with conventional precooling strategies that use predetermined setpoints that could precool the building when unnecessary and result in additional costs. Sensitivity analysis explored optimal precooling control parameters to provide the most financial benefit to customers. Control of the TES implemented a logic-

based algorithm that dispatched (charge or discharge) depending on time of day and thermal requirements of the building. Precooling and thermal energy storage were also combined to evaluate potential benefits together.

Chapter 2 quantified the benefit of cooling strategies to reduce customer on-peak demand by up to 75.6% and annual operational costs by up to 23.5%. Findings showed that implementing a precooling strategy, by means of a smart thermostat, offered the lowest pay back period for all three locations. This was primarily a result of the relatively high cost of TES for each location. Further, there were minimal additional economic improvements for combining precooling and TES because both strategies had similar effect to shift cooling loads to off-peak electrical rates. One benefit of TES is that the approach maintained a consistent indoor air temperature whereas the precooling strategy neglected customer thermal comfort. Potential future work could integrate thermal comfort considerations into the control schemes introduced in Chapter 2.

Reducing thermal loads can help utilities reduce peak demand and therefore reduce operating expenses by minimizing use of higher-cost peaker plants. These cost savings can be passed onto customers using time of use rate structures that incentivizes shifting electrical loads during typical times of electrical system peak demand. Widespread adoption of innovative cooling strategies has the potential to provide significant benefits for both electrical utilities and customers because thermal loads comprise 41% of total residential energy use in the United States. Expanding on this work, Chapter 3 identified opportunities to provide similar or improved benefits if electrical loads and distributed energy resources (DERs) are optimized.

Chapter 3 developed three microgrid control algorithms and compared results to assess technical and financial performance for a baseline logic-based control, model predictive control (MPC), and MPC with ancillary services allowed as a revenue stream. The logic-based control algorithm executes real-time dispatch at each time step using information on the current operating state of the energy asset and time-of-use (TOU) electricity rates, which is a similar approach to controls developed in Chapter 2 for dispatching TES. For Chapter 3, the two optimization-based control algorithms utilized much of the same formulation, with the algorithm including ancillary services expanding the optimization function and constraints to enable participation in spinning reserve and non-spinning reserve markets. Participation in additional wholesale markets (e.g. regulation, replacement, black-start, and voltage support) were not considered due to regulations and contracting processes guiding the involvement of DERs in these markets still being in their infancy or not available at all. A grid-tied microgrid comprised of 326 kW solar PV, 634 kW/ 634 kWh battery, and a 350 kW diesel generator was designed to serve a commercial building on the Arizona State University (ASU) campus. Measured electrical load and solar PV generation data were used.

Findings from Chapter 3 indicate that a microgrid using a logic-based controller could reduce customer annual operational costs by 26.7%. Using a model predictive control algorithm increased annual cost savings by 13.7% when compared to a logic-based algorithm. If participation in ancillary service markets was considered within the model predictive control algorithm, annual net operating expenses reduced by an additional 23.5% when compared to a logic-based algorithm. This additional savings are primarily attributed to reduced energy charges, reduced demand charges, reduced O&M expenses resulting

from less cycling of the batteries, and additional revenue streams from ancillary service markets if participation is enabled. These savings enabled by advanced controls can reduce project pay back times for customers and help accelerate the adoption of low carbon energy solutions while providing additional operating flexibility for utilities/ regional transmission organizations/ independent system operators.

Sensitivity analyses showed that decreasing the duration of time steps from 60 min. to 15 min. decreased annual net expenses by up to 12.5%, and increasing the prediction time horizon from 24 hours to 168 hours decreased annual net expenses by up to 3.5%. Shorter duration time steps enable control actions to be executed on a more frequent basis and longer prediction time horizons provide an improved understanding of future events to optimize asset dispatch in the present time step. Shorter duration time steps and longer prediction horizons create additional decision variables that must be calculated by the optimization solver. This additional computation cost may prohibit certain combinations of time steps and prediction time horizons.

Intraday dispatch simulations displayed operational behavior of all three control algorithms for average weekdays in January and July. All three control algorithms displayed similar battery dispatch tendencies. In general, batteries were charged with solar PV and discharged during on-peak times to reduce energy and demand charges. In contrast, the logic-based algorithm charges batteries earlier in the day to ensure that they are fully charged before on-peak times whereas MPC algorithms charge batteries when solar PV generation is greater than the critical load, thereby reducing the amount of solar PV sold back to the grid by up to 67.6%. A deviation to this general behavior was observed when using MPC without ancillary services algorithm in January. Instead of discharging during

on-peak times, the controllable load is shifted to maintain a constant net load with the gird to limit the on-peak demand charge. This behavior reduces battery cycling and the associated operations and maintenance cost. The reduced cycling is also expected to improve battery life (Correa et al. 2017). MPC algorithms charge batteries from solar PV or the grid immediately following the on-peak time of day to provide capacity to bid into ancillary services markets late in the day that have higher bid prices (revenue) than earlier in the day. The microgrid dispatch using MPC shows the ability to adjust operations depending on environmental conditions, load profiles, and pricing signals. This adaptive feature along with the inherent modularity and scalability of MPC approaches can potentially reduce the development time of controls for each unique microgrid configuration, retail electric rate structure, and ancillary service participation structure.

Case studies and control algorithms introduced in Chapter 3 focused solely on grid-tied operations of microgrids. Chapter 4 introduces techniques for control during islanded operation. Chapter 4 develops a method to quantify the resilience of microgrids using a Markov chain to statistically describe the capability to serve critical loads during islanded operations. Reliability metrics of dispatchable generating assets such as failure to start, failure to run, and availability were used in the Markov chain to evaluate the survivability. Autonomy, survivability, fuel consumption, and unserved load were introduced as metrics to evaluate the resilience of microgrids out to 7 days of grid outage. An optimization routine was developed to dispatch assets over the duration of the islanding event. Performance evaluations compared the resilience of a generator-only microgrid consisting of 5,250 kW in generators and a hybrid microgrid consisting of 2,250 kW generators, 3,450 kW / 13,800

kWh battery, and 16,479 kW solar PV. The hybrid microgrid was sized using XENDEE to optimally size assets for economic return during on-grid operation.

Sensitivity analyses identified optimal control parameters in the objective function to maximize on-site reserve generation capacity, minimize fuel consumption, and minimize curtailed load. Findings also identified that minimizing fuel consumption can worsen the survivability by up to 49.24% for hybrid microgrids because batteries are discharged to save fuel and then no longer can provide capacity to supplement failure of a generator or battery stack. Further sensitivity analyses varied the quantity of on-site fuel reserves to identify how much fuel is needed serve 100% of the critical load for a 168-hour outage. The hybrid microgrid was shown to require 37.5% less on-site fuel than the generator-only microgrid for a 168-hour islanding event. This fuel savings could be used to extend mission duration if the islanding event lasted longer than 168 hours. The hybrid microgrid also increased survivability by 10% relative to the generator-only system.

Additional analyses examined the dependence on solar PV and battery state of charge at the beginning of an islanding event. The hybrid microgrid was dependent on the full solar PV generation to ensure autonomy for 168 hours but could still achieve autonomy for more than 166 hours with 50% solar PV generation. Analyses also demonstrated that the battery starting state of charge must be above 70% to ensure autonomy for 168 hours. However, the batteries must only maintain a starting state of charge of 50% to be more likely to survive an islanding event than a generator-only microgrid. These analyses can be used to formulate operational goals of grid-connected control algorithms to ensure resilience and enable a thorough comparison of the benefits and drawbacks of generator-only microgrids and hybrid microgrids.

Chapter 3 and 4 controlled microgrids during on-grid and off-grid operation, respectively. Chapter 3 minimized operational expenses and regularly cycled batteries during on-peak times to reduce energy and demand charges. Chapter 4 maximized on-site generation reserve capacity and therefore maintained battery state of charge near 100% with minimum cycling during islanded operations. These results show how control algorithms can adapt energy asset behavior to achieve different operational objectives (minimize cost vs. maximize resilience).

5.2. Future Work

The studies in Chapters 2, 3, and 4 developed and demonstrated advanced controls for thermal and electrical energy systems. Results demonstrated the technical efficacy of different control algorithms and associated benefits for customers, utilities, and regional transmission operators/ independent system operators. Modifications and additions to these control approaches along with applications with different use cases can provide a more comprehensive understanding of the value propositions these generalized controls offer.

The proposed adaptive precooling strategy in Chapter 2 neglected occupant thermal comfort as a constraint while the proposed thermal energy storage strategy maintained an indoor air temperature within the specified ASHRAE standard (ANSI/ASHRAE 2013). Modifications to the precooling strategy to constrain indoor air temperature within the specified ASHRAE standards would provide a more direct comparison to the TES cooling strategy that does not deviate from the baseline indoor air temperature. Future work is also needed to understand the operational constraints of absorption chillers and heating ventilation and cooling systems to create a complete set of constraints for all thermal assets.

Chapter 2 demonstrated potential economic and technical benefits that thermal systems could provide. Chapters 3 and 4 both examined the operation of electrical systems but neglect considerations for thermal systems. Integrating controls for electrical and thermal systems into a unified control algorithm has the potential to increase benefits these systems can provide. Generators can be used for combined heat and power applications. Considering the exhaust heat as a source of energy can provide additional economic incentive to operate on-site generators. This has the potential to increase the annual operating hours similar to allowing them to participate in ancillary service markets as detailed in Chapter 3. Thermal energy can be used for heating applications in microgrids (e.g. hot water) or paired with an absorption chiller for cooling applications. However, additional input data is needed to model thermal loads of microgrids and calculate optimal dispatch using a model predictive control approach.

The Markov chain model developed in Chapter 4 describes the survivability of a microgrid over the duration of an islanding event using a pre-determined starting operating state. Slight modifications to the proposed control algorithm can enable real-time control in a similar manner to the model predictive control approach detailed in Chapter 3 while accounting for assets under maintenance or out of service. However, the Markov chain model developed in Chapter 4 cannot describe the survivability of a microgrid in real-time due to the inability to accurately adjust the operating state to account for maintenance of assets. Future work to modify the Markov chain model and allow operators to evaluate the survivability, autonomy, fuel usage, and loss of load of microgrids in real-time is still needed. This work can enable operators to evaluate the effects of asset maintenance schedules and control parameters in real-time. Lastly, this modification to the Markov

chain model would enable a feed-back loop to be integrated with the control algorithm to automatically adjust microgrid islanded operations based on predetermined resilience metrics.

Findings from Chapter 4 (e.g. minimum battery starting SOC of 70% to ensure autonomy for 168 hours) could be paired with the on-grid dispatch simulations using the model predictive control approaches in Chapter 3 to evaluate the economic and operational effects of imposing additional resilience constraints. A real-time feedback loop could also be integrated with the on-grid model predictive control algorithms to automatically adjust dispatch behavior to ensure minimum resilience metrics can be achieved in the event of a grid outage.

5.3. Closing Remarks

Advanced controls for electrical and thermal energy systems can leverage the functionality of individual energy assets in an aggregated fashion to provide increased value to multiple stakeholders in the energy industry. New industry regulations are enabling the participation of distributed energy resources and microgrids in wholesale energy markets that can help decrease pay back periods and thereby increase the rate of adoption. However, this progression inevitably increases the technical and economic complexities of a system that was originally designed for centralized generation and can potentially cause more harm than good. Advanced controls can facilitate the integration and coordination of these distributed assets with higher-level centralized generation and transmission entities to increase the operational flexibility of the entire system and provide low cost, low carbon, reliable energy sources to customers.

REFERENCES

ABB. n.d. “Introduction to Microgrids.” https://new.abb.com/distributed-energy-microgrids/introduction-to-microgrids.

———. 2019. “Model Predictive Control Technology Demystified.” 2019. https://new.abb.com/control-systems/features/model-predictive-control-mpc.

Abd-rabou, A M, A M Soliman, and A S Mokhtar. 2015. “Impact of DG Different Types on the Grid Performance” 2: 149–60.

Abraham, S., and R. Efford. 2004. “Final Report on the August 14, 2003 Blackout in the United States and Canada.” *,” US-Canada Power System Outage Task Force*.

Acosta, Adriana, Ana I. González, Jesús M. Zamarreño, and Víctor Álvarez. 2016. “Energy Savings and Guaranteed Thermal Comfort in Hotel Rooms through Nonlinear Model Predictive Controllers.” *Energy and Buildings* 129: 59–68. https://doi.org/10.1016/j.enbuild.2016.07.061.

Administration, U.S. Energy Information. 2018. “Monthly Energy Review November 2018,” no. November: 2018. https://www.eia.gov/totalenergy/data/monthly/pdf/sec7_5.pdf.

Afram, Abdul, and Farrokh Janabi-Sharifi. 2014. “Theory and Applications of HVAC Control Systems - A Review of Model Predictive Control (MPC).” *Building and Environment* 72: 343–55. https://doi.org/10.1016/j.buildenv.2013.11.016.

Aghdam, Farid Hamzeh, Javad Salehi, and Sina Ghaemi. 2018. “Contingency Based Energy Management of Multi-Microgrid Based Distribution Network.” *Sustainable Cities and Society* 41 (January): 265–74. https://doi.org/10.1016/j.scs.2018.05.019.

American Public Power Association. 2018. “Wholesale Electricity Markets and Regional Transmission Organizations,” no. 888. https://web.archive.org/web/20180412151454/https://www.publicpower.org/policy/wholesale-electricity-markets-and-regional-transmission-organizations.

Amirioun, M H, F Aminifar, H Lesani, and M Shahidehpour. 2019. “Electrical Power and Energy Systems Metrics and Quantitative Framework for Assessing Microgrid Resilience against Windstorms.” *Electrical Power and Energy Systems* 104 (January 2018): 716–23. https://doi.org/10.1016/j.ijepes.2018.07.025.

ANSI/ASHRAE. 2013. “Thermal Environmental Conditions for Human Occupancy.”

Applications, Institutional, Peter Asmus, Adam Cornelius, and Clint Wheelock. 2009. “Microgrids Islanded Power Grids and Distributed Generation For.”

Arababadi, Reza, and Kristen Parrish. 2015. “Developing and Modeling Potential Precooling Strategies for Residential Buildings in the Phoenix Climate.” *ASHRAE Transactions*, 1–7.

Arafeh, Samir A. 1978. “Hierarchical Control of Power Distribution Systems.” *IEEE*

TRANSACTIONS ON AUTOMATIC CONTROL AC-23 (2): 333–43.

Arcuri, Bruno, Catalina Spataru, and Mark Barrett. 2017. “Evaluation of Ice Thermal Energy Storage (ITES) for Commercial Buildings in Cities in Brazil.” *Sustainable Cities and Society* 29: 178–92. https://doi.org/10.1016/j.scs.2016.12.011.

Argonne, Zhou, Steve Capanna, Ookie Ma, Paul Spitsen, Ian Hamos, Dave Rench-, Patrick Gilman, et al. 2017. “2017 Renewable Energy Data Book.”

Arizona Public Service. 2017. “RATE SCHEDULE E-32 M MEDIUM GENERAL SERVICE (101 KW - 400 KW).”

Arizona State University. n.d. “Campus Metabolism.” https://cm.asu.edu/.

Asmus, Peter, Adam Forni, and Laura Vogel. 2018. “Microgrid Analysis and Case Studies Report.”

Ayar, Muharrem, Student Member, Serhat Obuz, Student Member, Rodrigo D Trevizan, Student Member, Arturo S Bretas, Senior Member, Haniph A Latchman, and Senior Member. 2017. “A Distributed Control Approach for Enhancing Smart Grid Transient Stability and Resilience” 8 (6): 3035–44.

“BankableEnergy.” 2018. 2018. https://www.bankableenergy.com/.

Bell, Dagfinn. 1998. “Evaluation of Optimal Control for Ice-Based Thermal Energy Storage Systems.” University of Colorado.

Berardi, Umberto. 2015. “Building Energy Consumption in US, EU, and BRIC Countries.” *Procedia Engineering* 118: 128–36. https://doi.org/10.1016/j.proeng.2015.08.411.

Berkeley, Lawrence, National Renewable, and Oak Ridge. n.d. “Validation and Uncertainty Characterization for Energy Simulation.”

Billinton, Li, and Wenyuan Li. 1994. *Reliability Assessment of Electric Power Systems Using Monte Carlo Methods*. New York: Plenum.

Biswal, Gyan Ranjan, R. P. Maheshwari, and M. L. Dewal. 2012. “System Reliability and Fault Tree Analysis of SeSHRS-Based Augmentation of Hydrogen: Dedicated for Combined Cycle Power Plants.” *IEEE Systems Journal* 6 (4): 647–56. https://doi.org/10.1109/JSYST.2012.2192065.

Booten, Chuck, and Paulo Cesar Tabares-Velasco. 2012. “Using EnergyPlus to Simulate the Dynamic Response of a Residential Building to Advanced Cooling Strategies.” In *2nd International Conference on Building Energy and Environment, Boulder, Colorado*.

Borazjani, Pouya, Noor Izzri Abdul Wahab, Hashim b. Hizam, and Azura Bt Che Soh. 2014. “A Review on Microgrid Control Techniques.” *2014 IEEE Innovative Smart Grid Technologies - Asia (ISGT ASIA)*, 749–53. https://doi.org/10.1109/ISGT-Asia.2014.6873886.

Brager, Gail S. 2013. “Benefits of Improving Occupant Comfort and Well-Being in Buildings.” *Proceedings of the 4th International Holcim Forum for Sustainable Construction: The Economy of Sustainable Construction* , no. Wilson 2004: 181–194. https://doi.org/10.1007/s00415-015-7871-8.

Braun, James E., and Nitin Chaturvedi. 2002. “An Inverse Gray-Box Model for Transient Building Load Prediction.” *HVAC&R Research* 8 (1): 73–99.

Braun, James E., and Kyoung-Ho Lee. 2006. “An Experimental Evaluation of Demand Limiting Using Building Thermal Mass in a Small Commercial Building.” *ASHRAE Transactions* 112 (1).

Braun, James E., Kent W. Montgomery, and Nitin Chaturvedi. 2001. “Evaluating the Performance of Building Thermal Mass Control Strategies.” *HVAC&R Research*, 403–28. https://doi.org/10.1080/10789669.2001.10391283.

Braun, Martin, Chenjie Ma, Paul Kaufmann, and J T. 2016. “Optimal Generation Dispatch of Distributed Generators Considering Fair Contribution to Grid Voltage Control” 87: 946–53. https://doi.org/10.1016/j.renene.2015.07.083.

Bruni, G., S. Cordiner, V. Mulone, V. Rocco, and F. Spagnolo. 2015. “A Study of Energy Management in Domestic Micro-Grids Based on Model Predictive Control Strategies.” *Energy Procedia* 102: 1012–16. https://doi.org/10.1016/j.egypro.2014.11.1013.

Bryan, W. 2012. “Emergency Situation Reports: Hurricane Sandy.”

Cagnano, A, A Caldarulo Bugliari, and E De Tuglie. 2018. “A Cooperative Control for the Reserve Management of Isolated Microgrids.” *Applied Energy* 218 (March): 256–65. https://doi.org/10.1016/j.apenergy.2018.02.142.

CAISO. n.d. “Ancillary Services Overview California ISO Ancillary Services Market,” 1–7. https://www.caiso.com/Documents/AncillaryServicesOverview.pdf.

California Independent System Operator. 2018. “California Independent System Operator Corporation Fifth Replacement Electronic Tariff.”

California ISO. n.d. “California ISO OASIS.” http://oasis.caiso.com/mrioasis/logon.do.

———. 2012. “What the Duck Curve Tells Us about Managing a Green Grid.” *California ISO, Shaping a Renewed Future*. Vol. Fact Sheet. https://doi.org/CommPR/HS/10.2013.

———. 2019. “Entering the Energy Market.” 2019. http://www.caiso.com/participate/Pages/default.aspx.

Cappers, Peter, C Anna Spurlock, Patrick Baylis, Meredith Fowlie, and Catherine Wolfram. 2016. “Time-of-Use as a Default Rate for Residential Customers: Issues and Insights.” *Lawrence Berkeley National Laboratory*, no. June: 1–53.

Castilla, M., J. D. Álvarez, J. E. Normey-Rico, and F. Rodríguez. 2014. “Thermal

Comfort Control Using a Non-Linear MPC Strategy: A Real Case of Study in a Bioclimatic Building." *Journal of Process Control* 24 (6): 703–13. https://doi.org/10.1016/j.jprocont.2013.08.009.

Cattaneo, Alessandro, Sreenath Chalil, and Scott Backhaus. 2018. "Integration of Optimal Operational Dispatch and Controller Determined Dynamics for Microgrid Survivability Consortium for Electric Reliability Technology Solutions." *Applied Energy* 230 (August): 1685–96. https://doi.org/10.1016/j.apenergy.2018.08.127.

Caves, Douglas W., and Laurits R. Christensen. 1980. "Econometric Analysis of Residential Time-of-Use Electricity Pricing Experiments." *Journal of Econometrics* 14 (3): 287–306. https://doi.org/10.1016/0304-4076(80)90029-9.

Ceres. 2015. "Pathway to a 21st Century Electric Utility," no. November.

Chambers, Tom. 2018. "Distributed Energy Resources and Power Quality." *IEEE Rural Electric Power Conference*, 37–41. https://doi.org/10.1109/REPC.2018.00015.

Chediak, Mark. 2017. "The Latest Bull Case for Electric Cars: The Cheapest Batteries Ever." 2017.

Chen, T. Y. 2001. "Real-Time Predictive Supervisory Operation of Building Thermal Systems with Thermal Mass." *Energy and Buildings* 33 (2): 141–50.

Chen, Thomas M, Senior Member, Juan Carlos Sanchez-aarnoutse, John Buford, and Senior Member. 2011. "Petri Net Modeling of Cyber-Physical Attacks on Smart Grid." *IEEE Transactions on Smart Grid* 2 (4): 741–49. https://doi.org/10.1109/TSG.2011.2160000.

Chen, Xiao, Qian Wang, and Jelena Srebric. 2015. "Model Predictive Control for Indoor Thermal Comfort and Energy Optimization Using Occupant Feedback." *Energy and Buildings* 102: 357–69. https://doi.org/10.1016/j.enbuild.2015.06.002.

Chilipi, Rajasekharareddy, Naji Al Sayari, Khalifa Al Hosani, and Abdul Rahiman Beig. 2016. "Control Scheme for Grid-Tied Distributed Generation Inverter under Unbalanced and Distorted Utility Conditions with Power Quality Ancillary Services" 10: 140–49. https://doi.org/10.1049/iet-rpg.2015.0095.

Clifford Power. 1999. "Wet Stacking of Generator Sets and How to Avoid It."

Cochran, Jaquelin, Mackay Miller, Michael Milligan, Erik Ela, Douglas Arent, Aaron Bloom, Matthew Futch, et al. 2013. "Market Evolution: Wholesale Electricity Market Design for 21st Century Power Systems." *Contract*, no. October 2013. https://doi.org/10.2172/1260327.

COINNEWS MEDIA GROUP LLC. n.d. "Current US Inflation Rates: 2009-2019." US INFLATION CALCULATOR. https://www.usinflationcalculator.com/inflation/current-inflation-rates/.

Colli, Alessandra. 2015. "Failure Mode and Effect Analysis for Photovoltaic Systems." *Renewable and Sustainable Energy Reviews* 50: 804–9.

https://doi.org/10.1016/j.rser.2015.05.056.

Collins, Elmer, Michael Dvorack, Jeff Mahn, Michael Mundt, and Michael Quintana. 2009. “RELIABILITY AND AVAILABILITY ANALYSIS OF A FIELDED PHOTOVOLTAlC,” 2316–21.

Coppez, G, S Chowdhury, and ... 2010. “The Importance of Energy Storage in Renewable Power Generation: A Review.” *Universities Power …*, 1–5. https://ieeexplore.ieee.org/abstract/document/5648970/.

Correa, Carlos Adrian, Alexis Gerossier, Andrea Michiorri, and Georges Kariniotakis. 2017. “Optimal Scheduling of Storage Devices in Smart Buildings Including Battery Cycling.” *2017 IEEE Manchester PowerTech, Powertech 2017*, 1–6. https://doi.org/10.1109/PTC.2017.7981199.

Delaney, John R. 2018. “The Best Smart Thermostats for 2019.” PCmag. 2018. https://www.pcmag.com/article/356755/the-best-smart-thermostats.

Department of Defense. 2014. “Department of Defense Directive 4180.01.”

———. 2017. “Army Directive 2017-07.”

Department of the Navy. n.d. “Department of the Navy’s Energy Program for Security and Independence.” https://doi.org/10.1016/0010-4485(78)90081-7.

Dorn, Derek. n.d. “MACRS Depreciation and Renewable Energy Finance.”

Dulau, Lucian Ioan, Mihail Abrudean, and Dorin Bica. 2014. “Effects of Distribution Generation on Electric Power Systems.” *Procedia Technology* 12: 681–86. https://doi.org/10.1016/j.protcy.2013.12.549.

EIA. 2016. “Annual Energy Outlook 2016.” *U.S. Energy Information Administration*, ES-5. https://doi.org/EIA-0383(2016).

———. 2018. “Electric Power Monthly with Data for September 2018.” *U.S. Energy Information Administration*, no. Novemebr.

Electric Power Research Institute. 2016. “Electric Power System Resiliency Challenges and Opportunities.”

Energy Information Administration. 2017. “2016 EIA Form 861:Electric Power Sales, Revenue, and Energy Efficiency.” https://eia.gov/electricity/data/eia861.

Energy, U.S. Department of. 2017. “Heat Pump Systems.” 2017. https://energy.gov/energysaver/heat-pump-systems.

EOS. n.d. “Eos Aurora Product Description.” http://www.eosenergystorage.com/wp-content/uploads/2017/01/eos_product_brouchure011817.pdf.

———. n.d. “EOS Energy Storage.” https://eosenergystorage.com/.

Ericson, Sean. 2019. “Calculating the Reliability of a Backup System,” 1–6.

ESTCP. 2019. “Environmental Security Technology Certification Program (ESTCP).”

Eto, Joseph H, and Kristina Hamachi Lacommare. 2008. “Tracking the Reliability of the U . S . Electric Power System : An Assessment of Publicly Available Information Reported to State Public Utility Commissions,” no. October.

Farah, Sleiman, Ming Liu, and Wasim Saman. 2019. “Numerical Investigation of Phase Change Material Thermal Storage for Space Cooling.” *Applied Energy* 239 (January): 526–35. https://doi.org/10.1016/j.apenergy.2019.01.197.

Fathima, A. Hina, and K. Palanisamy. 2015. “Optimization in Microgrids with Hybrid Energy Systems - A Review.” *Renewable and Sustainable Energy Reviews* 45: 431–46. https://doi.org/10.1016/j.rser.2015.01.059.

FERC. n.d. “Federal Energy Regulatory Commission Strategic Plan FY 2018-2022.”

Few, Sheridan, Oliver Schmidt, Gregory J. Offer, Nigel Brandon, Jenny Nelson, and Ajay Gambhir. 2018. “Prospective Improvements in Cost and Cycle Life of Off-Grid Lithium-Ion Battery Packs: An Analysis Informed by Expert Elicitations.” *Energy Policy* 114 (May 2017): 578–90. https://doi.org/10.1016/j.enpol.2017.12.033.

Figueroa-candia, Marcelo, Frank A Felder, and David W Coit. 2018. “Resiliency-Based Optimization of Restoration Policies for Electric Power Distribution Systems.” *Electric Power Systems Research* 161: 188–98. https://doi.org/10.1016/j.epsr.2018.04.007.

Fischer, E M, and R Knutti. 2015. “Anthropogenic Contribution to Global Occurrence of Heavy-Precipitation and High-Temperature Extremes” 5 (June). https://doi.org/10.1038/NCLIMATE2617.

Fu, Ran, David Feldman, Robert Margolis, Ran Fu, David Feldman, and Robert Margolis. 2018. “U . S . Solar Photovoltaic System Cost Benchmark : Q1 2018 U . S . Solar Photovoltaic System Cost Benchmark : Q1 2018,” no. November.

Fu, Ran, David Feldman, Robert Margolis, Mike Woodhouse, Kristen Ardani, Ran Fu, David Feldman, Robert Margolis, Mike Woodhouse, and Kristen Ardani. 2017. “U . S . Solar Photovoltaic System Cost Benchmark : Q1 2017 U . S . Solar Photovoltaic System Cost Benchmark : Q1 2017,” no. September. https://doi.org/https://dx.doi.org/10.7799/1375958.

Gandhi, Oktoviano, Carlos D. Rodríguez-Gallegos, Wenjie Zhang, Dipti Srinivasan, and Thomas Reindl. 2018. “Economic and Technical Analysis of Reactive Power Provision from Distributed Energy Resources in Microgrids.” *Applied Energy* 210 (August 2017): 827–41. https://doi.org/10.1016/j.apenergy.2017.08.154.

Generac Industrial Power. 2012. “Generac SD350 Industrial Diesel Generator Set Spec Sheet.” Vol. 156.

German, Alea, Marc Hoeschele, David Springer, and Davis Energy Group. 2014. “Maximising the Benefits of Residential Pre-Cooling.” *ACEEE Summer Study on*

Energy Efficiency in Buildings, 71–83.

Ghanbarian, Mohammad Mehdi, Majid Nayeripour, Amir Hosein Rajaei, Fatemeh Jamshidi, and Eberhard Waffenschmidt. 2017. "Model Predictive Control of Distributed Generation Micro-Grids in Island and Grid Connected Operation under Balanced and Unbalanced Conditions." *Journal of Renewable and Sustainable Energy* 9 (4): 0–17. https://doi.org/10.1063/1.4990823.

Giraldez, Julieta, Francisco Flores-espino, Sara Macalpine, Peter Asmus, Julieta Giraldez, Francisco Flores-espino, Sara Macalpine, and Peter Asmus. 2018. "Phase I Microgrid Cost Study : Data Collection and Analysis of Microgrid Costs in the United States Phase I Microgrid Cost Study : Data Collection and Analysis of Microgrid Costs in the United States," no. October.

Golnas, Anastasios. 2013. "PV System Reliability : An Operator ' s Perspective" 3 (1): 416–21.

Gomes, Mário Helder, and João Tomé Saraiva. 2010. "Allocation of Reactive Power Support, Active Loss Balancing and Demand Interruption Ancillary Services in MicroGrids." *Electric Power Systems Research* 80 (10): 1267–76. https://doi.org/10.1016/j.epsr.2010.04.013.

Goyal, Megha, and Arindam Ghosh. 2016. "Sustainable Energy , Grids and Networks Microgrids Interconnection to Support Mutually during Any Contingency." *Sustainable Energy, Grids and Networks* 6: 100–108. https://doi.org/10.1016/j.segan.2016.02.006.

Greenfield, Lawrence R. 2018. "An Overview of the Federal Energy Regulatory Commission and Federal Regulation of Public Utilities."

Grid Modernization Labortatory Consortium. 2017. "Grid Modernization: Metrics Analysis (GMLC1.1)," no. May.

Gruber, J. K., F. Huerta, P. Matatagui, and M. Prodanović. 2015. "Advanced Building Energy Management Based on a Two-Stage Receding Horizon Optimization." *Applied Energy* 160: 194–205. https://doi.org/10.1016/j.apenergy.2015.09.049.

Hadi, Muhammad Wardi, Nanang Hariyanto, and Jaeho Choi. 2016. "Stability Enhancement of Hybrid Diesel Generator and Photovoltaic Generator Based on Droop Control." *Proceedings of the 2015 IEEE Innovative Smart Grid Technologies - Asia, ISGT ASIA 2015*, 1–6. https://doi.org/10.1109/ISGT-Asia.2015.7387022.

Hajiah, Ali, and Moncef Krarti. 2012a. "Optimal Control of Building Storage Systems Using Both Ice Storage and Thermal Mass - Part I: Simulation Environment." *Energy Conversion and Management* 64: 499–508. https://doi.org/10.1016/j.enconman.2012.02.016.

———. 2012b. "Optimal Controls of Building Storage Systems Using Both Ice Storage and Thermal Mass - Part II: Parametric Analysis." *Energy Conversion and Management* 64: 509–15. https://doi.org/10.1016/j.enconman.2012.02.020.

Hasnain S.M. 1998. “Review on Sustainable Thermal Energy Storage Technologies, Part I: Heat Storage Materials and Techniques.” *Energy Conversion and Management* 39 (11): 1127–38. https://doi.org/10.1016/S0196-8904(98)00025-9.

Hawaii Electric Light. 2016. “REVISED SHEET NO. 71, Effective September 21, 2016.” 2016. https://www.hawaiianelectric.com/Documents/my_account/rates/hawaii_electric_light_rates/helco_rates_sch_tou_r.pdf.

———. 2017a. “REVISED SHEET NO. 50.4 , Effective July 1, 2017.” 2017. https://www.hawaiianelectric.com/Documents/my_account/rates/hawaii_electric_light_rates/helco_rates_pbf_current.pdf.

———. 2017b. “REVISED SHEET NO. 53, Effective January 1, 2018 to June 30, 2018.” 2017. https://www.hawaiianelectric.com/Documents/my_account/rates/hawaii_electric_light_rates/helco_rates_gi_fee_surcharge.pdf.

———. 2017c. “REVISED SHEET NO. 90, Effective January 1-31, 2018.” 2017. https://www.hawaiianelectric.com/Documents/my_account/rates/hawaii_electric_light_rates/helco_rates_ppac.pdf.

———. 2017d. “REVISED SHEET NO. 91, Effective June 1, 2017.” 2017. https://www.hawaiianelectric.com/Documents/my_account/rates/hawaii_electric_light_rates/helco_rates_rba.pdf.

Hazyuk, Ion, Christian Ghiaus, and David Penhouet. 2012. “Optimal Temperature Control of Intermittently Heated Buildings Using Model Predictive Control: Part II - Control Algorithm.” *Building and Environment* 51: 388–94. https://doi.org/10.1016/j.buildenv.2011.11.008.

HBM Prenscia. 2019. “Fault Tree Analysis.” 2019. https://www.weibull.com/basics/fault-tree/index.htm.

He, Zichang, and Wen Jiang. 2018. “A New Belief Markov Chain Model and Its Application in Inventory Prediction.” *International Journal of Production Research* 7543: 1–18. https://doi.org/10.1080/00207543.2017.1405166.

Hecht, Herbert. 2003. *Systems Reliability and Failure Prevention*. Artech House. https://ebookcentral-proquest-com.ezproxy1.lib.asu.edu/lib/asulib-ebooks/detail.action?docID=227632.

Hedman, Kory W, Student Member, Michael C Ferris, Richard P O Neill, Emily Bartholomew Fisher, Student Member, and Shmuel S Oren. 2010. “Co-Optimization of Generation Unit Commitment and Transmission Switching With N-1 Reliability” 25 (2): 1052–63.

Henninger, Robert H, and Michael Witte. n.d. “EnergyPlus Testing with HVAC Equipment Component Tests,” 1–23.

Henninger, Robert H, and Michael J Witte. n.d. “EnergyPlus Testing with ASHRAE

1052-RP Toolkit – Building Fabric Analytical Tests."

Henninger, Robert H, Michael J Witte, Drury B Crawley, and Case E Base. 2003. "EXPERIENCE TESTING ENERGYPLUS WITH THE IEA HVAC BESTEST E100-E200 SERIES," 467–74.

Henze, Gregor P., and Moncef Krarti. 1999. "The Impact of Forecasting Uncertainty on the Performance of a Predictive Optimal Controller for Thermal Energy Storage Systems." *ASHRAE Transactions* 105: 553.

Herter, K., and Y. Okuneva. 2014. "SMUD's Residential Summer Solutions Study 2011-2012." *Herter Energy Research Solutions. El Dorado Hills, CA*.

Hines, Paul, and Karthikeyan Balasubramaniam. 1977. "Cascading Failures in Power Grids."

Hirsch, Adam, Yael Parag, and Josep Guerrero. 2018. "Microgrids : A Review of Technologies , Key Drivers , and Outstanding Issues" 90 (March): 402–11. https://doi.org/10.1016/j.rser.2018.03.040.

Hirst, Eric, and Brendan Kirby. 1996. "Costs for Electric-Power Ancillary Services." *Electricity Journal* 9 (10): 26–30. https://doi.org/10.1016/S1040-6190(96)80153-9.

———. 2000. "Bulk-Power Basics : Reliability and Commerce." *North*.

Hoffman, Patricia, and Devon Streit. 2015. "United States Electricity Industry Primer." *Office of Electricity Delivery and Energy Reliability U.S. Department of Energy, DOE/OE-0017*, no. July: 1–94. https://doi.org/DOE/OE-0017.

Hu, Maomao, Fu Xiao, and Lingshi Wang. 2019. "Investigation of Demand Response Potentials of Residential Air Conditioners in Smart Grids Using Grey-Box Room Thermal Model." *Applied Energy* 207 (2017): 324–35. https://doi.org/10.1016/j.apenergy.2017.05.099.

Hunt, Kirby, Anthony Blekicki, Robert Callery, and First Solar. 2015. "Availability of Utility-Scale Photovoltaic Power Plants," 0–2.

Hussain, Akhtar, Van-hai Bui, and Hak-man Kim. 2019. "Microgrids as a Resilience Resource and Strategies Used by Microgrids for Enhancing Resilience." *Applied Energy* 240 (February): 56–72. https://doi.org/10.1016/j.apenergy.2019.02.055.

Ice Energy. 2018a. "Ice Bear 20." https://www.ice-energy.com/wp-content/uploads/2018/05/IB-20-ProductSheet-2017-US-D4.pdf.

———. 2018b. "Ice Bear 40." https://www.ice-energy.com/wp-content/uploads/2018/05/IB-20-ProductSheet-2017-US-D4.pdf.

Im, Piljae. 2016. "Multi-Year Plan for Validation of EnergyPlus Multi-Zone HVAC System Modeling Using ORNL's Flexible Research Platform," no. August.

Jamei, Mahdi, Eran Schweitzer, Anna Scaglione, and Kory W Hedman. n.d. "Gas and Electric Grid Unit Commitment with Coordinated N-1 Generator Contingency

Analysis." *2018 Power Systems Computation Conference (PSCC)*, 1–7. https://doi.org/10.23919/PSCC.2018.8442863.

Janko, Samantha A., Michael R. Arnold, and Nathan G. Johnson. 2016. "Implications of High-Penetration Renewables for Ratepayers and Utilities in the Residential Solar Photovoltaic (PV) Market." *Applied Energy* 180: 37–51. https://doi.org/10.1016/j.apenergy.2016.07.041.

Ji, Chuanyi, Yun Wei, Henry Mei, Jorge Calzada, Matthew Carey, and Steve Church. 2016. "Large Scale Data Analysis of Power Grid Resilience across Multiple US Service Regions," no. April 2018. https://doi.org/10.1038/nenergy.2016.52.

Johra, Hicham, and Per Heiselberg. 2017. "In Fl Uence of Internal Thermal Mass on the Indoor Thermal Dynamics and Integration of Phase Change Materials in Furniture for Building Energy Storage : A Review." *Renewable and Sustainable Energy Reviews* 69 (November 2016): 19–32. https://doi.org/10.1016/j.rser.2016.11.145.

Keeney, Kevin R., and James E. Braun. 1997. "Application of Building Precooling to Reduce Peak Cooling Requirements." *ASHRAE Transactions* 103 (1): 463–69.

Kerr, Richard A. 2011. "Humans Are Driving Extreme Weather ; Time to Prepare." https://doi.org/10.1126/science.334.6059.1040.

Khani, Davood, Ahmad Sadeghi, and Hossein Madadi. 2012. "Electrical Power and Energy Systems Impacts of Distributed Generations on Power System Transient and Voltage Stability" 43: 488–500. https://doi.org/10.1016/j.ijepes.2012.06.007.

Khongkhachat, Somkiart, and Surin Khomfoi. 2015. "Hierarchical Control Strategies in AC Microgrids." *ECTI-CON 2015 - 2015 12th International Conference on Electrical Engineering/Electronics, Computer, Telecommunications and Information Technology*, 1–6. https://doi.org/10.1109/ECTICon.2015.7206968.

Kintner-Meyer, M., and A. F. Emery. 1995. "Optimal Control of an HVAC System Using Cold Storage and Building Thermal Capacitance." *Energy and Buildings* 23 (1): 19–31. https://doi.org/10.1016/0378-7788(95)00917-M.

Klaassen, C. J., John M. House, and Iowa Energy Center. 2002. "Demonstration of Load Shifting and Peak Load Reduction with Control of Building Thermal Mass." *Teaming for Efficiency: Commercial Buildings: Technologies, Design, Performance Analysis, and Building Industry Trends* 3: 55.

Krarti, Moncef, Gregor P. Henze, and Dagfinn Bell. 1999. "Planning Horizon for a Predictive Optimal Controller for Thermal Energy Storage Systems." *ASHRAE Transactions* 105: 543.

Lammers, Imke. 2017. "Grid Resilience Governance of the Future : Analyzing the Role of Associations in Experimental Smart Grid Projects in The Netherlands Grid Resilience Governance of the Future : Analyzing the Role of Associations in Experimental Smart Grid Projects in The N," no. August. https://doi.org/10.1007/978-3-319-61813-5.

Lau, Eng Tseng, Kok Keong Chai, Yue Chen, and Jonathan Loo. 2018. “Efficient Economic and Resilience-Based Critical Infrastructures,” 1–20. https://doi.org/10.3390/en11123418.

Lawder, Matthew T, Vilayanur Viswanathan, and Venkat R Subramanian. 2015. “Balancing Autonomy and Utilization of Solar Power and Battery Storage for Demand Based Microgrids” 279: 645–55. https://doi.org/10.1016/j.jpowsour.2015.01.015.

Lazard. 2018. “Lazard’s Levelized Cost of Storage Analysis - Version 4.0.”

Lee, Hyojong, Shwetha Niddodi, Anurag Srivastava, and David Bakken. 2016. “Decentralized Voltage Stability Monitoring and Control in the Smart Grid Using Distributed Computing Architecture.” *2016 IEEE Industry Applications Society Annual Meeting*, 1–9. https://doi.org/10.1109/IAS.2016.7731871.

Lee, Kyoung-ho, and James E. Braun. 2008a. “Development of Methods for Determining Demand-Limiting Setpoint Trajectories in Buildings Using Short-Term Measurements.” *Building and Environment* 43 (10): 1755–68.

———. 2008b. “Model-Based Demand-Limiting Control of Building Thermal Mass.” *Building and Environment* 43 (10): 1633–46.

Lee, Kyoung-Ho, and James E. Braun. 2008. “A Data-Driven Method for Determining Zone Temperature Trajectories That Minimize Peak Electrical Demand.” *ASHRAE Transactions* 114 (2).

Lee, Robert. n.d. “City of Los Angeles.” Accessed January 1, 2018. http://www.uutinfo.org/uutinfo_city_info/los_angeles/uutinfo_los_angeles.htm.

Lin, P. O.Ting, Y. U.Cheng Chou, Yung Ting, Shian Shing Shyu, and Chang Kuo Chen. 2014. “A Robust System Reliability Analysis Using Partitioning and Parallel Processing of Markov Chain.” *Artificial Intelligence for Engineering Design, Analysis and Manufacturing: AIEDAM* 28 (4): 311–22. https://doi.org/10.1017/S0890060414000493.

Lin, Yanling, and Zhaohong Bie. 2016. “Study on the Resilience of the Integrated Energy System.” *Energy Procedia* 103 (April): 171–76. https://doi.org/10.1016/j.egypro.2016.11.268.

Liu, Yajie, Bo Guo, Tao Zhang, Rui Wang, and Yan Zhang. 2016. “Model Predictive Control-Based Operation Management for a Residential Microgrid with Considering Forecast Uncertainties and Demand Response Strategies.” *IET Generation, Transmission & Distribution* 10 (10): 2367–78. https://doi.org/10.1049/iet-gtd.2015.1127.

Lizana, Jesús, Ricardo Chacartegui, Angela Barrios-Padura, and José Manuel Valverde. 2017. “Advances in Thermal Energy Storage Materials and Their Applications towards Zero Energy Buildings: A Critical Review.” *Applied Energy* 203: 219–39. https://doi.org/10.1016/j.apenergy.2017.06.008.

Load Management Leadership. 2019. “The Future of Distributed Energy Resources.”

Los Angeles Department of Water and Power. 2016. “Electric Rate Schedules.” 2016. https://www.ladwp.com/ladwp/faces/wcnav_externalId/a-fr-elecrate-schel?_adf.ctrl-state=xogg89u6n_49&_afrLoop=350577774383580&_afrWindowMode=0&_afrWindowId=gdatcyg8s_1#%40%3F_afrWindowId%3Dgdatcyg8s_1%26_afrLoop%3D350577774383580%26_afrWindowMode%3D0%26_ad.

Luerssen, Christoph, Oktoviano Gandhi, Thomas Reindl, Chandra Sekhar, and David Cheong. 2019. “Levelised Cost of Storage (LCOS) for Solar-PV-Powered Cooling in the Tropics.” *Applied Energy* 242 (March): 640–54. https://doi.org/10.1016/j.apenergy.2019.03.133.

Luo, Na, Tianzhen Hong, Hui Li, Ruoxi Jia, and Wenguo Weng. 2017. “Data Analytics and Optimization of an Ice-Based Energy Storage System for Commercial Buildings.” *Applied Energy* 204: 459–75. https://doi.org/10.1016/j.apenergy.2017.07.048.

Mahmud, M A, M J Hossain, and H R Pota. 2011. *Analysis of Voltage Rise Effect on Distribution Network with Distributed Generation*. *IFAC Proceedings Volumes*. Vol. 44. IFAC. https://doi.org/10.3182/20110828-6-IT-1002.01305.

Majumder, Ritwik, Arindam Ghosh, Gerard Ledwich, Saikat Chakrabarti, and Firuz Zare. 2010. “Improved Power Sharing among Distributed Generators Using Web Based Communication.” *IEEE PES General Meeting, PES 2010*, no. July: 25–29. https://doi.org/10.1109/PES.2010.5589288.

Majzoobi, Alireza, and Amin Khodaei. 2017. “Application of Microgrids in Providing Ancillary Services to the Utility Grid.” *Energy* 123: 555–63. https://doi.org/10.1016/j.energy.2017.01.113.

Mammoli, Andrea, and Matthew Robinson. 2018. “Numerical Analysis of Heat Transfer Processes in a Low-Cost, High-Performance Ice Storage Device for Residential Applications.” *Applied Thermal Engineering* 128: 453–63. https://doi.org/10.1016/j.applthermaleng.2017.09.043.

Marler, R T, and J S Arora. 2004. “Survey of Multi-Objective Optimization Methods for Engineering” 395: 369–95. https://doi.org/10.1007/s00158-003-0368-6.

Marler, R Timothy, and Jasbir S Arora. 2010. “The Weighted Sum Method for Multi-Objective Optimization : New Insights,” 853–62. https://doi.org/10.1007/s00158-009-0460-7.

Martin-martínez, F, and M Rivier. 2016. “A Literature Review of Microgrids : A Functional Layer Based Classi Fi Cation” 62: 1133–53. https://doi.org/10.1016/j.rser.2016.05.025.

Mashayekh, Salman, Michael Stadler, Gonçalo Cardoso, Miguel Heleno, Sreenath Chalil Madathil, Harsha Nagarajan, Russell Bent, Marc Mueller-stoffels, Xiaonan Lu, and Jianhui Wang. 2017. “Security-Constrained Design of Isolated Security-Constrained

Design of Isolated Multi-Energy Microgrids," no. September.

Mazumder, Sumit, Arindam Ghosh, and Firuz Zare. 2013. "Improving Power Quality in Low-Voltage Networks Containing Distributed Energy Resources." *International Journal of Emerging Electric Power Systems* 14 (1): 67–78. https://doi.org/10.1515/ijeeps-2013-0022.

McKane, Aimee. 2010. "Automated Demand Response: The Missing Link in the Electricity Value Chain." *Lawrence Berkeley National Laboratory*. http://escholarship.org/uc/item/4kz048j2.pdf.

Mehleri, E. D., L. G. Papageorgiou, N. C. Markatos, and H. Sarimveis. 2012. *A Model Predictive Control Framework for Residential Microgrids*. *Computer Aided Chemical Engineering*. Vol. 30. Elsevier B.V. https://doi.org/10.1016/B978-0-444-59519-5.50066-6.

Mei, Xiong, and Guangcai Gong. 2018. "Predicting Airborne Particle Deposition by a Modi Fi Ed Markov Chain Model for Fast Estimation of Potential Contaminant Spread" 185 (October 2017): 137–46. https://doi.org/10.1016/j.atmosenv.2018.04.050.

Meng, Lexuan, Adriana Luna, Enrique Rodríguez Díaz, Bo Sun, Tomislav Dragicevic, Mehdi Savaghebi, Juan C. Vasquez, Josep M. Guerrero, Moisès Graells, and Fabio Andrade. 2016. "Flexible System Integration and Advanced Hierarchical Control Architectures in the Microgrid Research Laboratory of Aalborg University." *IEEE Transactions on Industry Applications* 52 (2): 1736–49. https://doi.org/10.1109/TIA.2015.2504472.

Miao, Shuwei, Guangtao Ning, Yingzhong Gu, Jiahao Yan, and Botao Ma. 2018. "Markov Chain Model for Solar Farm Generation and Its Application to Generation Performance Evaluation" 186. https://doi.org/10.1016/j.jclepro.2018.03.173.

Miller, Stephen S. 2008. "Extending Traditional Planning Methods to Evaluate the Potential for Cascading Failures in Electric Power Grids," 1–7.

Molyneaux, Lynette, Liam Wagner, Craig Froome, and John Foster. 2012. "Resilience and Electricity Systems : A Comparative Analysis" 47: 188–201. https://doi.org/10.1016/j.enpol.2012.04.057.

Momoh, James. 2012. *Smart Grid: Fundamentals of Design and Analysis*. IEEE. https://ieeexplore-ieee-org.ezproxy1.lib.asu.edu/document/6183637.

Monesha, S, S Ganesh Kumar, and M Rivera. n.d. "Microgrid Energy Management and Control : Technical Review." *2016 IEEE International Conference on Automatica (ICA-ACCA)*, 1–7. https://doi.org/10.1109/ICA-ACCA.2016.7778452.

Morstyn, Thomas, Branislav Hredzak, Ricardo P. Aguilera, and Vassilios G. Agelidis. 2018. "Model Predictive Control for Distributed Microgrid Battery Energy Storage Systems." *IEEE Transactions on Control Systems Technology* 26 (3): 1107–14. https://doi.org/10.1109/TCST.2017.2699159.

Moskowitz, Scott. 2017. “Trends Shaping the Energy Storage Inverter Market: Falling Prices, Fragmentation, New Features.” *Greentech Media*, September 2017. https://www.greentechmedia.com/articles/read/trends-shaping-the-energy-storage-inverter-market#gs.dazFXeo.

MQ Power. 2007. “750kW Containerized Diesel Generator Set.” Carson.

Mrowca, B. 2011. “Emergency Diesel Generator Failure Review 1999 - 2001.” *EDG Failure Review*. http://www.nrc.gov/NRR/OVERSIGHT/ASSESS/faqs_by_id.pdf.

Müller, Sven C, Marc Osthues, Christoph Rekowski, Ulf Häger, and Christian Rehtanz. 2013. “Techno-Economic Evaluation of Corrective Actions for Efficient Attainment of (N-1) -Security in Operation and Planning.” https://doi.org/10.1109/PESMG.2013.6672676.

Muresan, Adela. 2016. “Who Lives Largest? The Growth of Urban American Homes in the Last 100 Years.” Real Estate Broad. 2016. https://www.propertyshark.com/Real-Estate-Reports/2016/09/08/the-growth-of-urban-american-homes-in-the-last-100-years/.

Musgrove, A. R.de L., H. J. Ehmke, and K. J. Stocks. 1989. “Optimum Design and Operation of Ice-Storage Air-Conditioning Systems under Australian TOU Tariffs.” *Energy* 14 (9): 525–35. https://doi.org/10.1016/0360-5442(89)90023-6.

Naja, Javad, Ali Peiravi, and Josep M Guerrero. 2018. “Power Distribution System Improvement Planning under Hurricanes Based on a New Resilience Index” 39 (December 2017): 592–604. https://doi.org/10.1016/j.scs.2018.03.022.

National Renewable Energy Laboratory. 2014. “Advanced Inverter Functions To Support High Levels of Distributed Solar Policy and Regulatory the Need for Advanced.” *NREL Technical Report NREL/TP-5200-57991*, 1–8.

———. 2016. “BEopt.” https://beopt.nrel.gov/.

Navarro, Lidia, Alvaro De Gracia, Shane Colclough, Maria Browne, Sarah J Mccormack, Philip Grif, and Luisa F Cabeza. 2016. “Thermal Energy Storage in Building Integrated Thermal Systems : A Review . Part 1 . Active Storage Systems” 88. https://doi.org/10.1016/j.renene.2015.11.040.

Navidbakhsh, Mahdi, Ali Shirazi, and Sepehr Sanaye. 2013. “Four e Analysis and Multi-Objective Optimization of an Ice Storage System Incorporating PCM as the Partial Cold Storage for Air-Conditioning Applications.” *Applied Thermal Engineering* 58 (1–2): 30–41. https://doi.org/10.1016/j.applthermaleng.2013.04.002.

Navigant Research. 2018. “Market Data: Microgrid.”

———. 2019. “Microgrid Deployment Tracker 2Q19.” 2019.

NERC. 2019a. “Reliability Standards for the Bulk Electric Systems of North America.” *Standard*, 1–1044. http://www.nerc.com/docs/standards/rs/Reliability_Standards_Complete_Set.pdf.

———. 2019b. “State of Reliability 2019.” *Nerc*, no. June.

NERC Resources Subcommittee. 2011. “Balancing and Frequency Control.” Princeton. https://www.nerc.com/docs/oc/rs/NERC Balancing and Frequency Control 040520111.pdf.

Nguyen, S V T. 2012. “Microgrid Study : Energy Security for DoD Installations,” no. June.

Norris, J.R. 1998. *Markov Chains*. Illustrate. Cambridge University Press.

Office of Public Accountability/Ratepayer Advocate. 2018. “Measuring Electric Service Reliability.”

Ogunjuyigbe, A S O, T R Ayodele, and O O Akinola. 2016. “Impact of Distributed Generators on the Power Loss and Voltage Profile of Sub-Transmission Network.” *Journal of Electrical Systems and Information Technology* 3 (1): 94–107. https://doi.org/10.1016/j.jesit.2015.11.010.

Ohama, Raun. 2017. “Total Interior Area Hawaii.” Honolulu: Hawaii Information Services.

Oró, E., A. de Gracia, A. Castell, M. M. Farid, and L. F. Cabeza. 2012. “Review on Phase Change Materials (PCMs) for Cold Thermal Energy Storage Applications.” *Applied Energy* 99: 513–33. https://doi.org/10.1016/j.apenergy.2012.03.058.

Pacific Northwest National Laboratory. 2002. “A Primer on Electric Utilities, Deregulation, and Restructuring of U.S. Electricity Markets.”

Pacific Northwest National Laboratory, Oak Ridge National Laboratory. 2010. “Guide to Determining Climate Regions by County.” https://www1.eere.energy.gov/buildings/publications/pdfs/building_america/ba_climateguide_7_1.pdf.

Parisio, Alessandra, Evangelos Rikos, and Luigi Glielmo. 2016. “Stochastic Model Predictive Control for Economic/Environmental Operation Management of Microgrids: An Experimental Case Study.” *Journal of Process Control* 43: 24–37. https://doi.org/10.1016/j.jprocont.2016.04.008.

Parisio, Alessandra, Evangelos Rikos, Luigi Glielmo, and Senior Member. 2014. “A Model Predictive Control Approach to Microgrid Operation Optimization” 22 (5): 1813–27.

Parisio, Alessandra, Evangelos Rikos, George Tzamalis, and Luigi Glielmo. 2014. “Use of Model Predictive Control for Experimental Microgrid Optimization.” *Applied Energy* 115: 37–46. https://doi.org/10.1016/j.apenergy.2013.10.027.

Pencenak, Z. K., M. Stadler, and K. Fahy. 2019. “Efficient Multi-Year Economic Energy Planning in Microgrids.” *Applied Energy* 255.

Pereira, M., D. Munoz De La Pena, and D. Limon. 2016. “Robust Economic Model

Predictive Control of a Community Micro-Grid." *2016 IEEE 55th Conference on Decision and Control, CDC 2016* 100: 2739–44. https://doi.org/10.1109/CDC.2016.7798676.

PJM. n.d. "Market for Electricity." https://learn.pjm.com/electricity-basics/market-for-electricity.aspx.

Power, Generac Industrial. 2016. "Total Cost of Ownership Diesel vs . Natural Gas Generators," 1–5.

Prívara, Samuel, Jan Široký, Lukáš Ferkl, and Jiří Cigler. 2011. "Model Predictive Control of a Building Heating System: The First Experience." *Energy and Buildings* 43 (2–3): 564–72. https://doi.org/10.1016/j.enbuild.2010.10.022.

Prodan, Ionela, and Enrico Zio. 2014. "A Model Predictive Control Framework for Reliable Microgrid Energy Management." *International Journal of Electrical Power and Energy Systems* 61: 399–409. https://doi.org/10.1016/j.ijepes.2014.03.017.

Project, Salt River. 2015. "STANDARD PRICE PLAN FOR RESIDENTIAL TIME-OF-USE SERVICE."

Prowell, S. J., and J. H. Poore. 2004. "Computing System Reliability Using Markov Chain Usage Models." *Journal of Systems and Software* 73 (2): 219–25. https://doi.org/10.1016/S0164-1212(03)00241-3.

PwC. 2014. "The Road Ahead - Gaining Momentum from Energy Transformation." *Pwc*, 1–32. http://www.pwc.com/en_GX/gx/utilities/publications/assets/pwc-the-road-ahead.pdf.

Ramakrishnan, M. 2016. "Integration of Functional Reliability Analysis and System Hardware Reliability through Monte Carlo Simulation." *Annals of Nuclear Energy* 95: 54–63. https://doi.org/10.1016/j.anucene.2016.04.032.

Raquel, Parks. n.d. "Microgrids : Legal and Regulatory Hurdles for a More Resilient Energy Infrastructure," 173–202.

Ratnam, Elizabeth L., and Steven R. Weller. 2018. "Receding Horizon Optimization-Based Approaches to Managing Supply Voltages and Power Flows in a Distribution Grid with Battery Storage Co-Located with Solar PV." *Applied Energy* 210 (August 2017): 1017–26. https://doi.org/10.1016/j.apenergy.2017.08.163.

Rawlings, James B, and David. Q Mayne. 2009. *Model Predictive Control: Theory and Design*. Madison: Nob Hill Publishing.

Rebecca, Smith. 2014. "Assault on California Power Station Raises Alarm on Potential for Terrorism; April Sniper Attack Knocked Out Substation, Raises Concern for Country's Power Grid." *Wall Street Journal*, 2014.

Reishus Consulting LLc. 2017. "Electricity Ancillary Services Primer," no. August.

Rismanchi, B., R. Saidur, H. H. Masjuki, and T. M I Mahlia. 2012. "Energetic, Economic

and Environmental Benefits of Utilizing the Ice Thermal Storage Systems for Office Building Applications." *Energy and Buildings* 50: 347–54. https://doi.org/10.1016/j.enbuild.2012.04.001.

Roberts, David, Alvin Chang, and Vox. 2018. "Meet the Microgrid, the Technology Poised to Transform Electricity." https://www.vox.com/energy-and-environment/2017/12/15/16714146/greener-more-reliable-more-resilient-grid-microgrids.

Rodrigues, Yuri, Maíra Monteiro, Morad Abdelaziz, Liwei Wang, Antonio Z De Souza, and Paulo Ribeiro. 2020. "Electrical Power and Energy Systems Improving the Autonomy of Islanded Microgrids through Frequency Regulation." *Electrical Power and Energy Systems* 115 (August 2019): 105499. https://doi.org/10.1016/j.ijepes.2019.105499.

Roege, Paul E, Zachary A Collier, James Mancillas, John A Mcdonagh, and Igor Linkov. 2014. "Metrics for Energy Resilience" 72: 249–56. https://doi.org/10.1016/j.enpol.2014.04.012.

Ruan, Yingjun, Qingrong Liu, Zhengwei Li, and Jiazheng Wu. 2016. "Optimization and Analysis of Building Combined Cooling, Heating and Power (BCHP) Plants with Chilled Ice Thermal Storage System." *Applied Energy* 179 (2016): 738–54. https://doi.org/10.1016/j.apenergy.2016.07.009.

Sadamoto, Tomonori, Aranya Chakrabortty, Takayuki Ishizaki, and Jun-ichi Imura. 2018. "Dynamic Modeling , Stability , and Control of Power Systems with Distributed Energy Resources." *ArXiv E-Prints*, 1–36.

Saleh, Khaled A, Hatem H Zeineldin, and Ehab F El-saadany. 2017. "Optimal Protection Coordination for Microgrids Considering N − 1 Contingency" 13 (5): 2270–78.

Salt River Project. n.d. "How to Read a Residential Bill." Accessed January 10, 2017. https://www.srpnet.com/billing/home/read.aspx.

Sanaye, Sepehr, and Mohammad Hekmatian. 2016. "Ice Thermal Energy Storage (ITES) for Air-Conditioning Application in Full and Partial Load Operating Modes." *International Journal of Refrigeration* 66: 181–97. https://doi.org/10.1016/j.ijrefrig.2015.10.014.

Sanaye, Sepehr, and Ali Shirazi. 2013. "Thermo-Economic Optimization of an Ice Thermal Energy Storage System for Air-Conditioning Applications." *Energy and Buildings* 60: 100–109. https://doi.org/10.1016/j.enbuild.2012.12.040.

Schirrer, Alexander, Markus Brandstetter, Ines Leobner, Stefan Hauer, and Martin Kozek. 2016. "Nonlinear Model Predictive Control for a Heating and Cooling System of a Low-Energy Office Building." *Energy and Buildings* 125: 86–98. https://doi.org/10.1016/j.enbuild.2016.04.029.

Schossig, Thomas, and Walter Schossig. 2013. "DISTURBANCES AND BLACKOUTS – LESSONS LEARNED TO MASTER THE ENERGY TURNAROUND," no.

October.

Sen, Sachidananda, and Vishal Kumar. 2018. “Microgrid Control: A Comprehensive Survey.” *Annual Reviews in Control* 45 (March): 118–51. https://doi.org/10.1016/j.arcontrol.2018.04.012.

Shen, Lijuan, Beatrice Cassottana, and Loon Ching Tang. 2018. “Statistical Trend Tests for Resilience of Power Systems.” *Reliability Engineering and System Safety* 177 (April): 138–47. https://doi.org/10.1016/j.ress.2018.05.006.

Sherlock, Molly F. 2018. “The Energy Credit : An Investment Tax Credit for Renewable Energy,” 7–8.

Shi, L., Y. Luo, and G. Y. Tu. 2014. “Bidding Strategy of Microgrid with Consideration of Uncertainty for Participating in Power Market.” *International Journal of Electrical Power and Energy Systems* 59: 1–13. https://doi.org/10.1016/j.ijepes.2014.01.033.

Small, Forrest, and L Frantzis. 2010. “The 21st Century Electric Utility: Positioning for a Low-Carbon Future.” *Ceres - Igniting 21st Century Solutions for a Sustainable Economy*, no. July.

Springer, David, and Davis Energy Group. 2007. *SMUD Off-Peak Over-Cooling Project: Final Project Report*. California Energy Commission.

Stadler, Michael, and A Nasle. 2019. “Planning and Implementation of Bankable Microgrids.” *The Electricty Journal*.

Stelloh, Tim. 2019. “California Braces for More Fires, Blackouts as Part of State’s New ‘Normal.’” NBC News. 2019. https://www.nbcnews.com/news/us-news/california-braces-more-fires-blackouts-wind-comes-roaring-back-state-n1073136.

Stott, By Peter. 2016. “How Climate Change Affects Extreme Weather Events” 352 (6293).

Studies, Case, Emerging Applications, and Their Benefits. 2019. “PUTTING DISTRIBUTED ENERGY RESOURCES TO WORK IN WHOLESALE Case Studies of Emerging Applications and Their,” no. September.

sunrun. 2019. “Building a More Resilient Grid.”

Taft, J D. 2017a. “Electric Grid Market- Control Structure,” no. June.

———. 2017b. “Electric Grid Resilience and Reliability for Grid Architecture,” no. November.

Tang, Rui, and Shengwei Wang. 2019. “Model Predictive Control for Thermal Energy Storage and Thermal Comfort Optimization of Building Demand Response in Smart Grids.” *Applied Energy* 242 (March): 873–82. https://doi.org/10.1016/J.APENERGY.2019.03.038.

Temple, James. 2018. “The $2.5 Trillion Reason We Can’t Rely on Batteries to Clean up

the Grid." 2018.

The Gridwise Alliance. 2013. "Improving Electric Grid Reliablity and Resilience: Lessons Learned from Superstorm Sandy and Other Extreme Events."

The World Bank. n.d. "Pump Price for Diesel Fuel (US$ per Liter)." https://data.worldbank.org/indicator/ep.pmp.desl.cd.

Ton, Dan, and Merrill Smith. 2012. "The U.S. Department of Energy's Microgrid Initiative."

Turner, W. J.N., I. S. Walker, and J. Roux. 2015. "Peak Load Reductions: Electric Load Shifting with Mechanical Pre-Cooling of Residential Buildings with Low Thermal Mass." *Energy* 82: 1057–67. https://doi.org/10.1016/j.energy.2015.02.011.

Tuttle, David P., Gurcan Gulen, Robert Hebner, Carey W. King, David B. Spence, Juan Andrade, Jason A. Wible, Ross Baldick, and Roger Duncan. 2016. "The History and Evolution of the U.S. Electricity Industry," 24. http://energy.utexas.edu/.

U.S. Department of Energy. n.d. "Tips on Saving Money and Energy in Your Home Contents."

———. 2017. "EnergyPlus." *U.S. Department of Energy's*. https://energyplus.net/.

U.S. Energy Information Administration. n.d. "U.S. Total Energy Statistics."

———. 2018a. "Levelized Cost and Levelized Avoided Cost of New Generation Resources in the Annual Energy Outlook 2018." *Independent Statistics & Analysis*.

———. 2018b. "Nearly Half of Utility-Scale Capacity Installed in 2017 Came from Renewables." 2018.

U.S. Environmental Protection Agency. 1997. "Guiding Principles for Monte Carlo Analysis." *Us Epa*, no. March: 1–35. https://doi.org/EPA/630/R-97/001.

U.S. Government Information. 2005. *ENERGY POLICY ACT OF 2005*.

Undrill, John. 2018. "Primary Frequency Response and Control of Power System Frequency," no. February. https://www.ferc.gov/industries/electric/indus-act/reliability/frequency-control-requirements/primary-response.pdf.

United States Environmental Protection Agency. 2017. "U.S. Electricity Grid & Markets." 2017. https://www.epa.gov/greenpower/us-electricity-grid-markets.

United States of America Federal Energy Regulatory Commission. 2018. *Electric Storage Participation in Markets Operated by Regional Transmission Organizations and Independent System Operators*. *18 CFR Part 35*. https://doi.org/10.1017/CBO9781107415324.004.

Units, Rooftop. 2017. "Landmark ® Rooftop Units."

University of Michigan, Center for Sustainable Systems. 2018. "U . S . Grid Energy Storage."

http://css.umich.edu/sites/default/files/U.S._Grid_Energy_Storage_Factsheet_CSS15-17_e2018.pdf.

US Department of Energy. 2008. “Energy Efficiency Trends in Residential and Commercial Buildings,” no. October: 1–32.

Venkata Rao, Ravipudi. 2018. *Jaya: An Advanced Optimization Algorithm and Its Engineering Applications*. *Jaya: An Advanced Optimization Algorithm and Its Engineering Applications*. https://doi.org/10.1007/978-3-319-78922-4.

Venkatasubramanian, Vaithianathan, and Yuan Li. 2004. “Analysis of 1996 Western American Electric Blackouts.” *Bulk Power System Dynamics and Control* 4: 22–27.

Vugrin, Eric, Anya Castillo, and Cesar Silva-monroy. 2017. “Resilience Metrics for the Electric Power System : A Performance-Based Approach,” no. February.

Wang, Jianxiao, Haiwang Zhong, Wenyuan Tang, Ram Rajagopal, Qing Xia, Chongqing Kang, and Yi Wang. 2017. “Optimal Bidding Strategy for Microgrids in Joint Energy and Ancillary Service Markets Considering Flexible Ramping Products.” *Applied Energy* 205: 294–303. https://doi.org/10.1016/j.apenergy.2017.07.047.

Wang, Jiaren, Ning Xie, Wenxian Wu, Dong Han, Chengmin Wang, and Binruo Zhu. 2018. “Resilience Enhancement Strategy Using Microgrids in Distribution Network.” *Global Energy Interconnection* 1 (5): 537–43. https://doi.org/10.14171/j.2096-5117.gei.2018.05.002.

Wang, Jing, Wangda Zuo, Landolf Rhode-barbarigos, Xing Lu, Jianhui Wang, and Yanling Lin. 2020. “Literature Review on Modeling and Simulation of Energy Infrastructures from a Resilience Perspective.” *Reliability Engineering and System Safety* 183 (November 2017): 360–73. https://doi.org/10.1016/j.ress.2018.11.029.

West, Samuel R., John K. Ward, and Josh Wall. 2014. “Trial Results from a Model Predictive Control and Optimisation System for Commercial Building HVAC.” *Energy and Buildings* 72: 271–79. https://doi.org/10.1016/j.enbuild.2013.12.037.

Widergren, S, A Shankar, B Kelley, J Taft, and R Melton. 2018. “Toward a Practical Theory of Grid Resilience,” no. April.

Wijesuriya, Sajith, Matthew Brandt, and Paulo Cesar Tabares-Velasco. 2018. “Parametric Analysis of a Residential Building with Phase Change Material (PCM)-Enhanced Drywall, Precooling, and Variable Electric Rates in a Hot and Dry Climate.” *Applied Energy* 222 (March): 497–514. https://doi.org/10.1016/j.apenergy.2018.03.119.

Wilcox, S, and W Marion. 2008. “Users Manual for TMY3 Data Sets.” *Renewable Energy*, no. May: 51. https://doi.org/NREL/TP-581-43156.

Wilson, E, C Engebrecht Metzger, S Horowitz, and R Hendron. 2014. “2014 Building America House Simulation Protocols.”

Witte, Michael J, Robert H Henninger, and Drury B Crawley. 2004. “EXPERIENCE

TESTING ENERGYPLUS WITH THE ASHRAE 1052-RP BUILDING FABRIC ANALYTICAL TESTS," 1–8.

Xu, Jun, Yuanyuan Zou, and Yugang Niu. 2014. "Multi-Time Scale Hierarchical Predictive Control for Energy Management of Microgrid System with Smart Users." *26th Chinese Control and Decision Conference, CCDC 2014*, 3055–60. https://doi.org/10.1109/CCDC.2014.6852699.

Xu, Peng. 2006. "Evaluation of Demand Shifting with Thermal Mass in Two Large Commercial Buildings." Ernest Orlando Lawrence Berkeley National Laboratory, Berkeley, CA (US).

Xu, Yinliang, Kun Ji, Yan Lu, Yuebin Yu, and Wenxin Liu. 2013. "Optimal Building Energy Management Using Intelligent Optimization." In *Automation Science and Engineering (CASE), 2013 IEEE International Conference On*, 95–99. IEEE.

Xue, Xue, and Wang Shengwei. 2012. "Interactive Building Load Management for Smart Grid." In *Power Engineering and Automation Conference (PEAM), 2012 IEEE*, 1–5. IEEE.

Yau, Y. H., and Behzad Rismanchi. 2012. "A Review on Cool Thermal Storage Technologies and Operating Strategies." *Renewable and Sustainable Energy Reviews* 16 (1): 787–97. https://doi.org/10.1016/j.rser.2011.09.004.

Ye, Yixin, Ignacio E Grossmann, Jose M Pinto, and Sivaraman Ramaswamy. 2018. "Markov Chain MINLP Model for Reliability Optimization of System Design and Maintenance," no. 2002: 1–6. https://doi.org/10.1016/B978-0-444-64241-7.50242-1.

Yu, Moduo, Wentao Huang, Nengling Tai, Xiaodong Zheng, Pan Wu, and Weidong Chen. 2018. "Transient Stability Mechanism of Grid-Connected Inverter-Interfaced Distributed Generators Using Droop Control Strategy." *Applied Energy* 210 (March 2017): 737–47. https://doi.org/10.1016/j.apenergy.2017.08.104.

Zachar, Michael, and Prodromos Daoutidis. 2016. "Nonlinear Economic Model Predictive Control for Microgrid Dispatch." *IFAC-PapersOnLine* 49 (18): 778–83. https://doi.org/10.1016/j.ifacol.2016.10.260.

Zhang, Xinan, Jie Bao, Ruigang Wang, Chaoxu Zheng, and Maria Skyllas-Kazacos. 2017. "Dissipativity Based Distributed Economic Model Predictive Control for Residential Microgrids with Renewable Energy Generation and Battery Energy Storage." *Renewable Energy* 100: 18–34. https://doi.org/10.1016/j.renene.2016.05.006.

Zhang, Yan, Tao Zhang, Rui Wang, Yajie Liu, and Bo Guo. 2015. "Optimal Operation of a Smart Residential Microgrid Based on Model Predictive Control by Considering Uncertainties and Storage Impacts." *Solar Energy* 122: 1052–65. https://doi.org/10.1016/j.solener.2015.10.027.

Zhao, Long, Zhiyong Yang, and Wei Jen Lee. 2017. "The Impact of Time of Use (TOU) Rate Structure on Consumption Patterns of The Residential Customers." *IEEE*

Transactions on Industry Applications 9994 (c). https://doi.org/10.1109/TIA.2017.2734039.

Zhenzhen, Song. 2015. “The Evaluation of Parameter M in the Big M Method of Linear Programming Song Zhenzhen,” no. Meita: 37–40.

Zhou, Yang, and Carl Ngai-man Ho. 2016. “A Review on Microgrid Architectures and Control Methods.” *2016 IEEE 8th International Power Electronics and Motion Control Conference (IPEMC-ECCE Asia)*, 3149–56. https://doi.org/10.1109/IPEMC.2016.7512799.

Zhu, Yihai, and Jun Yan. 2014. “Revealing Cascading Failure Vulnerability in Power Grids Using Risk-Graph.” *IEEE Transactions on Parallel and Distributed Systems* 25 (12): 3274–84. https://doi.org/10.1109/TPDS.2013.2295814.